



THESE

présentée pour obtenir le grade de

**Docteur de l'Ecole Nationale Supérieure
des Télécommunications**

Spécialité: Informatique et Réseaux

Hicham Anouar

Conception et Optimisation de Protocoles d'Accès Multiple au Canal pour les Réseaux Ad Hoc sans Fil

Thèse soutenue le 29 Juin 2006, devant le jury composé de :

Pierre Humblet	Rapporteur
Andrzej Duda	Rapporteur
Isabelle Demeure	Examineur
Mounir Ghogho	Examineur
Marceau Coupechoux	Examineur
Christian Bonnet	Directeur de thèse

Thèse réalisée au sein de l'Institut Eurecom

© Hicham Anouar 2006

AUTHOR ADDRESS:

Hicham Anouar

Institut Eurecom

Departement de CommunicationMobile

2229, route des Crêtes

B.P. 193

06904 Sophia-Antipolis France

Tel: +33 4 93 00 81 50

Email: hicham.anouar@eurecom.fr



THESIS

In Partial Fulfillment of the Requirements
for the Degree of Doctor of Philosophy
from Ecole Nationale Supérieure des Télécommunications

Specializing: Computer Sciences and Networking

Hicham Anouar

Design and Optimization of Multiple Access Protocols for Ad Hoc Wireless Networks

Defended on June 29, 2006, before the committee composed by:

Pierre Humblet	Reader
Andrzej Duda	Reader
Isabelle Demeure	Examiner
Mounir Ghogho	Examiner
Marceau Coupechoux	Examiner
Christian Bonnet	Thesis supervisor

Remerciements

Je remercie mon directeur de thèse M. Christian Bonnet pour avoir accepté d'encadrer mon travail, pour son aide précieuse, technique et morale, et pour sa grande patience durant toutes les phases de cette thèse.

Je remercie aussi tous les membres du jury qui par leurs commentaires ont participé à améliorer la qualité de ce travail.

Mes remerciements vont aussi à tous les doctorants et tous le personnel de l'institut Eurecom pour leur sympathie et la bonne ambiance qu'ils génèrent au sein de l'institut.

Enfin, Ce travail n'aurait pas pu être accompli sans l'amour et le soutien de toute ma famille, mes parents, ma soeur Khadija, et mes frères Youssef, Kamal et Yassin. ***Merci pour tout, cette thèse vous est dédiée.***

Dans cette thèse, nos principales objectives sont la conception, l'analyse et l'optimisation de protocoles CAC existants ou nouveaux pour les réseaux ad hoc sans fil, et l'étude des limites fondamentales de l'estimation du temps d'arrivée des signaux à très large bande.

Pour les réseaux simple-bond, nous nous concentrons sur la dérivation de schémas de retransmissions optimaux qui maximisent la capacité totale du réseau. Nous nous intéressons spécialement aux schémas quasi-aveugles dans le sens qu'ils nécessitent juste une information sur la taille du réseau. En effet, les schémas existants se basent soit sur l'estimation du nombre de paquets en attente de retransmission, soit sur d'autres informations obtenues par la mesure de l'activité du canal. L'information sur la taille du réseau est la plus simple à obtenir dans les réseaux simple-bond. Nous considérons alors spécialement le protocole ALOHA synchronisé (chapitre 2) et le protocole CAC du standard IEEE 802.11 connu sous le nom DCF (chapitre 3).

Les limitations physiques ou système des puissances d'émission produisent des situations où les nœuds ne partagent pas tous le même voisinage. Les protocoles CAC ont alors à résoudre en plus le problème du terminal caché qui détériore les performances de tout mécanisme basé sur l'écoute ou la réservation du canal. Pour résoudre correctement le problème du terminal caché, on introduit dans le chapitre (4) un nouveau mécanisme de réservation du canal afin de protéger la réception des paquets de données. Ensuite, on analyse les performances du protocole résultant, et on propose un algorithme distribué basé sur la théorie des Approximations Stochastiques pour contrôler les retransmissions.

L'utilisation des canaux multiples dans les réseaux ad hoc sans fil peut fournir une amélioration de performances en réduisant les collisions et en permettant des transmissions simultanées, augmentant ainsi l'utilisation du canal radio et sa réutilisation spatiale. Dans le chapitre (5), nous proposons un nouveau protocole ALOHA pour les réseaux ad hoc multi-canaux et nous dérivons ensuite un schéma de retransmission qui a les mêmes caractéristiques que celles du schéma obtenu pour le protocole DCF en topologie simple-bond, et ceci sans écoute du canal.

La signalisation UWB est un exemple de technologie de transmission qui peut être employée pour fournir des systèmes multi-canaux. Dans le chapitre (6) de la thèse, on étudie les performances fondamentales de quelques estimateurs cohérents et non-cohérents du temps d'arrivée des signaux UWB. La connaissance de ces performances est nécessaire pour la synchronisation et pour l'exploitation des capacités de localisation des signaux UWB.

Contents

Remerciements	1
Résumé	3
List of Figures	9
List of Tables	13
Acronyms	15
1 Introduction	17
1.1 Motivations	18
1.2 Objectives	22
1.3 Thesis Outline & Contributions	23
I Single Hop Networks	27
2 ALOHA Protocol	29
2.1 Introduction	29
2.1.1 Contribution	30
2.2 Performance Analysis and Optimization of Slotted ALOHA . .	31
2.2.1 Stability	32
2.2.2 Optimization	32
2.3 Conclusion	39
3 IEEE 802.11 DCF Protocol: Analysis & Optimization	43
3.1 Introduction and Related Works	43
3.1.1 Contribution	46
3.2 Binary Exponential Backoff Scheme	47
3.2.1 Delay Statistics	52
3.2.2 Short-Term Fairness	53
3.3 Optimal Constant-Window Backoff Scheme	56

3.3.1	Derivation of τ_{op} and W_{op}^s	57
3.3.2	Derivation of q_t	58
3.3.3	Loss in System Performances	58
3.4	Numerical Results	61
3.4.1	Throughput	61
3.4.2	Delay & Fairness	67
3.5	Buffered Terminals Model	68
3.6	Simulation results	72
3.7	Conclusion	76
 II Multiple Hop Networks		77
4	IEEE 802.11 DCF Protocol: Enhancement & Optimization	79
4.1	Introduction	79
4.1.1	Contribution	82
4.2	Effectiveness of RTS/CTS Handshaking in IEEE 802.11 DCF .	83
4.2.1	The Masked Node Problem	83
4.2.2	The False Blocking Problem and its Propagation	84
4.3	Protocol Enhancement: The RTS/R-CTS Handshaking	85
4.4	Performance Analysis	87
4.5	Backoff Window Optimization	90
4.6	Conclusion	95
5	Design & Optimization of MAC protocol for Multi-channel Networks	97
5.1	Introduction	97
5.1.1	Contribution	100
5.2	Protocol Description	100
5.2.1	State Diagram	101
5.3	Delay-Throughput Analysis	103
5.3.1	Saturation Throughput Analysis	104
5.3.2	General Load Analysis	112
5.4	Conclusion	114
5.A	Appendix	116
5.A.1	Transition Rates For General Load	116

III	Case study: Ultra-Wideband Networks	119
6	Time Delay estimation of UWB Signals	121
6.1	System Model	124
6.2	Lower Bound on Mean Square Estimation Error	125
6.2.1	The Improved Ziv-Zakai Lower Bound	125
6.2.2	Case of perfect 2nd. order statistics information	125
6.2.3	Numerical Results	130
6.3	Performance of Sub-optimal estimators	132
6.3.1	Upper Bound on Mean Square Estimation Error	133
6.3.2	Mis-Matched Maximum Likelihood Estimator	134
6.3.3	Case of No 2nd Order Statistics Information: Equal Gain Combining (EGC)	135
6.3.4	Discrete Time Estimation by Energy Maximization	135
6.3.5	Numerical Results	137
6.4	Conclusion	140
6.A	Appendix	142
6.A.1	Derivation of the Improved Ziv-Zakai Lower Bound	142
6.A.2	Derivation of the detection error probability	144
6.A.3	Proof of Theorem 6.3.1	145
7	General Conclusion & Perspectives for Future Works	149
	Résumé (in french)	153
	Bibliography	173
	List of Publications	185

List of Figures

1.1	The Backoff function	19
1.2	The hidden node problem	19
2.1	Expected drift and steady-state probabilities Vs. backlog state	33
2.2	Aloha state diagram	33
2.3	Throughput and optimal retransmission probabilities of homogeneous network of size $M = 20$	35
2.4	Expected drift and steady-state probabilities Vs. backlog state under optimal retransmission probabilities	38
2.5	Throughput of Homogeneous Network of Size $M=20$ for Various Retransmission Probabilities	40
2.6	Packet delay of Homogeneous Network of Size $M=20$ for Various Retransmission Probabilities	41
3.1	Markov chain model	49
3.2	Channel capture by node 1	54
3.3	Channel capture probability Vs. $W1$	56
3.4	Optimal transmission probabilities and the corresponding optimal backoff windows (normalized to the saturation optimal window) vs. arrival rates	59
3.5	Bounds on system performances	60
3.6	Throughput	62
3.7	Repartition of Success probability of the BEB Scheme	64
3.8	Repartition of Success probability of the OCB Scheme	65
3.9	Throughput for Optimal Exact Window and Optimal Saturation Window	66
3.10	Throughput Vs. Network size	67
3.11	Normalized delay	68
3.12	Jain fairness Index	69

3.13	Queueing model throughput Vs. simulation	72
3.14	Queueing model delay Vs. simulation	73
3.15	Delay fairness	74
3.16	Throughput short-term fairness	75
4.1	Illustration of the masked node problem	83
4.2	DATA collision caused by masked nodes	84
4.3	The RTS/R-CTS handshaking	86
5.1	State diagram	102
5.2	Case of no collision	103
5.3	State diagram in saturation conditions	106
5.4	Optimal Retransmission Delay To	110
5.5	Network Throughput	111
5.6	Network Throughput vs. Packet duration L for $N = 10$	111
5.7	Network Throughput vs. Packet duration L for $N = 50$	112
5.8	Optimal Retransmission Delay and Real Load R Vs Mean Ar- rival rate η	113
5.9	User Channels Utilization in General Load Conditions	114
6.1	IZZLB on RMSE of single frame and muliframe estimators Vs. average SNR, and $T_d=15ns, 20ns$	131
6.2	IZZLB on RMSE of single frame and muliframe estimators Vs. observation length T_f , and $SNR=-10dB, +10dB$	132
6.3	Discrete Time Energy Detector	136
6.4	IZZLB and upper bounds on RMSE of single frame estimators Vs. average SNR	138
6.5	Upper bounds on RMSE of muliframe estimators Vs. average SNR	138
6.6	Upper bound on RMSE of the energy maximization scheme Vs. SNR for various integration window lengths and PDF $\alpha = 2139$	
6.7	RMSE of energy maximization estimator Vs. integration win- dow length, for various integrating step Δ , various power decay factor α , $T_f=100ns$, $T_d=20ns$, and $SNR=-10dB$	140
7.1	Le schema de retransmission	154
7.2	le problème du terminal caché	155
7.3	Débit obtenu par ALOHA dans un réseau de taille $n=20$ sous différents choix de probabilités de retransmission	160

7.4	Délai obtenu par ALOHA dans un réseau de taille $n=20$ sous différents choix de probabilités de retransmission	161
7.5	Débit d'un réseau de taille $n=50$	163
7.6	délai normalisé d'un réseau de taille $n=50$	163
7.7	Indice d'équité de Jain sur le délai d'un réseau de taille $n=50$.	164
7.8	Débit du modèle theorique vs. simulation	164
7.9	Délai du modèle theorique vs. simulation	165
7.10	Illustration du mécanisme RTS/R-CTS	166
7.11	Exemple du fonctionnement du protocole ALOHA multi-canaux	167
7.12	Débit du réseau	168
7.13	Network Throughput vs. Packet duration L for $N = 10$	168
7.14	Network Throughput vs. Packet duration L for $N = 50$	169
7.15	Débit utilisateur Vs. charge du trafic	170
7.16	La bande IZZLB sur la bariance de l'erreur d'estimation . . .	170
7.17	Bande supérieure sur la variance de l'erreur d'estimation de l'estimateur effectuant une collection d'énergie	172

List of Tables

3.1	Parameter set used for numerical results	61
-----	--	----

Acronyms

Here are the main acronyms used in this document. The meaning of an acronym is usually indicated once, when it first occurs in the text.

ACK	Acknowledgment
BEB	Binary Exponential Backoff
CC	Common Channel
COSA	Code Division Multiple Access
CRLB	Crammer-Rao Lower Bound
CSMA/CA	Carrier Sense Multiple Access / Collision Avoidance
CS	Carrier Sense
CSR	Carrier Sensing Range
CTS	Clear To Send
DCF	Decentralized Coordination Function
DIFS	DCF Inter-Frame Space
EGC	Equal Gain Combining
EIED	Exponential Increase Exponential Decrease
EIFS	Extended Inter-Frame Space
FHSS	Frequency Hopping Spread Spectrum
GSM	Global System for Mobile Communications
FCC	Federal Communications Commission
FCR	Fast Collision Resolution
FDMA	Frequency Division Multiple Access
ID	Identifier
IPA	Infinitesimal Perturbation Analysis
IR	Impulse Radio
ITB	Inter-Transmission Backoff
IZZLB	Improved Ziv-Zakai Lower Bound
KW	Kiefer-Wolfowitz

LRT	Likelihood Ratio Test
MAC	Medium Access Control
MILD	Multiplicative Increase Linear Decrease
ML	Maximum Likelihood
MSE	Mean Square Error
NAV	Network Allocation Vector
NS2	Network Simulator 2
OCB	Optimal Constant Backoff
PHY	Physical Layer
RBS	Receiver-Based Scheme
RM	Robins-Monro
RMSE	Root Mean Square Error
RTS	Request To Send
RTS/R-CTS	Request To Send/Repeated-Clear To Send
SNR	Signal to Noise Ratio
SA	Stochastic Approximation
SIFS	Short Inter-Frame Space
SS	Steady State
TDMA	Time Division Multiple Access
TIS	Transmitter-Initiated Scheme
TR	Transmission Range
UMTS	Universal Mobile Telecommunications Services
UWB	Ultra-Wideband
WLAN	Wireless Local Area Network
WPAN	Wireless Personal Area Networks

Chapter 1

Introduction

Wireless networks have gained immense popularity over the past few years. The predominant use of these wireless technologies has been in single-hop networks that operate with infrastructure support. Since the great success of wireless telephony systems (GSM, UMTS...) and wireless local area network (WLAN) standards (IEEE802.11, Bluetooth...), up-and-coming mobile users/applications will require even greater amount of network capacity and flexibility as a natural evolution of the use of communications technologies towards multimedia access anytime anywhere. This motivates a significant research activity in building wireless ad-hoc networks which may be of use as private wireless networks, sensor networks, mobile ad hoc networks, emergency communication system, etc.

A mobile Ad Hoc network is a self organizing system of wireless nodes that requires no fixed infrastructure. In the event any two nodes cannot communicate directly, each node must act as a relay, forwarding packets on the behalf of other nodes. The main characteristics of these type of networks, whose the consequences must be carefully addressed when designing specific communication protocols, are the lack of central controller, the difficulty to synchronize the network, and the possible multihop topology.

1.1 Motivations

In wireless systems, the physical channel is scarce, so its utilization is of great importance; hence, Medium Access Control (MAC) protocol is a critical part of the network stack that determines to a large extent the correct and efficient operation of the network. The main objective of MAC protocols for wireless networks is to share efficiently and fairly communication medium among many contending users. These protocols and their performances differ according to the environment in question and the system requirements to be satisfied. Generally, MAC protocols may be broadly classified into two groups based on their strategy for determining access rights: deterministic access protocols and random access protocols.

Deterministic access protocols assign to each node in the network a permanent transmission schedule indicating in which of the synchronized time-slots or data channels (frequencies, spreading codes or their combinations) the node may transmit. These protocols have bounded delay but suffer low performance at low load. Moreover if the network topology changes, these protocols may potentially become inefficient and unstable as maintaining transmission schedules, in multihop topology, may use all network capacity. Random access protocols are well suited for flat architecture and bursty data traffic, and do not require global network synchronization. Their performances however are mainly governed by their capabilities to handle efficiently retransmissions of collided packets.

In wireless ad hoc networks, multiple stations use the radio channel to communicate without presence of any fixed infrastructure. In this case, multiple access is basically distributed and random, and collisions are unavoidable.

Single hop networks represent situations where all nodes in the network are in the transmission range of each others. In this case, the main challenge in designing a *good* MAC protocol is to manage optimally the retransmissions of collided packets. The retransmission scheme has to delay the next transmission attempt long enough in time to avoid repeated collisions, but not so far in order not to waste channel utilization (Fig. 1.1).

Due to power limitations, nodes in ad hoc networks are not always in the transmission range of each others. In this case, nodes may be requested to act as temporal relays in order to ensure the connectivity of the network. The multiple access issue becomes then more complicated as new problems

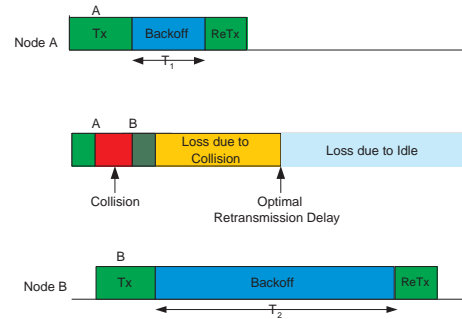


Figure 1.1: The Backoff function

occur, mainly, the hidden node problem. The hidden node problem does not permit efficient and complete signaling of control messages on the networks. So it affects any carrier sensing or reservation-based MAC protocol. As an example, consider the operation of a carrier sense multiple access (CSMA) protocol on the topology shown in Fig. 1.2. In this topology, node C does not hear packet transmissions from node A. Thus, node C may transmit a packet to node D, while node A transmits a packet to node B. These simultaneous transmissions lead to a collision at node B, destroying the packet sent by node A. In this scenario, node C is referred to as a hidden node with respect to node A.

The use of multiple channels in wireless ad hoc networks may provide some performance advantages by reducing collisions and enabling more concurrent transmissions, and thus better bandwidth usage and spatial reuse, even with the same aggregate physical capacity as in single channel networks. The multiple channels may be obtained through frequency division multiple

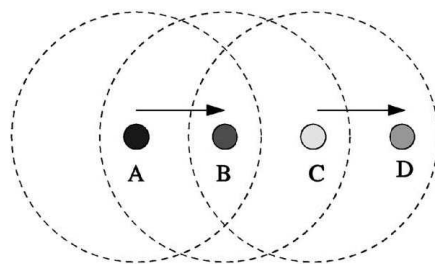


Figure 1.2: The hidden node problem

access (FDMA) and code division multiple access (CDMA) (frequency hopping, time hopping, and direct sequence spread spectrum) techniques.

Research on wireless network capacity has typically considered wireless networks with a single channel [1–3], although the results are applicable to a wireless network with multiple channels as well, provided that at each node there is a dedicated interface per channel. With a dedicated interface per channel, a node can use all the available channels simultaneously. However, the number of available channels in a wireless network can be fairly large, so it is too expensive to have a dedicated interface per channel at each node. When nodes are not equipped with a dedicated interface per channel, then capacity degradation may occur, compared to using a dedicated interface per channel. However in [4], it has been shown that in a random network of size n with up to $O(\log n)$ channels, even with a single interface per node, there is no capacity degradation. This implies that it may be possible to build near capacity-optimal multi-channel networks with few channels and one interface per node. This further implies that time has come to benefit from the panoply of multiplexing techniques offered by advances in transmission technologies in the design of efficient MAC protocols. In fact, when looking at existing standards for WLANs, we can observe that MAC protocols are not designed adequately to exploit the characteristics of the underlying transmission technologies.

As example, IEEE 802.11b and IEEE 802.11a define physical (PHY) layer standards that are faster than that of IEEE 802.11. In IEEE 802.11b, there can be 3 PHY channels concurrently in use, while In IEEE 802.11a, there can be 8 PHY channels concurrently in use. However, the two standards will use the MAC protocol of IEEE 802.11 or IEEE 802.11e¹ independently from physical layer specifications. In current IEEE 802.11/11b/11a standards, the different PHY channels are mainly utilized to partition wireless LANs into multiple base station systems.

To take benefit of channelized system, the multiple access scheme has to address additional design problems. Particularly, how to distribute efficiently the access demands on the different channels? This issue is known as the channel assignment problem.

Ultra-Wideband (UWB) signaling is an example of transmission technology that may be used to provide channelized system. Recently, UWB signaling has grown in popularity since the Federal Communications Commission

¹IEEE 802.11e [5] is a quality of service (QOS) extension of IEEE 802.11

(FCC) regulations in the United States [6] have defined emission masks for UWB signals. The FCC ruling allows for coexistence with traditional and protected radio services and enables the potential use of UWB transmission without allocated spectrum. This is achieved by constraining UWB transmission systems to operate at a very low spectral density, approximately equal to the power spectral density of thermal noise. Thus, interference from UWB transmitters to others UWB users as well as other wireless systems with overlapping spectrum bandwidth resembles thermal noise at the receiver. As result, scarce spectrum may be used more efficiently.

The potential classes of UWB device are many, ranging from imaging systems (ground-penetrating radar, wall-imaging system, medical systems, and surveillance systems) to vehicular radar systems, and communications and measurement systems. The technology offers significant potential for the deployment of short-range communication systems (Wireless Personal Area Networks (WPAN) supporting high rate applications.

Within the IEEE, two standardization groups have been created to investigate on UWB technology. The first one is the Task Group 3a (TG3) [7] which focuses on the definition of a physical layer alternative to IEEE 802.15.3 standard based on UWB signaling. The newly defined PHY will respond to consumers demand in the area of multimedia distribution and will work with the already designed MAC [8]. The second one is the TG4 [9] which is working toward a standard for specifying a low-rate low-power standard, offering localization capability, and low cost WPAN technology based on UWB signaling.

The widely used form of UWB signaling is based on impulse radio (IR) [10]. IR-based UWB (IR-UWB) technology utilizes signals of very short durations ($\leq ns$) with very low spectral densities, is resistant to channel multipath, has very good time-domain resolution allowing for location and tracking applications, and is relatively low-complexity and low-cost. Due to low power density, duty cycle transmission, and dense UWB multipath channel [10,11], very fine synchronization is required for reliable transmission in UWB systems.

In ad hoc networks based on UWB signaling (no base station to perform synchronization), this issue becomes crucial as transmitter and receiver nodes have to synchronize before each transmission. Thus, robust synchronization schemes have to be designed, and information about the performance of the synchronization (synchronization time and error statistics) has to be taken into account when building the system protocol stack.

For example, if the synchronization time needed to achieve acceptable level of performance is high, then we have to think about a master node to synchronize the network. Hence, the design of the MAC and routing protocol must be adapted. Or, if the needed time to synchronize is low, we have to specify data packet length adequately to achieve good performance.

In addition, UWB capabilities in providing ranging and localization information may be of great interest in building efficient power control, MAC, and routing protocol in ad hoc networks.

The issues of synchronization and localization are closely related to the time delay estimation subject. In fact, signal synchronization consists on two phases: coarse timing estimation phase that corresponds to a time-delay estimation procedure, followed by signal tracking phase to produce fine timing information. The Location information is also built upon the time delay information by using different localization algorithms. For these reasons, we focus in this thesis on time delay estimation study of UWB signals.

1.2 Objectives

In this thesis, our main objectives are to design, analyze, and optimize existent or new MAC protocols for ad hoc networks.

For single hop networks, we focus on deriving optimal backoff schemes that maximize the overall network throughput. We further look only for blind schemes that do not require any feedback information or cooperation between nodes. With blind we denote schemes that require only information about the network size. This information is simple to obtain in single hop networks. For this, we consider slotted ALOHA [12] and the IEEE 802.11 decentralized coordination protocols (DCF) [13].

For multihop networks, we address again the backoff scheme optimization issue, but we do not constraint the resulting solutions to be blind. We look also for new handshaking mechanism to ensure correct operation of DCF in multihop topologies.

In the perspective of using UWB signaling for future ad hoc networks, we first investigate on the design and the optimization of a new MAC protocol that take benefit from the multi-channel capabilities of UWB systems. Second, we examine fundamental performance of some coherent and non-coherent synchronization schemes for UWB communications.

1.3 Thesis Outline & Contributions

In the first part of the thesis, we address the optimization of retransmission scheme for ALOHA and DCF protocols in single hop networks. Optimization is carried out in order to maximize the overall network throughput. Our ambition is to design simple and blind optimal retransmission mechanisms under this configuration.

In chapter 2, we review the performance of slotted ALOHA protocol in single-hop network and we discuss its bistability behavior. We derive the optimal retransmission probability for a given network size and packet arrival probability. We prove then that the protocol is stable under this optimal retransmission scheme. Unfortunately, the optimal scheme is not blind as it requires information about the packet arrival probability. This information is hard to obtain in case of heterogeneous network where users have different traffic load.

To overcome this problem, we decide to use the optimal retransmission probability obtained for in saturated network under all traffic loads. We find then that the achieved protocol is quasi-optimal in term of throughput, but not in term of packet delay.

In chapter 3, we first give a detailed and novel analysis of the queueing operation of IEEE802.11 DCF protocol under general load conditions. We derive the delay statistics of the protocol, and we prove the short term unfairness of its binary exponential backoff scheme. We introduce then an optimal constant-window backoff scheme and we show that is sufficient to use the saturation's optimal window under all traffic loads to achieve nearly quasi-optimal throughput and delay under all traffic loads. The intuition behind this choice is that in CSMA system, the idle slot duration is small compared to the collision duration, so the loss in the achieved throughput when using the saturation's optimal window (the largest one for a given network size) under all loads is small. Our backoff scheme is then blind as it requires only information about the size of the network.

In the second part of this thesis we address MAC protocol design and enhancement for multihop networks.

In chapter 4, we introduce a modified handshaking scheme to guarantee full protection of ongoing transmissions in IEEE 802.11 DCF protocol. Then,

we analyze the performance of the resulting protocol, and we propose a distributed algorithm based on stochastic approximations theory to control the backoff window length of each node in order to maximize the network throughput.

In chapter 5, we propose a multi-channel ALOHA-like protocol for multihop networks. To relieve the channel assignment problem, a common channel (CC) is dedicated for broadcasting initial signalization message RTS (Request To Send), while other channels are used randomly by all nodes to complete communications setup and eventually for data transfers. This simplifies the channel assignment functionality since no inter-node collaboration is needed. Each node is equipped with a single half-duplex transceiver, but may switch to all channels. Physical carrier sensing is also avoided, even on data channels. On the CC, because it is of no interest since the RTS message is of small duration, and as each node may operate only on a single channel at time, sensing all data channels may be time consuming so that information collected during the sensing phase may be out-of-date at the end of the sensing operation.

The performances of the proposed protocol are analyzed in saturation conditions and shown to be very good if the retransmission scheme over the common channel is well designed. The analysis is then extended to consider general load conditions. We show again that it is sufficient to use the optimal saturation window under all loads to achieve near maximal throughput. This is a similar result to the one obtained by DCF in single hop situation, but here without the use of carrier sensing.

In chapter 6 of the thesis, we address the performance of some coherent and no-coherent time-delay estimation schemes of IR-UWB signals. We are specially interested in deriving lower and upper bounds on the mean square error (MSE) obtained by these schemes. As UWB systems are expected to operate at low signal-to-noise ratio (SNR) (80211.15.4 low-power low rate standard), the improved Ziv-Zakai lower bound (IZZLB) [14] is then more suited to characterize the lower bound on the MSE, than the Cramer-Rao lower bounds (CRLB) [15, 16].

We apply the IZZLB to derive the lower bound on MSE of maximum likelihood estimator based on perfect knowledge of the 2nd. order statistics of the receiver signal.

When studying practical synchronization schemes that are based on imperfect or no information about the channel state, we are interested in characterizing upper bounds on their performance, which in addition serve as general

upper bound on the MSE of an optimal estimator. For this purpose, we give first a new upper bound on signal parameter estimation suited to characterize sub-optimal estimation schemes. We analyze a mis-matched maximum likelihood (ML) estimator based on the knowledge of noisy second order statistics of the channel, and estimator with no information performing only equal gain combining (EGC) of the received signal. The last estimator we review is of great interest for practical implementation, i.e, it is based on a simple discrete-time energy detector that requires no information about the channel state. The performance of the different estimators are then compared and show that the energy detection scheme would achieve good performance with a few numbers of signal's repetition and adequate integration window's length.

General conclusions and directions for future works are presented in chapter 7.

Part I

Single Hop Networks

Chapter 2

ALOHA Protocol

2.1 Introduction

Historically, the pure ALOHA protocol [17] was first used in the ALOHA system, a single-hop terminal access network developed in 1970 at the University of Hawaii, employing packet-switching on a radio channel. Pure ALOHA permits a user to transmit any time it desires. If it receives an acknowledgment from the destination within some appropriate time-out period, then it knows that no conflict occurred. Otherwise it assumes that a collision occurred and it must retransmit the packet. To avoid continuously repeated conflicts, the retransmission delay is randomized, spreading thus the users (re)transmissions over time. A slotted version, referred to Slotted ALOHA [12], is obtained by dividing time into slots of duration equal to the transmission time of a single packet and its acknowledgment. Each user is then required to synchronize its transmission with slots. When two packets collide, they will overlap completely rather than partially, providing an increase in channel efficiency over pure ALOHA. Due to conflicts and idle channel time, the maximum channel efficiency achieved by ALOHA is only 18% for pure ALOHA and 36% for slotted ALOHA. The slotted version has the advantage of efficiency, but in multihop network, the synchronization may be hard to achieve.

One important dynamic-characteristic of ALOHA-type networks is that they possess two statistically stable equilibrium points, one in a desirable low-delay region (low number of backlogged packets), and the other in an undesirable high-delay region (high number of backlogged packets). Since the stability is only statistical in nature, the system oscillates between these two points, while the system performance are mainly governed by the steady state behavior [18,19]. In [20], the authors have proved the stability of control schemes where retransmission probabilities are function of the backlog state. Several works have then proposed dynamic control procedures to keep the system in a desired operating regime, [20–22], although these schemes cannot be implemented in a distributed fashion. Decentralized control strategies, as introduced in [22, 23], are sub-optimal as they rely only on simple feedback information [23], or on some performance or metrics estimate obtained by channel activity sensing [22].

A different class of random access control protocols, known as recursive conflict resolution algorithms [24–27], have been built upon the idea of optimally exploiting the observed ternary feedback information (idle, success, and collision) to resolve eventual collisions. Even if these protocols reach stable throughput higher than slotted ALOHA, their main drawbacks are that they operate only on synchronized networks and require from all user to share the same feedback information. For synchronized networks, practical reservation-based protocol have been shown to achieve good performance [28, 29].

2.1.1 Contribution

In this chapter, we review the performance of slotted ALOHA protocol in single-hop network and we discuss its bistability behavior. We derive the optimal retransmission probability that maximize the network throughput for a given network size and packet arrival probability. We prove then that the protocol is stable under this optimal retransmission scheme. Unfortunately, the optimal scheme is not blind as it requires information about users' load. This information is further hard to obtain in case of heterogeneous network where users have different traffic loads.

To overcome this problem, we decide to use the optimal retransmission probability obtained for saturated regime regardless of the exact system load. We find then that this choice results in a small loss in the throughput and relatively higher loss in packet delay, compared to the first retransmission scheme.

2.2 Performance Analysis and Optimization of Slotted ALOHA

The Markovian model we use was first introduced simultaneously in [18, 19], it analyzes the protocol operation by considering the joint-backlog state of all users in the network.

We consider a slotted ALOHA channel with user population consisting of $M \geq 2$ users. Each user can be in one of two states: blocked or idle. In the idle state, each user generates and transmits a new packet within a time slot with probability r . A packet which had a channel collision and is waiting for retransmission is said to be backlogged. Each user retransmit a backlogged packet in the current slot with probability p . From the time a user generates a packet until that packet is successfully received, the user is said to be blocked in the sense it cannot handle another transmission.

Let N^t be a stochastic process representing the total number of blocked users (backlogged packets) at time t . The sequence of system states N^t forms a discrete-time Markov chain with state-transition probabilities matrix ST whose entries are given by

$$ST_{ij} = \begin{cases} 0 & ; \quad j \leq i - 2 \\ ip(1-p)^{i-1}(1-r)^{M-i} & ; \quad j = i - 1 \\ (1-p)^i(M-i)r(1-r)^{M-i-1} + [1-ip(1-p)^{i-1}](1-r)^{M-i} & ; \quad j = i \\ (M-i)r(1-r)^{M-i-1} [1-(1-p)^i] & ; \quad j = i + 1 \\ \binom{M-i}{j-i} r^{j-i}(1-r)^{M-j} & ; \quad j \geq i + 2 \end{cases} \quad (2.1)$$

For $0 < p < 1$, $0 < r \leq 1$, the Markov chain is irreducible, aperiodic, and positive recurrent, with a vector of steady-state (SS) probabilities $u = (u_0, u_1, \dots, u_M)^T$ satisfying the equation $u^T = u^T ST$. However, deriving analytical expression of u from the last equation is difficult to obtain.

Conditioning on $N^t = n$, the channel input rate is given by

$$S_{in}^n = (M - n)r \quad (2.2)$$

And the expected channel throughput S_{out}^n , representing the probability of exactly one packet transmission, is

$$S_{out}^n = (1-p)^{n-1}(1-r)^{M-n-1} [Mr(1-p) + n(p-r)] \quad (2.3)$$

2.2.1 Stability

Using drift analysis [18] or fluid approximation [19], one may illustrate the bistable behavior of ALOHA.

In fact, at equilibrium, the expected channel throughput S_{out}^n is equal to the channel traffic input S_{in}^n . In Fig. 2.1 we plot the expected system drift function defined as $f_n(n) = S_{out}^n - S_{in}^n$, and the backlog steady-state probabilities Vs. backlog state for network of size $M = 50$ and different arrival probabilities r and retransmission probabilities p . We observe that depending on the pair $\{r, p\}$ the system may have one or two stable equilibrium points. In the case of two equilibrium points, the stable point with the highest steady-state probability will drive the system to operate mainly in its region. In (c) the stable point with the highest steady state probability is in the low-delay region while in (d) it is in the high-delay region. The bi-stable behavior of ALOHA can be explained as follows; Depending on the actual system's state, the use of a certain retransmission probability p can resolve efficiently the collisions and thus bring the system into a low backlog state, or may have an opposite effect and increase the actual system load, producing hence higher collision's rate.

Further, optimal retransmission mechanism derived from this analytical model, [22,23], requires information about the network's backlog state, this parameter may be highly variable so it is difficult to track its value.

2.2.2 Optimization

To avoid the need of information on backlog state, we use an equilibrium point analysis to derive the optimal retransmission probability of ALOHA protocol in case of homogenous users. In steady-state, we assume that each user k is in the idle state with probability P_i and in the backoff state with probability P_b . $P_i + P_b = 1$, $k = 1, \dots, M$. The dynamic of each user are illustrated in Fig.2.2.

Each user has a mean traffic load g per slot consisting of new and retransmitted packets given as: $g = rP_i + pP_b$. The total network load is then $G = Mg$. We define p_s as the transmission success probability $p_s = (1 - G/M)^{M-1}$.

The network throughput is defined as the probability of exactly one trans-

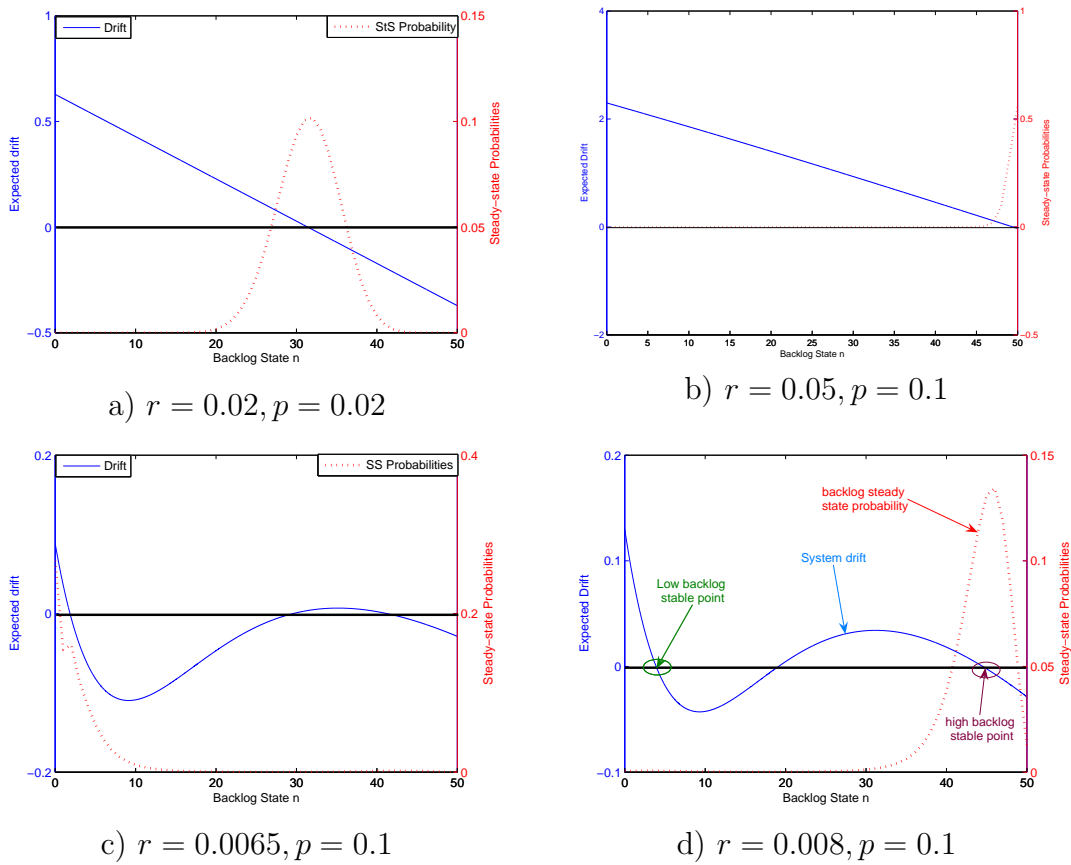


Figure 2.1: Expected drift and steady-state probabilities Vs. backlog state

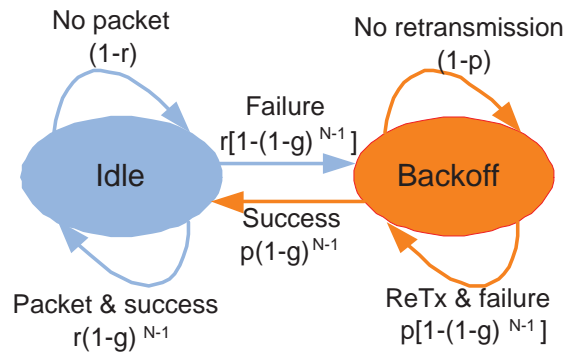


Figure 2.2: Aloha state diagram

mission per slot

$$S_M = G \left(1 - \frac{G}{M}\right)^{M-1} \quad (2.4)$$

And it reaches its maximal value for $G = 1$ ($G^k = \frac{1}{M}, k = 1, \dots, M$).

Successful transmission of a packet may occur at the first attempt at the idle state, or eventually after several retransmission attempts from the backoff state. Conditioned on packet arrival, the mean packet transmission delay is given as (the slot duration is equal to 1)

$$\begin{aligned} E[D] &= p_s + (1 - p_s) \sum_{i=1}^{\infty} (i+1)(1 - pp_s)^{i-1} p_s \\ &= 1 + \frac{1 - \left(1 - \frac{G}{M}\right)^{M-1}}{p \left(1 - \frac{G}{M}\right)^{M-1}} \end{aligned} \quad (2.5)$$

At steady-state, the dynamics of each user satisfies the following global balance equation

$$rP_i \left[1 - \left(1 - \frac{G}{M}\right)^{M-1}\right] = pP_b \left(1 - \frac{G}{M}\right)^{M-1} \quad (2.6)$$

To Find the value of p leading to $G = 1$ we have to solve the following system of equations:

$$\begin{cases} P_i + P_b = 1 \\ rP_i + pP_b = \frac{1}{M} \\ rP_i \left[1 - \left(1 - \frac{G}{M}\right)^{M-1}\right] = pP_b \left(1 - \frac{G}{M}\right)^{M-1} \end{cases} \quad (2.7)$$

Solving eq.2.7 gives the following optimal values of the system parameters P_i , P_b and p

$$P_i^* = \frac{\epsilon}{Mr} \quad (2.8)$$

$$P_b^* = \frac{Mr - \epsilon}{Mr} \quad (2.9)$$

$$p^* = \frac{r(1 - \epsilon)}{Mr - \epsilon} \quad (2.10)$$

$$\text{Where } \epsilon = \left(1 - \frac{1}{M}\right)^{M-1} \quad (2.11)$$

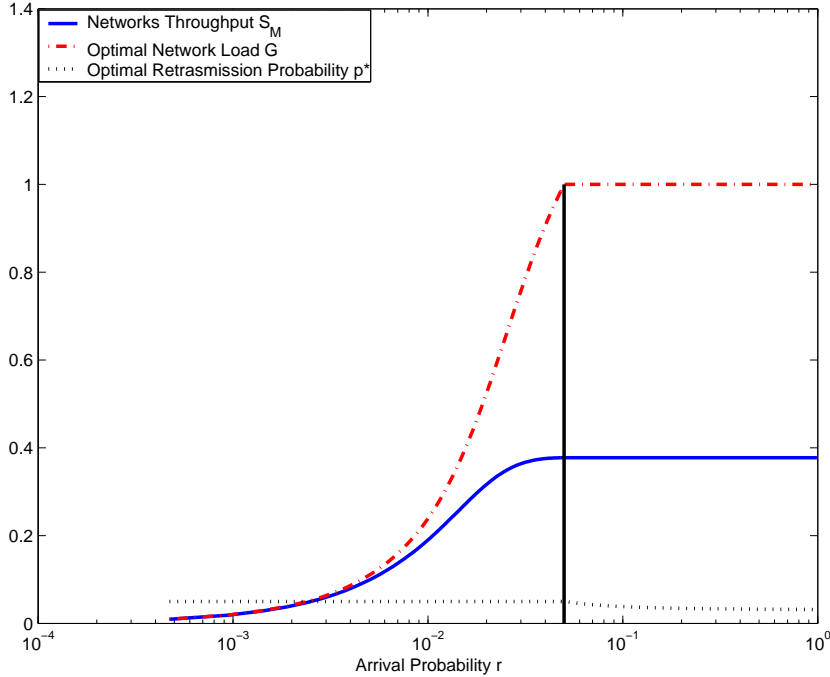


Figure 2.3: Throughput and optimal retransmission probabilities of homogeneous network of size $M = 20$

We observe that the optimization is not blind as it depends on the packet arrival probability r in addition to the network size M . We observe also that the optimization is not always feasible; for $r < \epsilon/M$ the optimal retransmission probability is negative. Moreover, there is also an upper bound on p^* that users must not exceed. We take this maximal value as $1/M$ (This is the worst case where we suppose that there is M collided packets in a slot). Under this choice, p^* is well defined for $r \geq 1/M$ in the sense that $0 < p^* \leq 1/M$.

In Fig. 2.3, we plot the network throughput and the corresponding retransmission probabilities and traffic load G Versus packet arrival probabilities. For $r \leq 1/M$, the achieved throughput and the traffic load G increase with r until achieving ϵ and 1 respectively. Then, for $r \geq 1/M$ the traffic load saturate at its optimal value 1 as well as the throughput at ϵ . The corresponding optimal retransmission probability decreases and quickly saturate at a lower limit $\frac{1-\epsilon}{M-\epsilon}$.

In the following, we prove that under our non-blind optimal retransmission scheme, ALOHA has only one stable equilibrium point.

Theorem 2.2.1 : *Under the following choice of retransmission probabilities $p = \frac{r(1-\epsilon)}{Mr-\epsilon}$ for $r \geq 1/M$, and $p = 1/M$ for $r < 1/M$ ALOHA has one and only one stable equilibrium point.*

Proof : We prove the theorem by showing that the drift function f_n has only one root in $[0 M]$.

At the boundaries of the interval $[0 M]$ we have

$$f_n(0) = Mr [1 - (1-r)^{M-1}] > 0 \quad (2.12)$$

$$f_n(M) = -Mp(1-p)^{M-1} < 0 \quad (2.13)$$

It is then sufficient to show that f_n is strictly decreasing function.

$$\frac{\partial f_n(n)}{\partial n} = -r - (1-r)^{M-n-1}(1-p)^{n-1} \left[p - r + \log \left(\frac{1-p}{1-r} \right) [Mr(1-p) + n(p-r)] \right] \quad (2.14)$$

For $r \geq 1/M$, we have $p = \frac{r(1-\epsilon)}{Mr-\epsilon} < r$. We can also lower-bound p as follows $p > \frac{1-\epsilon}{M-\epsilon}$ ($r = 1$).

We get then

$$\frac{\partial f_n(n)}{\partial n} < -r - (1-r)^{M-n-1}(1-p)^{n-1}[p-r] \quad (2.15)$$

$$< -r + \frac{(1-p)^{M-1}}{1-r}(r-p) \quad (2.16)$$

$$< r - \frac{1 - \frac{1-\epsilon}{M-\epsilon}}{1 - \frac{1}{M}}(r-p) \quad (2.17)$$

$$< r - \frac{Mr(Mr-1)}{(M-\epsilon)(Mr-\epsilon)} \quad (2.18)$$

$$< \frac{Mr^2\epsilon + r\epsilon - Mr}{(M-\epsilon)(Mr-\epsilon)} \quad (2.19)$$

$$< \frac{2Mr^2\epsilon - Mr}{(M-\epsilon)(Mr-\epsilon)} \quad (\text{as } Mr \geq 1) \quad (2.20)$$

$$< \frac{Mr(2r\epsilon - 1)}{(M-\epsilon)(Mr-\epsilon)} \quad (\text{as } \max(\epsilon) = 1/2 \text{ for } M = 2) \quad (2.21)$$

$$< 0 \quad (2.22)$$

Now in case of $r < 1/M$ we have $p = 1/M > r$, and $n < M(1 - \epsilon)$ (taking $r = 1/M$). We get then

$$\begin{aligned} \frac{\partial f_n(n)}{\partial n} &< -r - (1-r)^{M-n-1}(1-p)^{n-1} \left[\frac{1}{M} - r + \log \left(1 - \frac{1}{M} \right) [1 - \epsilon + r(M\epsilon - 1)] \right] \\ &< -(1-r)^{M-n-1}(1-p)^{n-1} \left[\frac{1}{M} + \log \left(1 - \frac{1}{M} \right) [1 - \epsilon + r(M\epsilon - 1)] \right] \end{aligned} \quad (2.23)$$

$$< -(1-r)^{M-n-1}(1-p)^{n-1} \left[\frac{1}{M} + \log \left(1 - \frac{1}{M} \right) \left[1 - \frac{1}{M} \right] \right] \quad (2.24)$$

The function $g(M) = 1/M + \log(1 - 1/M)(1 - 1/M)$ is strictly monotonic decreasing function of M . $g(2) = 1/2(1 - \log(2))$ and $\lim_{M \rightarrow \infty} g(M) = 0$. Thus, $g(M) \geq 0$ for $M \in [2, \infty]$. We conclude then that $\frac{\partial f_n(n)}{\partial n} < 0$. ■

In Fig. 2.4 we plot the expected system drift and the steady-state probabilities for the same network configuration as in section 2.2.1 but under our retransmission scheme. We see then that under all situations, the system has only one stable equilibrium point.

To avoid the need of estimating r , we decide to use the optimal retransmission probability p_{sat}^* obtained for saturated regime regardless of the exact system load. Form Eq. (2.10), p_{sat}^* is given as

$$p_{sat}^* = \frac{1 - \epsilon}{M - \epsilon} \quad (2.25)$$

This choice is motivated as follows:

- For small values of r , the packet collision probability is too small so that the backoff mechanism is almost never used. Thus, using p_{sat}^* , which is the smallest value of p^* for a given network size, has no effect on the system's performance and results on small loss in the throughput compared to the non-blind optimal retransmission scheme.
- For high values of r , the system is almost in saturation condition. So again, the use of p_{sat}^* in this situation has no effect on system's performances.
- For intermediates values of r , the collision probability is not too small, neither so high, so the users will face significant unfairness from the

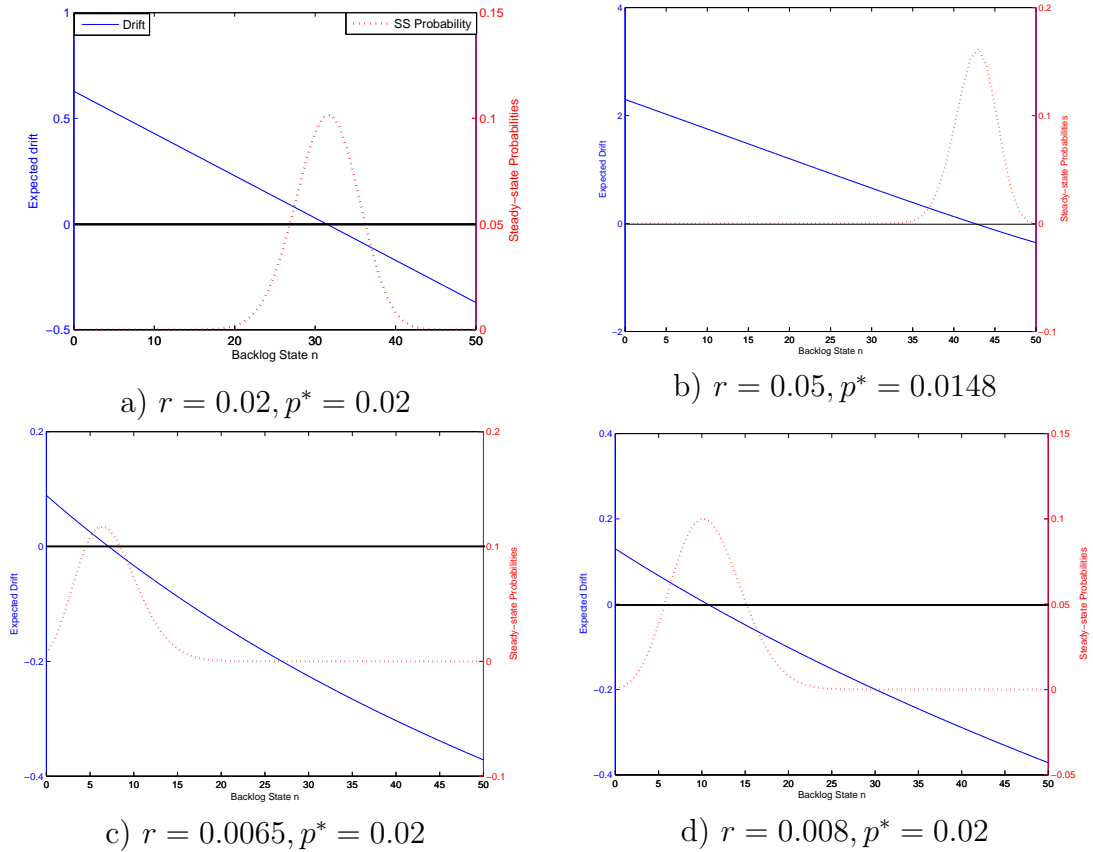


Figure 2.4: Expected drift and steady-state probabilities Vs. backlog state under optimal retransmission probabilities

system: lucky users get immediate access, unlucky ones produce collision and have to enter backoff state.

This behavior is inherent to any random access mechanism, independently from the design of the backoff mechanism. If the retransmission probability is high, the possible collisions will not be handled efficiently. If it is small, the unfairness behavior will be aggravated.

Even with an optimal retransmission mechanism, this undesirable effect may be reduced but not resolved. For this reason, the use of the p_{sat}^* may be tolerable.

In Fig. 2.5, we plot the network throughput against arrival probability under our non-blind and blind retransmission schemes and under different choices

of fixed retransmission probability: $p = 1/M^2$, $p = 0.1$. We observe then that for small values of r , the different schemes perform similarly. Since r is small, the choice of the retransmission probability has no effect as collision probability of new generated packets is small. As r continues to increase, the throughput achieved by the fixed retransmission probability schemes degrade seriously. For $p = 1/M^2$, the retransmission rate is very small which results in high idle slot probability $G \ll 1$. For $p = 0.1$, the retransmission rate is very high which results in high collision probability $G \gg 1$. The choice of p_{sat}^* seems to be very efficient as $p^*(r)$ converges quickly to the saturation value. As predicted, the only significant loss of this scheme is located in the a small intermediate region of r . However, In ALOHA systems, idle slot duration is equal to packet duration. So if we choose to use P_{sat}^* under all traffic loads then the loss in the packet delivery time may be high, especially for long data packet. To see this, we plot in Fig. 2.6 the mean packet delay for the same parameters as for the throughput. Then, we observe that the loss in delay of the blind scheme is relatively high compared to the non-blind one, and it is located on wide range of arrival probability.

2.3 Conclusion

In addressing single-hop ALOHA networks, our ambition was to find simple blind retransmission control schemes. Our motivation for this highly desirable result was that users in single-hop networks have access to the same channel state information. Indeed, our simple retransmission scheme based on setting $p = p_{sat}^*$ (it require just the information about the number of users M in the network) seems to operate near optimality. However, even if the loss in system throughput is small compared to the achievable capacity, the loss in packet delay may be not acceptable. Fortunately, we will see in the next chapter that a similar scheme similar operates optimally for IEEE Decentralized Coordination Function protocol (DCF). It benefices from two features of DCF, carrier sense capability to protect ongoing transmission and asymmetry of idle and collision durations.

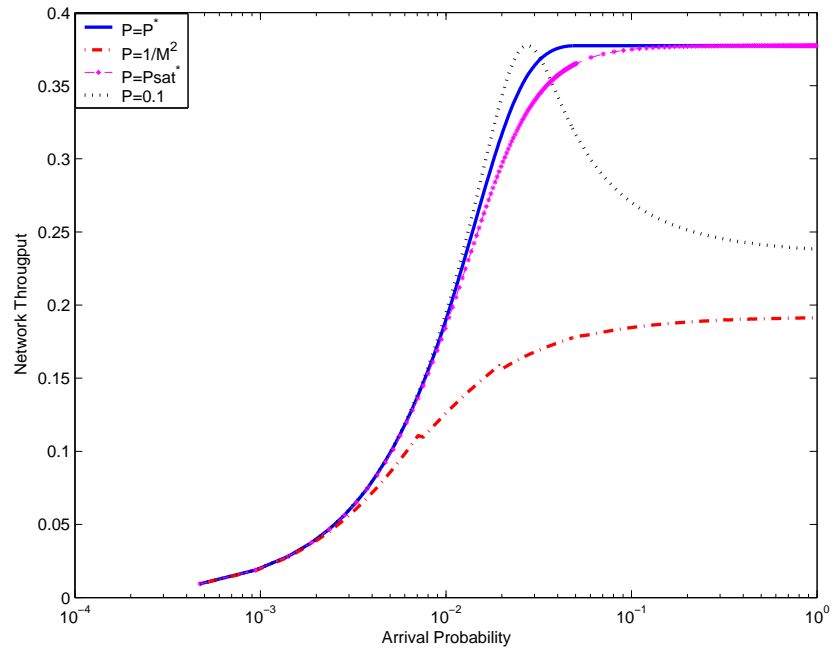


Figure 2.5: Throughput of Homogeneous Network of Size $M=20$ for Various Retransmission Probabilities

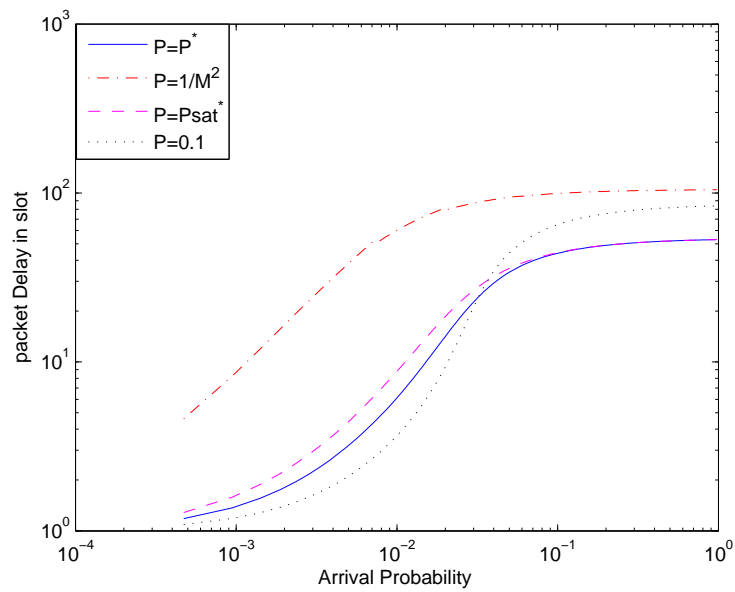


Figure 2.6: Packet delay of Homogeneous Network of Size $M=20$ for Various Retransmission Probabilities

Chapter 3

IEEE 802.11 DCF Protocol: Analysis & Optimization

3.1 Introduction and Related Works

Perhaps the main improvement in the MAC protocol design was the introduction of carrier sense multiple access (CSMA) technique by Kleinrock and Tobagi [30]. The terminology *(carriersense)* does not necessarily imply the use of a carrier, but simply the ability to quickly detect use of the channel. CSMA reduces the level of interference (caused by overlapping packets) in the random multi-access environment by allowing terminals to sense the carrier due to other users' transmissions; based on this channel state information (busy or idle), the terminal takes an action prescribed by the particular CSMA protocol being used (persistent, non-persistent, etc). In particular, a terminal never transmits when it senses that the channel is busy. In single-hop networks where all terminals share the same channel (carrier sense is efficient) CSMA protocols may achieve very good performances if the re-transmission scheme is well designed.

In the popular, and widely used IEEE802.11 standard for WLANs [13], the primary medium access control (MAC) technique is called distributed coordination function (DCF). DCF is a carrier sense multiple access with colli-

sion avoidance (CSMA/CA) scheme and slotted binary exponential backoff (BEB) rules. Since the introduction of the standard, many works have been interested in the analytical evaluation of its performance; most of them were based on the model of Bianchi, [31], and consider saturation throughput and delay analysis ([32–34] to cite few). In real networks, packets may be queued at node’s buffer before being handled by the MAC protocol, and typical data traffics are bursty or streamed at low rates so that stations do not operate usually in saturated regime. Recent works have addressed the finite load performance of IEEE802.11 DCF with queueing at node’s (queues with infinite capacity) [35, 36] or with simplifying assumptions [37].

The analysis of queueing model of MAC protocols is a challenging task, and generally does not permit to obtain closed-form expressions of quantities of interest. In this work, we use a two-stage technique to analyze a queueing model of DCF protocol. In order to acquire closed-form expression of system performance, a Markov chain model is first used to analyze the non-queueing operation of the system. The traffic load in this case is modeled as a probability of having a packet to transmit q , this probability is taken into account whenever the protocol is able to handle a new packet. In this way, q allows us to consider the fact that packet arrivals may occur anytime during the operation of the system. From the non-queueing model, we obtain the service-time statistics corresponding to a given q . In the second phase, we consider a queueing model of the system with a given arrival process $\lambda(t)$ and queue length K . Thus, the probability of having a packet to transmit q corresponds to the probability q_0 of having at least one packet in the queue. In order to link the two models, we use a recursive algorithm that updates the q value used in the Markov model to specify the service time statistics, to match the resulting q_0 from the queueing model.

It is well recognized that the key optimization issue of random access protocols is the design of an optimal retransmission scheme that keeps access rate to the multiple-access channel around its capacity. Obviously, an optimal retransmission scheme must achieve this capacity under all network conditions and must be distributed. The optimality of the scheme depends on how accurate is the information it has about the multiple access channel state.

IEEE802.11 DCF uses a BEB retransmission scheme. The BEB scheme has the advantage of being simple and does not require cooperation among users or any information about the channel state, it tries to blindly adapt the contention window to the channel congestion level based only on its experience, i.e., the contention window is increased in case of collision and it is reset to

its initial value in case of success. Its performances however are shown to be sub-optimal, in term of the achieved throughput as it needs several attempts to find approximately the best contention window, and also in term of short-term fairness as it favors the first successful user to compete again for the channel with small contention window against potentially others users with much higher contention window. Works in [38, 39] have derived specific fairness metric to illustrate this.

The enhancement of the DCF based BEB have been extensively addressed in the literature, the proposed schemes may be categorized into two classes:

1. Fully blind schemes: as in BEB, the change of the contention window's length is made upon collision or success but in a different manner than BEB (MILD [40], FCR [41], EIED [42] to cite few) in order to better reach the optimal backoff window and/or increase short-term fairness.
2. coherent schemes: here the optimization is made in order to dynamically adapt the contention window to meet directly some objective optimization condition. The objective condition is derived from an analytical model and its verification is made by measuring (estimating) some specific performance metrics, [43–46] to cite few. Even if these schemes identify and try to reach an optimal operating point of the system, the way they update the backoff window is not optimal as in the blind schemes.

Early in the work of Bianchi [31], the notion of optimal backoff window that optimizes the saturation network throughput has been introduced. Unfortunately, the calculation of this optimal window requires information about the network size N and the average duration of collisions $E[T_{col}]$. Even if N could be easily obtained in single-hop network, channel activity sensing is required to estimate $E[T_{col}]$ in case of heterogeneous network where users employ different physical rates and/or packet sizes.

As DCF provides equal long-term access rate to different users, several studies have shown that it is unable to fairly and efficiently manage heterogeneous networks [36, 43, 47–50]. As solution, time-based scheduling that guarantee equal channel time access to different users have been shown to increase both the throughput and fairness of the MAC protocol [48].

In order to achieve trivially time-based scheduling with DCF, it is sufficient to normalize the packet duration by normalizing the packet-size/physical-rate ratio, i.e., each physical rate is to be used with a corresponding packet

size in order to get unique packet duration on the channel and hence, a priori, fair input to the system. In this case, we can implement the optimal-window backoff scheme of [31] without estimating $E[T_{col}]$.

3.1.1 Contribution

In this chapter, we consider backoff-window optimization issue of finite load single-hop networks based on the idea in [31]. In order to avoid estimating collision durations, we suppose that packet durations are normalized. Obviously, the optimal backoff-window in this case will depend also on the traffic load. However, we will show that is sufficient to use the saturation's optimal window under all loads to achieve nearly the maximum achievable throughput. Our main contributions are:

- New analytical model to consider finite load performance of DCF without queueing at nodes buffers.
- Proof of the short term unfairness of the binary exponential scheme by using channel capture probability as fairness metric.
- Accurate delay statistics model considering self-loop probability on every backoff state.
- Derivation of the contention window size for the optimal constant-window backoff (OCB) scheme. The optimal window is achieved only for arrival rates greater than a specific threshold (saturation regime), below this threshold the optimal window is simply of length 2. However, we prove in this work that the saturation optimal window is quasi-optimal under all traffic loads.
- Deep analysis of the operations of the BEB and OCB schemes with respect to load variations using numerical results. We show that OCB performs better than BEB, in term of throughput, delay, and fairness, while remaining quasi-insensitive to traffic load.
- Analytical model to consider finite queueing capacity of nodes based on the delay statistics model of the non-queueing model. Using results on M/G/1/K queues, we will use a recursive algorithm to link the delay statistics produced by a given traffic load to a corresponding arrival process (Markovian in our case) and queue length.

The chapter is organized as follows. In section 3.2 we introduce the analytical model, we derive the throughput and the delay statistics, and we show the unfairness of the BEB retransmission scheme. In section 3.3 we introduce the optimal constant window backoff scheme and give bounds on performances loss when using only the saturation window for all arrival probabilities. The performances of the two schemes are then deeply analyzed in section 3.4. The finite capacity queueing model is given in section 3.5, simulation results in section 3.6 and concluding remarks are provided in section 3.7.

3.2 Binary Exponential Backoff Scheme

The analytical model we use is based on the work of Bianchi [31] but extends it to consider general load performance (with backoff freezing and finite retry limit).

We consider a network of n nodes evolving in single hop configuration. The key approximation of the Bianchi's model is to assume that the channel is busy with fixed probability p independently from the backoff counter value (equilibrium point analysis). Each node state is identified by its backoff window counter and backoff stage. The backoff counter and stage are modeled as a bidimensional discrete-time Markov process $(s(t), b(t))$ where $s(t)$ and $b(t)$ denote respectively the backoff stage and the backoff counter at time instant t . If the channel is busy the backoff counter is frozen for the duration of the current transmission. Otherwise, it is decreased when the channel is sensed again idle. Hence, transitions time of the Markov process depend on the current state of the channel. To alleviate this problem, a second approximation is made by defining an average time slot as the unit-time of the Markov chain. This unit-time is an average of the three possible time slot durations that correspond to successful transmission, collision or idle, weighted by their probability of occurrence:

$$T_{avg} = p_{idle}\sigma + p_{suc}T_{suc} + p_{col}T_{col} \quad (3.1)$$

σ is the idle slot duration. For the basic access mode, T_{suc} and T_{col} are given as

$$T_{suc} = 2\delta + H + E[P] + SIFS + Ack + DIFS \quad (3.2)$$

$$T_{col} = \delta + H + E[P] + EIFS \quad (3.3)$$

And for the RTS/CTS access mode

$$T_{suc} = 4\delta + H + E[P] + 3SIFS + RTS + CTS + ACK + DIFS \quad (3.4)$$

$$T_{col} = \delta + RTS + EIFS \quad (3.5)$$

p_{idle} , p_{suc} and p_{col} will be derived in the following.

When the backoff counter reaches 0 the node is allowed to transmit. In case of a collision, the node must double its contention window to reduce collision probability (binary exponential backoff). Otherwise it resets its contention window to its initial value. The scheme defines also a maximum number $m+1$ of retransmission trials after which the packet is dropped, and a maximum window's size order m' .

Let $\pi_{i,j}$ denotes the steady state probability of node to be in backoff stage i with backoff counter at j . $i \in \{0..m\}$, $j \in \{0..W_i - 1\}$ and W_i denotes contention window value at stage i . According to the standard we have:

$$W_i = \begin{cases} 2^i W_0 & \text{for } i \leq m' \\ 2^{m'} W_0 & \text{for } i \geq m' \end{cases} \quad (3.6)$$

where W_0 is the initial value of the contention window.

To avoid channel capture, each node must wait a random backoff time after each successful packet transmission. We add then the new states $(-1, j)$, $j \in \{0..W_0 - 1\}$ to model node's state during inter-packets transmission (Inter-transmission backoff (ITB) states).

In order to consider the non-saturated regime we define q as the probability of having a packet to transmit (all nodes have the same q^1), and to keep the analysis tractable we do not consider for the moment queueing at node's buffer (each node has at maximum one packet per time). In a queueing model, q corresponds to the probability of having at least one packet in the buffer.

Others works have addressed the performance analysis of 802.11 DCF under finite load conditions. In [35, 36], the authors analyzed the finite load performance of 802.11 considering queueing at nodes buffers. The analysis is more complex so they consider queues with infinite capacity. We mention also the work in [37] where the case of users with heterogeneous finite loads and with small buffers is analyzed. Using the assumptions of small buffers, the authors in [37] have modeled the arrival probability as the probability of

¹extension to heterogeneous arrival case is straightforward [37]

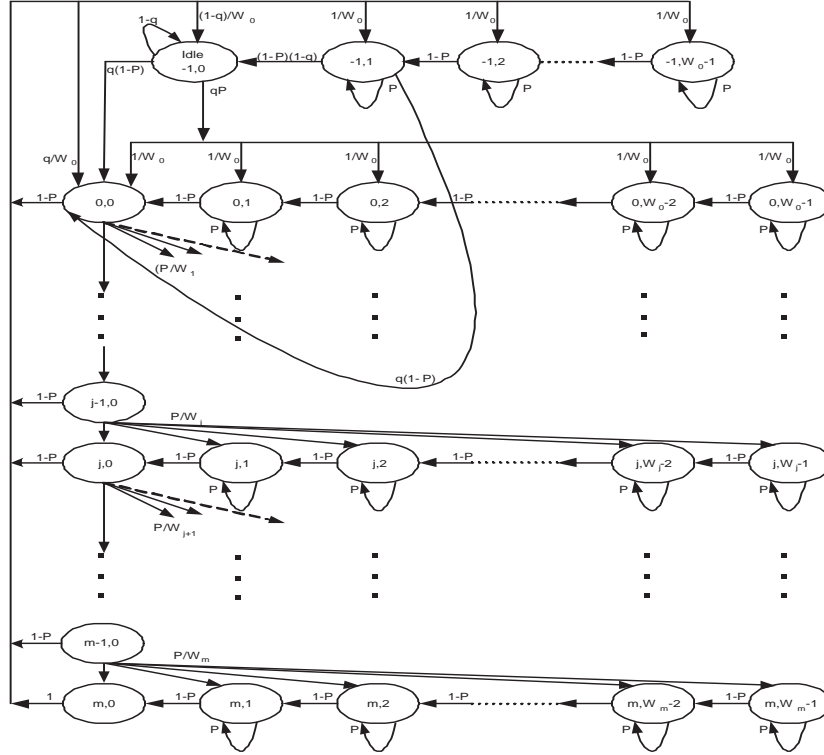


Figure 3.1: Markov chain model

having at least one arrival during the mean system time T_{avg} , which in fact remove the queuing effect as it is true only when the buffer size is equal to 1. Here, we proceed differently, from the no-queueing model parameterized by the packet availability probability q , we derive the delay statistics and then we relate them to the finite capacity queueing model (section 3.5).

Fig. 3.1 illustrates the Markov chain model used for the no-queueing model. After a packet transmission (success or drop), a node may transit to the following states:

- $(0, 0)$: if it chooses 0 as backoff value and it has a packet to transmit

$$p\{(0, 0)|(i, 0)\} = \frac{(1-p)q}{W_0} \quad i \in \{0, m-1\} \quad (3.7)$$

$$p\{(0, 0)|(m, 0)\} = \frac{q}{W_0} \quad (3.8)$$

- $(-1, 0)$: if it chooses 0 as backoff value but has no packet to transmit.

$$p\{(-1, 0)|(i, 0)\} = \frac{(1-p)(1-q)}{W_0} \quad (3.9)$$

$$p\{(-1, 0)|(m, 0)\} = \frac{1-q}{W_0} \quad (3.10)$$

In this case, the node will stay in this state waiting for a new packet to transmit; *Idle* state.

- $(-1, j)$, $j \in \{1..W_0 - 1\}$: if it chooses j as backoff value.

$$p\{(-1, j)|(i, 0)\} = \frac{(1-p)}{W_0} \quad i \in \{0, m-1\} \quad (3.11)$$

$$p\{(-1, j)|(m, 0)\} = \frac{1}{W_0} \quad (3.12)$$

At the end of the ITB (state $(-1, 1)$), the node may transit to the $(0, 0)$ state if it has a packet to transmit. Otherwise, it goes to the *Idle* state.

$$p\{(0, 0)|(-1, 1)\} = (1-p)q \quad (3.13)$$

$$p\{(-1, 0)|(-1, 1)\} = (1-p)(1-q) \quad (3.14)$$

Transitions from the *idle* state occur at new packet arrival. If the medium is sensed idle during DIFS, the node proceeds directly with packet transmission and transits to the state $(0, 0)$. Otherwise, it executes the BEB scheme.

$$p\{(0, 0)|(-1, 0)\} = (1-p)q \quad (3.15)$$

$$p\{(0, j)|(-1, 0)\} = \frac{pq}{W_0} \quad j \in \{0..W_0 - 1\} \quad (3.16)$$

Solving the global balance equations leads to the following steady state probabilities

- for the last $m - 1$ backoff stages:

$$\pi_{i,j} = \frac{(W_i - j)p^i}{W_i(1-p)} \pi_{0,0} \quad j \in \{1, W_i - 1\} \quad (3.17)$$

$$\pi_{i,0} = p^i \pi_{0,0} \quad (3.18)$$

$$\pi_{0,0} \left[\sum_{i=0}^m p^i + \sum_{i=0}^m \sum_{j=1}^{W_i-1} \frac{(W_i-j)p^i}{W_i(1-p)} + \sum_{j=1}^{W_0-1} \frac{(W_0-j)p(1-q)}{W_0(1-p)} + \frac{1-q}{q} \right] = 1 \quad (3.22)$$

$$\pi_{0,0} = \begin{cases} \left[\frac{W_0(1-p)[1-(2p)^{m'+1}] + (1-2p)^2[1-p^{m'+1}] + 2^{m'}W_0(1-2p)[p^{m'+1}-p^{m+1}]}{2(1-p)^2(1-2p)} \right. \\ \quad \left. + (1-q) \left[\frac{p(W_0-1)}{2(1-p)} + \frac{1}{q} \right] \right]^{-1} & m \geq m' \\ \left[\frac{W_0(1-p)[1-(2p)^{m+1}] + (1-2p)^2[1-p^{m+1}]}{2(1-p)^2(1-p)} + (1-q) \left[\frac{p(W_0-1)}{2(1-p)} + \frac{1}{q} \right] \right]^{-1} & m \leq m' \\ \left[\frac{(W_0+1-2p)[1-p^{m+1}]}{2(1-p)^2} + (1-q) \left[\frac{p(W_0-1)}{2(1-p)} + \frac{1}{q} \right] \right]^{-1} & m' = 0 \text{ (constant window)} \end{cases} \quad (3.23)$$

- for the inter-transmission backoff states:

$$\pi_{-1,j} = \frac{(W_0-j)}{W_0(1-p)} \pi_{0,0} \quad j \in \{1, W_0-1\} \quad (3.19)$$

$$\pi_{-1,0} = \frac{1-q}{q} \pi_{0,0} \quad (3.20)$$

- and for the first backoff stage

$$\pi_{0,j} = \frac{(W_0-j)p(1-q)}{W_0(1-p)} \pi_{0,0} \quad j \in \{1, W_0-1\} \quad (3.21)$$

The normalizing equation and the resulting steady state probability of being in state (0,0) are given in Eqs. (3.22,3.23). The probability of transmission in a given slot is then

$$\tau = \sum_{i=0}^m \pi_{i,0} = \frac{1-p^{m+1}}{1-p} \pi_{0,0} \quad (3.24)$$

Then the probabilities of busy, idle, success, and collision are given as

$$p = 1 - (1-\tau)^{n-1} \quad (3.25)$$

$$p_{idle} = (1-\tau)^n \quad (3.26)$$

$$p_{suc} = n\tau(1-\tau)^{n-1} \quad (3.27)$$

$$p_{col} = 1 - p_{idle} - p_{suc} \quad (3.28)$$

and the throughput is defined as

$$Thrp = \frac{p_{suc}L}{T_{avg}} = \frac{p_{suc}L}{p_{idle}\sigma + p_{suc}T_{suc} + p_{col}T_{col}} \quad (3.29)$$

where L is the data packet length.

3.2.1 Delay Statistics

We define packet success delay as the time duration a packet lasts in the system since it is being handled by the MAC layer until the reception of acknowledgement of its successful reception.

A successful transmission may occur at one of the several backoff stages. The *average* time that a packet spends in the first backoff stage before its first transmission depends on whether the packet comes directly from the idle state or from ITB states. Conditioned on being in the first transmission stage $(0, 0)$, this time is

$$\begin{aligned} D_0 &= \left[1 - \frac{q(1-p)\pi_{-1,0}}{\pi_{0,0}} \right] \sum_{j=1}^{W_0-1} \frac{j}{W_0} D_B \\ &= [1 - (1-q)(1-p)] \frac{W_0-1}{2} D_B \end{aligned} \quad (3.30)$$

D_B denotes the average time that nodes spent in every backoff state. Many analysis of 802.11 delay take D_B equal to T_{avg} and ignore the self-loop probability p on every backoff state. In fact, D_B is geometrically distributed with parameter p and variates depending on the states of the $(n-1)$ remaining nodes

$$D_B = \sum_{k=0}^{\infty} p^k (1-p)(kT_B + \sigma) = \frac{pT_B + (1-p)\sigma}{1-p} \quad (3.31)$$

where T_B denotes the average slot duration seen by a node in backoff state when the channel is busy. Conditioned on channel busy probability p , T_B is

$$T_B = \frac{(n-1)\tau(1-\tau)^{n-2}[T_{suc} - T_{col}] + [1 - (1-\tau)^{n-1}]T_{col}}{p} \quad (3.32)$$

Similarly, for the other backoff stages, the *average* time that a packet spends in the stage i before its transmission

$$D_i = D_{i-1} + \frac{W_i-1}{2} D_B + T_{col} \quad i \in \{1 \dots m\} \quad (3.33)$$

D_{i-1} represents the time that the packet spends in the system until it's $(i-1)$ th. transmission, T_{col} the fact that the last transmission was not successful, and $\frac{W_i-1}{2} D_B$ is the average backoff time at the current backoff stage. Conditioned on starting transmission at the state $(0, 0)$, transmission success probability at the i th stage is

$$p_i^{suc} = \frac{\pi_{i,0}(1-p)}{\pi_{0,0}} = p^i(1-p) \quad i \in \{0 \dots m\} \quad (3.34)$$

The delay of a successful transmission can then be seen as a geometric random variable taking values in the set

$$\{D_i^{suc} = D_i + T_{suc}, i = 0 \dots m\}.$$

Alternatively, the *average* delay of packet drop is simply

$$E[D_{drop}] = D_m + T_{col} \quad (3.35)$$

With drop probability (conditioned on starting transmission at $(0, 0)$ state)

$$p_{drop} = p^{m+1} \quad (3.36)$$

Conditioned on effectively starting packet transmission (at state $(0, 0)$) success and drop probabilities sum to 1

$$\sum_{i=0}^m p_i^{suc} + p_{drop} = 1 \quad (3.37)$$

3.2.2 Short-Term Fairness

The use of exponential backoff retransmission scheme in 802.11 DCF leads to short-term unfairness. This is mainly because the scheme favors the first successful user to transmit again.

There exist several metrics to measure the fairness of a MAC protocol, the most popular is the one proposed by Jain et al. [51], but it can not be used for analytical purposes.

Many studies have then tried to characterize the short-term fairness issue by deriving specific fairness metrics [38], [39]. In [39], the authors define as metric the distribution of the number of inter-transmissions that other hosts may perform between two transmissions of a given host. They derive this metric for IEEE802.11 by considering the analytically tractable case of two nodes in saturation conditions and found that the distribution of the number of inter-transmission K is independent of the contention window size. This means that changing the window size has no impact on fairness, so they conclude that unfairness of 802.11 DCF is not related to the use of the exponential backoff scheme.

In [39], the derivation of the distribution of K was possible by approximating the discrete uniform distribution by a continuous one. In doing so, the authors neglect the collision probability and so the analysis did not take into

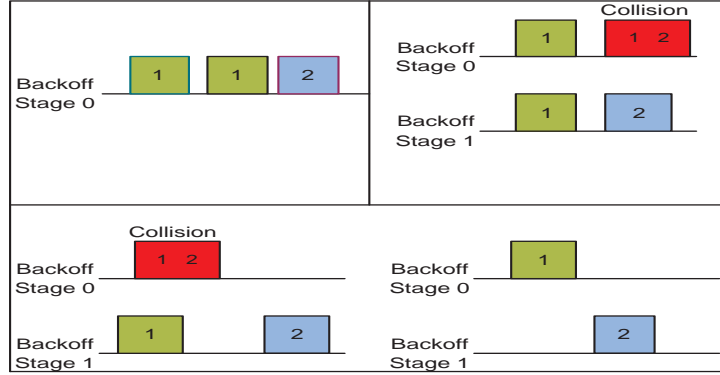


Figure 3.2: Channel capture by node 1

account the exponential backoff scheme.

To prevent analytical difficulties faced when deriving the distribution of K , we use as metric the channel capture probability, i.e., the probability that a node sends successfully and consecutively 2 packets. As this probability is smaller the scheme is fairer (for TDMA this probability is 0 as nodes use the channel alternatively). We derive this probability also only for the case of two nodes in saturation and we consider only two backoff stages. The goal is just to have an idea on the way the protocol performs in this simple scenario. Consider two nodes 1 and 2, and let $w_{i,j}^k$ denote the k .th backoff window value chosen by node i when it enters backoff stage j . We denote the backoff window size at stage i by W_i and we suppose that the two nodes start simultaneously at stage 0.

The channel may be captured by node 1 only in the three following transmission cases: ‘11’, ‘1C1’ or C11 (Fig. 3.2). C denotes collision.

The event 11 represents a situation where node 1 chooses consecutively two backoff values $w_{1,0}^1$ and $w_{1,0}^2$ such that the backoff value $w_{2,0}^1$ chosen by node 2 is greater than $w_{1,0}^1 + w_{1,0}^2$. The probability of this event is

$$\begin{aligned}
 p(11) &= p(w_{1,0}^1 < w_{2,0}^1 \text{ \& } w_{1,0}^2 < w_{2,0}^1 - w_{1,0}^1) \\
 &= \sum_{i=0}^{W_0-1} \sum_{j=i+1}^{W_0-1} \sum_{k=0}^{j-i-1} \frac{1}{W_0^3} = \frac{W_0^2 - 1}{6W_0^2}
 \end{aligned} \tag{3.38}$$

We can see that this probability increases with increasing W_0 and it’s independent of the choice of W_1 .

The event 1C1 represents a situation where the backoff values chosen by node

1 at the first backoff stage, and then after a collision at the second backoff stage, are smaller than those of node 2. The probability of this event is

$$\begin{aligned}
p(1C1) &= p(w_{10}^1 < w_{20}^1 \& w_{20}^1 = w_{10}^1 + w_{10}^2 \& w_{11}^1 < w_{21}^1) \\
&= \left[\frac{1}{W_0} \sum_{i=0}^{W_0-1} \sum_{j=i+1}^{W_0-1} \frac{1}{W_0^2} \right] \left[\sum_{i=0}^{W_1-1} \sum_{j=i+1}^{W_1-1} \frac{1}{W_1^2} \right] \\
&= \frac{(W_0 - 1)(W_1 - 1)}{4W_0^2W_1} \tag{3.39}
\end{aligned}$$

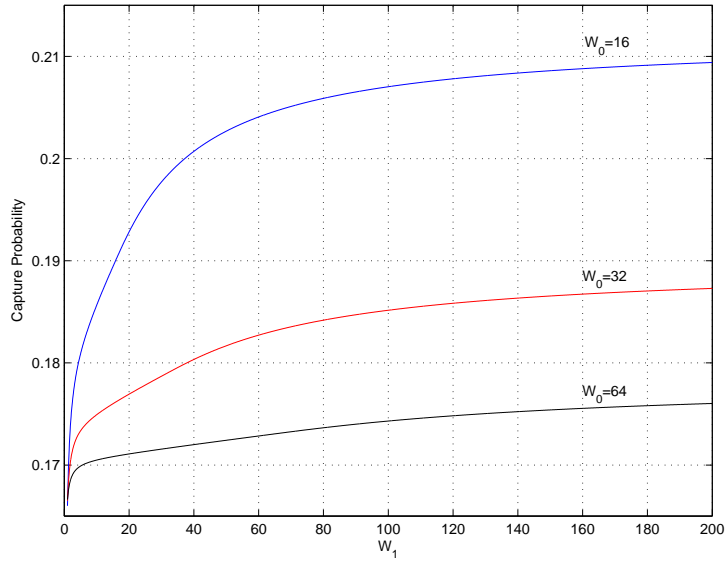
We observe that this probability decreases with increasing W_0 (collision probability is decreased) and increases with increasing W_1 .

The third event represents a situation where after a collision, node 1 succeeds to transmit first its packet, then it goes-back to the first backoff stage and transmit again before node 2. The probability of the third event is

$$\begin{aligned}
p(C11) &= p(w_{10}^1 = w_{20}^1 \& w_{11}^1 < w_{21}^1 \& w_{20}^2 < w_{21}^1 - w_{11}^1) \\
&= \left[\frac{1}{W_0} \sum_{i=0}^{W_1-1} \sum_{j=i+1}^{W_1-1} \sum_{k=0}^{j-i-1} \frac{1}{W_0W_1^2} \right] \\
&= \begin{cases} \frac{W_1^2-1}{6W_0^2W_1} & W_1 \leq W_0 \\ \frac{3W_1^2+W_0^2-3W_0W_1-1}{6W_0W_1^2} & W_1 > W_0 \end{cases} \tag{3.40}
\end{aligned}$$

We observe again that this probability increases with increasing W_1 . In fact, after a collision the first successful node has a smaller contention window than the other node so it has more chance to retransmit again.

The channel capture probability is the sum of probabilities of the last three events. As we have seen, the channel capture probability increases with increasing W_1 (Fig. 3.3) which means that binary exponential backoff scheme is less fair than constant backoff scheme ($W_1 = W_0$). We observe also that BEB is fairer for increasing size of the initial backoff window. The result is for the case of two nodes but give a general idea on the behavior of the protocol. Intuitively, if the network size increases, the collision probability increases, and so, the probability that nodes will alternate transmissions after collision decreases as they have different windows. The same argument can be used to prove the same behavior for increasing number of backoff stages. We are then facing a capacity-fairness tradeoff; after a collision, if the contention window is increased, the system becomes unfair, but in the same time the

Figure 3.3: Channel capture probability Vs. W₁

collision probability is decreased.

Historically, the BEB scheme was introduced to blindly adapt the contention window to the traffic load in order to reduce collisions. Recently, it was shown in [52] that the BEB achieves a success probability of $\ln 2/2$ which is lower than the capacity of a constant backoff scheme (e^{-1} for slotted Aloha with uniform retransmission). It is then legitimate to think about a constant backoff scheme that blindly adapt or that is insensitive to traffic load.

3.3 Optimal Constant-Window Backoff Scheme

Motivated by the results on short-term unfairness of BEB, we analyze in depth the case of constant backoff window. In this case, the backoff window must be optimized to maximize the throughput and must be fixed to not decrease fairness.

The optimal backoff window can be seen as the transmission probability τ_{op} , below which the channel utilization is reduced due to high probability of idle slots and above which reduction of throughput is due to high collision probability. The goal of the optimization is then to adapt the backoff window

to achieve this τ_{op} . Obviously, under general load conditions, the backoff window must be optimized with respect to traffic intensity (q). However, it is also obvious that the $\{\tau_{op}\}$ will not be achieved for small arrival rate ($q \leq q_t$, q_t is a threshold on arrival rate) even with the minimal backoff window ($W_0 = 1$). For this reason, we propose in this work to use the optimal backoff window of the saturated regime W_{op}^s for all arrival rates. The intuition behind this choice is that below q_t the system is lightly loaded so that the probability of going into backoff is very small and thus the effect of using a large W is minimal. Above q_t , the loss incurred by using a backoff window $W_0 = W_{op}^s \geq W_{op}$ is due to the fact that idle slot probability is higher than the optimal one, but in this case, the packet collision probability is lower than the optimal one, since in CSMA system the idle slot duration is small compared to the collision duration, the loss in the achieved throughput is small. In the following, we derive first the optimal transmission probability τ_{op} and the arrival rate threshold q_t . Once q_t identified, we show that for arrival rates below q_t almost all transmissions succeed without involving the backoff scheme, and for $q \geq q_t$ we give an upper bound on the throughput loss.

3.3.1 Derivation of τ_{op} and W_{op}^s

When we differentiate the *Thrp* with respect to τ , we find that is maximal for transmission probability τ_{op} verifying²

$$\tau_{op} = \frac{\alpha - (1 - \tau_{op})^n}{\alpha n} \quad \text{where} \quad \alpha = \frac{T_{col}}{T_{col} - \sigma} \quad (3.41)$$

From Eq.(3.23) we have for the constant backoff case ($m' = 0$) in saturation conditions ($q = 1$)

$$\tau = \frac{2(1 - p)}{(W_0 + 1 - 2p)} = \frac{2(1 - \tau)^{n-1}}{[W_0 - 1 + 2(1 - \tau)^{n-1}]} \quad (3.42)$$

The saturation optimal fixed backoff window is then

$$W_{op}^s = 1 + \frac{2(1 - \tau_{op})^n}{\tau_{op}} \quad (3.43)$$

²The existence and uniqueness of τ_{op} can be simply verified [31]

3.3.2 Derivation of q_t

We look now under which condition on q the τ_{op} could not be achieved even with the minimal allowed value of the backoff window $W_0 = 1$ (no backoff³). From Eq. 3.23 we have for $W_0 = 1$

$$\tau = \frac{q(1-p)}{qp+1-p} \quad (3.44)$$

With a little algebra we find that the situation of $\tau \leq \tau_{op}$ is possible for

$$q \leq q_t = \frac{\tau_{op}(1-p_{op})}{1-p_{op}-\tau_{op}p_{op}} \quad (3.45)$$

$$\text{Where } p_{op} = 1 - (1 - \tau_{op})^{n-1} \quad (3.46)$$

In Fig 3.4, we plot the Optimal transmission probabilities and the corresponding optimal backoff windows Vs arrival rates. We can see that for arrival probabilities $q \leq q_t$ the achieved transmission rates are below the optimal ones even with backoff window equal to 1. We say then that the system is in lightly loaded regime. Above q_t , τ_{op} is achieved by increasing the backoff window's size. We observe also that the optimal backoff window increases, in a first phase, exponentially and then, in a second phase, slowly converges to the saturation optimal window. During the first phase of increase we say that the system is in transition regime while during the second phase it is in saturation regime.

In the following, we give bounds on throughput loss when using the saturation optimal window under all load rather than the exact optimal window that take into account the value of traffic load.

3.3.3 Loss in System Performances

Case of $q \leq q_t$

As we have said before, in this case the system is lightly loaded and almost all transmissions are successful without backoff. To see this we can express the transmission success probability outside the backoff state as

$$P_{suc}^{NB} = n\pi_{-1,0}q(1-p)^2 = n(1-q)(1-p)^2\pi_{0,0} \quad (3.47)$$

³We take $W_0 = 1$ only for analytical purpose, in real system the lowest value of W_0 we may take is 2

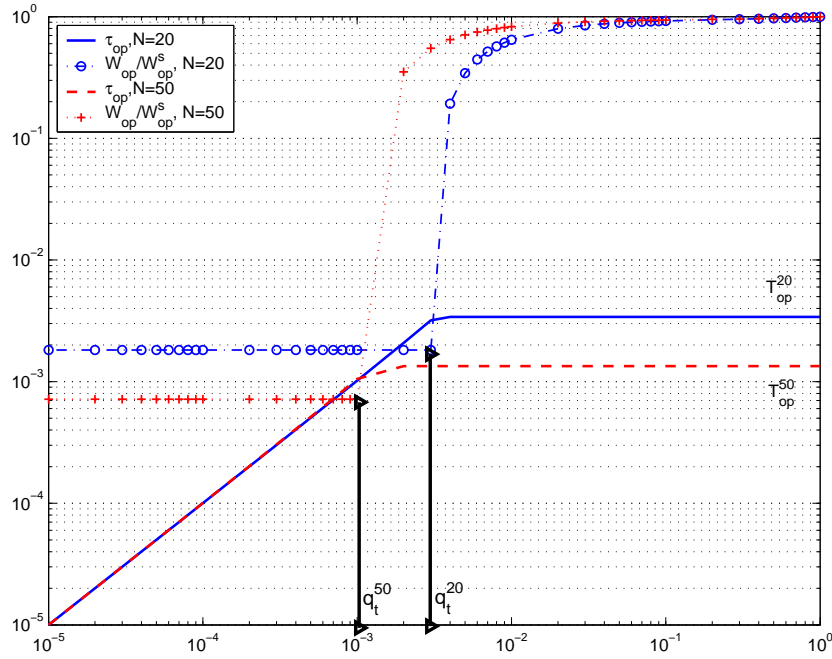


Figure 3.4: Optimal transmission probabilities and the corresponding optimal backoff windows (normalized to the saturation optimal window) vs. arrival rates

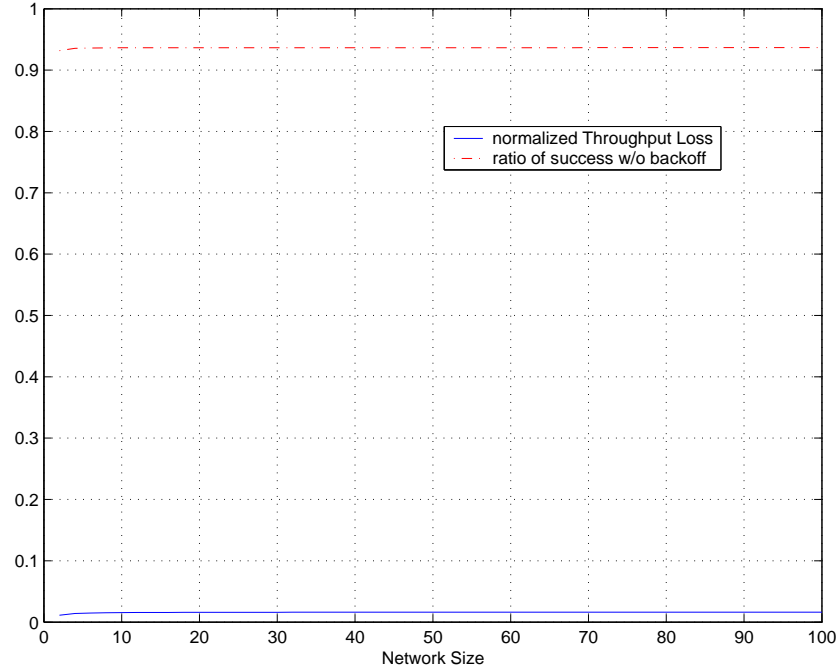


Figure 3.5: Bounds on system performances

While total transmission success probability is given as

$$p_{suc} = n\tau(1-p) = n(1-p^{m+1})\pi_{0,0} \quad (3.48)$$

As $q \leq q_t$, we have $\tau \leq \tau_t$, where τ_t is the transmission probability corresponding to q_t . Thus, we can lower bound the ratio of p_{suc}^{NB} over p_{suc} as follow

$$\frac{P_{suc}^{NB}}{p_{suc}} \geq (1-q_t)(1-p_t)^2 \quad (3.49)$$

$$\text{Where } p_t = 1 - (1 - \tau_t)^{n-1} \quad (3.50)$$

In Fig. 3.5 we plot this lower bound Vs. network size and we can see that about 94% of transmissions success occurs without backoff. We conclude then that the use of the saturation optimal window in this case has almost no effect on system performances.

δ	σ	<i>SIFS</i>	<i>DIFS</i>	<i>EIFS</i>	<i>H</i>	$E[P]$	<i>RTS/CTS</i>	<i>ACK</i>
$1\mu s$	$20\mu s$	$10\mu s$	$50\mu s$	$364\mu s$	416	8184	352	304

Table 3.1: Parameter set used for numerical results

Case of $q \geq q_t$

In this case the τ_{op} is achieved if the backoff window is optimally adapted to the arrival rate. The maximum system throughput is then achieved. Using Eq. 3.41 we can express this maximum throughput as follow

$$Thrp_{max} = \frac{(1 - p_{op})E(P)}{(1 - p_{op})T_{suc} + p_{op}T_{col}} \quad (3.51)$$

From this last expression of the maximal throughput we can deduce that the optimal operation of the protocol is similar to having only one node in saturation condition who succeed its transmissions with probability $1 - p_{op}$ and fails with probability p_{op} .

Now, we want to measure the loss in the achieved throughput if we do not use the optimal window to achieve τ_{op} but only the saturation optimal window. As $q \geq q_t$, we have $\tau \geq \tau_q$, we can thus upper bound the normalized throughput loss as follow

$$\frac{Thrp_{max} - Thrp}{Thrp_{max}} \leq \frac{Thrp_{max} - Thrp_t}{Thrp_{max}}$$

In Fig. 3.5 we plot this bound Vs. networks size and we find that the loss does not exceed 1.6%.

3.4 Numerical Results

In this section, we compare the performance of the IEEE802.11 DCF based BEB with the proposed optimal constant backoff (OCB) scheme. Table 3.1 summarizes the parameters used for our numerical results.

3.4.1 Throughput

Fig. 3.6 shows the achieved throughput Vs. packet arrival probability for network of size $n = 50$. The optimal window for OCB scheme in this case

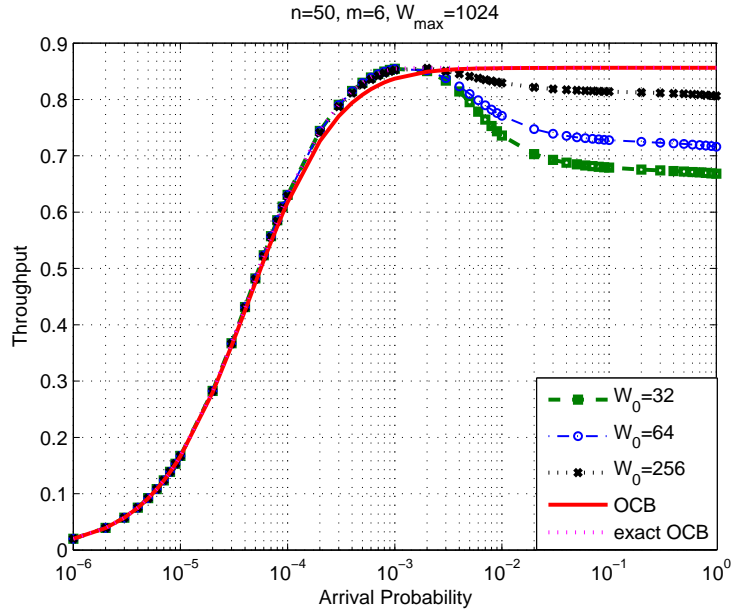


Figure 3.6: Throughput

is 1392 slots. We consider multiple BEB cases with different initial backoff window $W_0 = 16, 64, 256$. We see then that during the lightly loaded regime ($q \leq 10^{-3.5}$ in this case), both OCB and BEB (independently from W_0) perform similarly and increase their channel utilization with increasing q . During the transition regime ($10^{-3.5} \leq q \leq 10^{-2.8}$), we observe that the BEB throughput is slightly higher than the OCB one. Finally in the saturation regime ($q \geq 10^{-3.5}$), and depending on W_0 , the throughput achieved by BEB scheme decreases and then saturates, while the OCB throughput saturates at a higher value.

To understand the operation of the two schemes, we plot in Fig. (3.7,3.8) the repartition of success probability (is the successful transmissions occur from *idle* state or from backoff states?), the collision probability and the idle probability Vs. packet arrival probability q . We consider the case of $W_0 = 64$ for BEB. For both schemes we observe that during the 1st phase, success and collision probabilities increase with increasing load while idle probability remains almost equal to 1 which means that the system is lightly loaded. As result, all success is almost from the *idle* state which means that almost all packets are transmitted directly at their arrivals without any backoff delay.

In the 2nd phase, for the BEB scheme, the collision probability continues to increase with load while idle probability starts to decrease seriously. BEB begins then to have significant transmission success from the backoff state while success from the *idle* state saturates. At the end of this phase, the two success probabilities are equal. The same phenomena is observed for OCB, except the idle probability that decreases also but remains close to 1, and a less significant success from backoff states which means that almost all success is still produced at *idle* state.

To explain this and how the difference in success probability repartition produces the small difference in the channel utilization, we can say that during this transition phase, the probability of busy slot at packet arrival increases for the two schemes. They start then to execute occasionally their backoff procedures. As the BEB scheme begins with a relatively small value of W_0 , its busy slot probability is bigger than for OCB (the users are not delayed for a long time), so it enters more frequently into backoff states, but as the system is still lightly loaded, it succeeds its transmission without excessive backoff delay (the panel of backoff windows (from W_0 to W_{max}) is sufficient to statistically multiplex efficiently all access demands). The OCB scheme operates differently; as its backoff window is bigger (1392), its busy slot probability is smaller than for BEB (high idle probability), so it enters less frequently the backoff state. But in the same time, as the system is lightly loaded, even if the system delays far enough the unlucky users who find the system busy at their packet arrival, the channel is not used frequently during this time which explains the small loss in channel utilization.

During the 3rd phase, the total success probability of the two schemes saturate as well as the idle and collision probabilities (and so the throughput). For the BEB, success from backoff states continues to increase with load becoming the only significant source of transmission success. While for the OCB scheme, success from backoff states becomes significant only at values of q approaching 1. The degradation of throughput of BEB can be seen as a failure of the scheme to adapt its window to access demands (high collision probability). The OCB scheme is more efficient during this phase, as its backoff window is tailored for a saturated regime. Even if it continues to delay unlucky user for a longer time than BEB, the channel utilization get higher as the load increases.

Another important observation is that even if BEB achieves higher success probability than OCB, the resultant throughput is lower! This gives us a more precise idea on the philosophy of the scheme; In fact, OCB fixes the

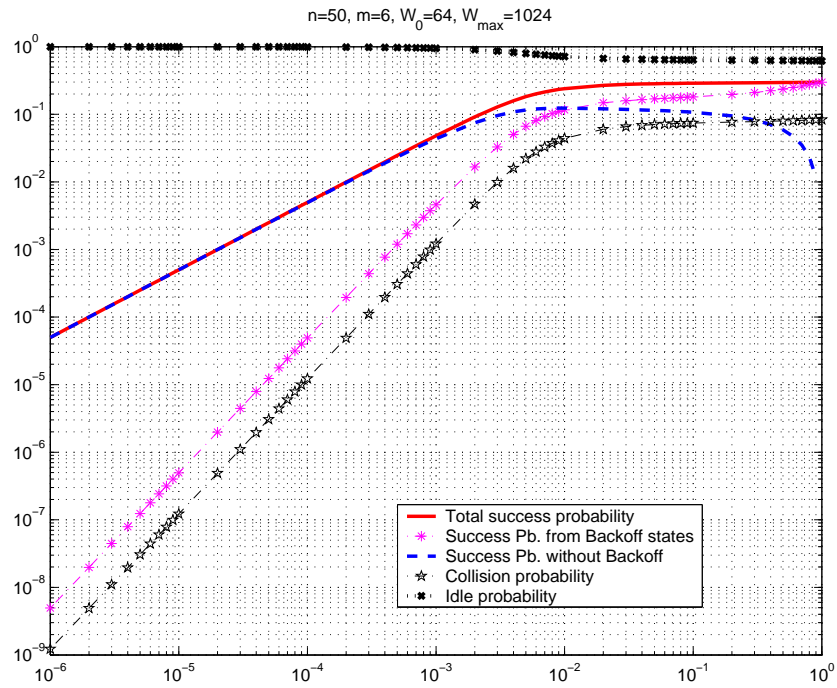


Figure 3.7: Repartition of Success probability of the BEB Scheme

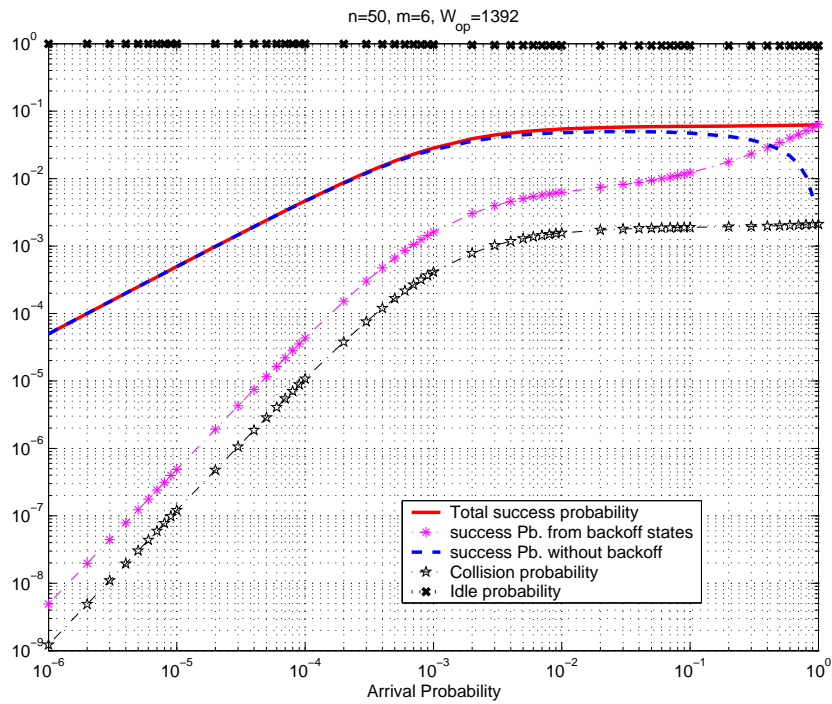


Figure 3.8: Repartition of Success probability of the OCB Scheme

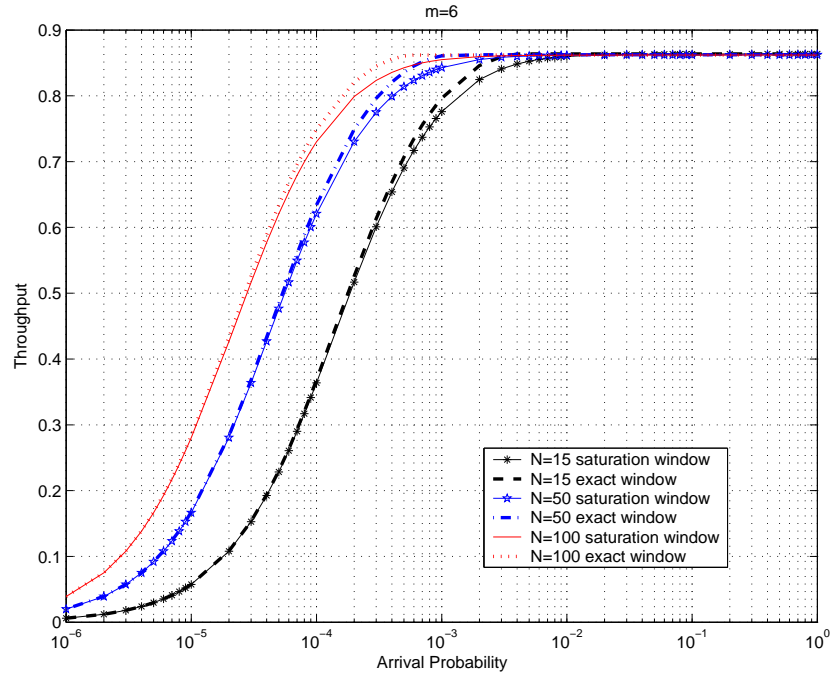


Figure 3.9: Throughput for Optimal Exact Window and Optimal Saturation Window

optimal window in order to keep transmission probability in an optimal level. At this optimal level loss due to idle slots is equal to loss due to collision. Below this optimal level, idle slot probability increases while success and collision probabilities decrease. Above the optimal transmission level, success increases but also collisions. In carrier sense multiple access scheme, idle slot duration is shorter than collision, the scheme tries then to equalize the duration of idle and collision events which explains the large value for the contention window and so the smaller success probability.

OCB seems then to operate at optimal level regardless of traffic intensity except during the transition phase. In Fig. 3.9, we compare the throughput achieved by OCB to the one achieved by exactly optimizing the backoff window to the traffic load q . As predicted by the bound we observe that the loss of OCB is small for all network size considered, and is located on a small interval that corresponds to the transition phase.

To illustrate better the superiority of OCB over BEB, we plot in fig. 3.10 the achieved throughput of the two schemes in saturation vs. network size.

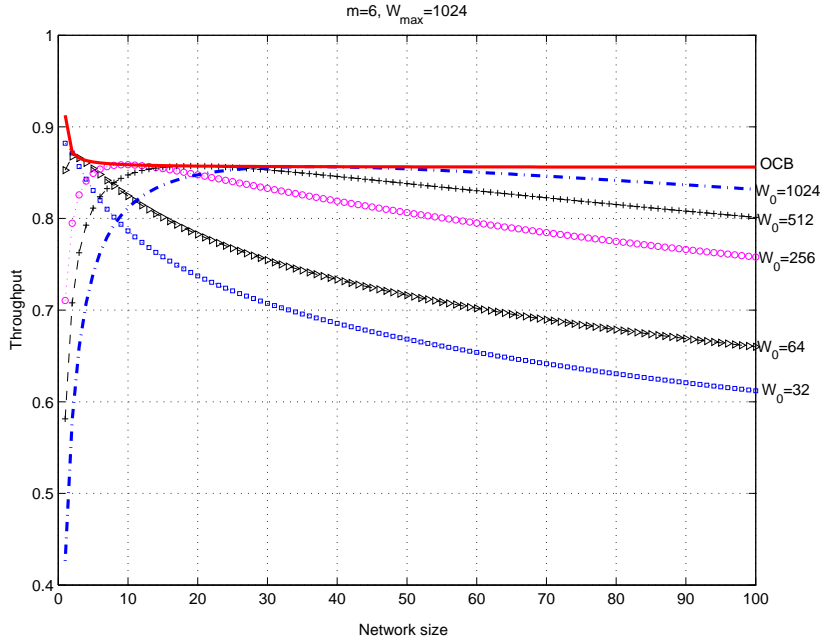


Figure 3.10: Throughput Vs. Network size

We observe that OCB performs better than BEB at all network size. We observe also that BEB operates differently depending on its initial backoff window value. We can see that every value of W_0 has only a limited interval of network sizes where it performs optimally which shows the inability of BEB to adapt efficiently the backoff window to the access demands.

3.4.2 Delay & Fairness

Fig. 3.11 depicts the normalized achieved delay (to packet transmission time T_{suc}) Vs. packet arrival probability. We observe a logical behavior with respect to the throughput, i.e., no excess delay in the non-backoff regime, delay of OCB slightly greater than BEB in the transition regime and lower in saturation regime. Moreover, we can see that OCB packet's mean delay at saturation approximates $50 * T_{suc}$, which is the delay of a pure TDMA scheme with 50 users in saturation.

To illustrate the BEB unfairness, we use the Jain's fairness index relative to the delay. The Jain's fairness can be related to the delay statistics as follow

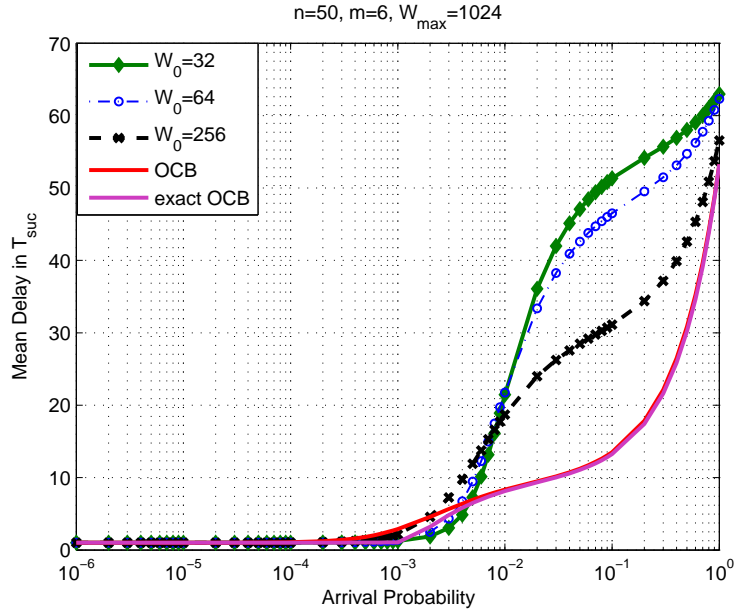


Figure 3.11: Normalized delay

$$Jain's\ index = \frac{1}{1 + \frac{var(D)}{E[D]^2}} \quad (3.52)$$

Fig. 3.12 pictures the Jain index for the same setting as previously. We can see that OCB is less fair than BEB during the transition phase but much more fair in saturation regime. We observe also that during the transition phase, the system can not guarantee equal service time even with the exact window OCB scheme. As the system is not really loaded, neither unloaded, packets got service depending on the system's state at their arrival time: lucky users got immediate service while others are delayed. During the saturation regime, OCB becomes fairer as all packet get access from backoff states while BEB remain unfair due to its intrinsic unfairness.

3.5 Buffered Terminals Model

In real networks, packets may be queued at node's buffer before being handled by the MAC protocol. It's then necessary to include the queuing delay in the characterization of the system performance. In section 3.2.1, we have

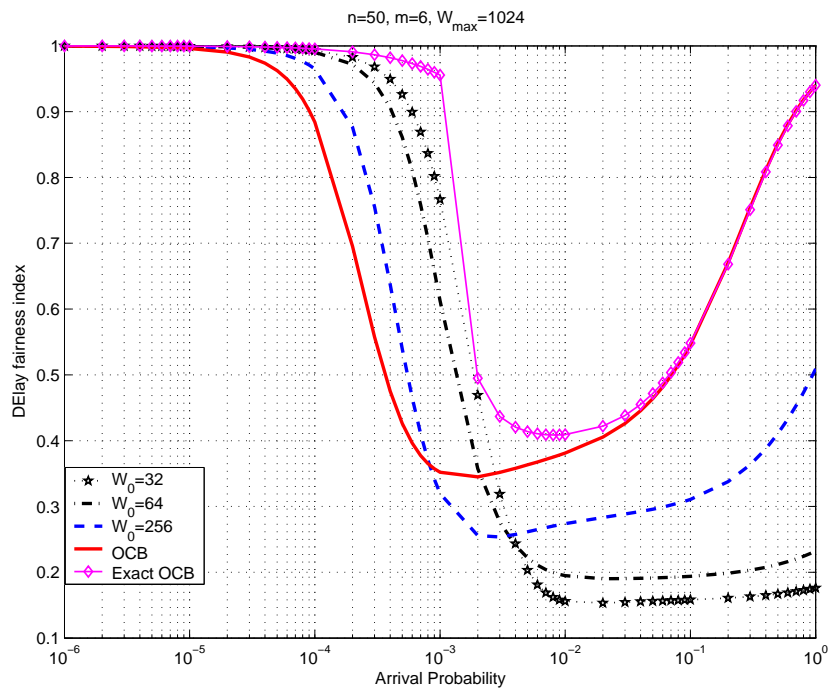


Figure 3.12: Jain fairness Index

derived the delay statistics of the protocol for a given packet availability q . We consider now each terminal with a queue of size $(K-1)$ packets, the probability q corresponds then to the probability that the queue is not empty. We assume that packet arrivals at each terminal is Poissonian process with mean λ , hence each node buffer can be modeled as a finite capacity single server queue $M/G/1/K$. The number of packet in the system at the embedded points corresponding to the time instants just after a job completion (successful transmission or drop) forms a Markov chain. We define the packet service time as the packet success delay in case of successful transmission or the packet drop delay in the contrary case. The average packet service time at the MAC layer is then

$$\mu = \sum_{i=0}^m D_i^{suc} p_i^{suc} + D_{drop} p_{drop} \quad (3.53)$$

Let (π_k^d, π_k) denote respectively the steady state probability of having k packets in the queueing system at departure instants, and at arbitrary instants. $k \in \{0 \dots K-1\}$. And let $Q_{i,j}^d$ denotes the system transition probabilities upon departure, we have then [53]

$$Q_{0,k}^d = \begin{cases} \alpha_k & 0 \leq k \leq K-2 \\ 1 - \sum_{i=0}^{K-2} \alpha_i & k = K-1 \end{cases} \quad j = 0 \quad (3.54)$$

$$Q_{j,k}^d = \begin{cases} \alpha_{k-j+1} & j-1 \leq k \leq K-2 \\ 1 - \sum_{i=0}^{K-j-1} \alpha_i & k = K-1 \end{cases} \quad 1 \leq j \leq K-1 \quad (3.55)$$

Where α_k represents the probability of having k arrivals during a service time

$$\alpha_k = \sum_{i=-1}^m \frac{(\lambda D_i^{suc})^k}{k!} e^{-\lambda D_i^{suc}} p_i^{suc} + \frac{(\lambda D^{drop})^k}{k!} e^{-\lambda D^{drop}} p_{drop} \quad (3.56)$$

The global balance equations and the normalization condition are given as follow

$$\pi_k^d = \sum_{j=0}^{K-1} \pi_k^d Q_{j,k}^d, \quad 1 = \sum_{k=0}^{K-1} \pi_k^d \quad (3.57)$$

Therefore, the steady state probabilities at arbitrary instants are given by

$$\pi_k = \frac{1}{\pi_0^d + \rho} \pi_k^d, \quad k \in \{0 \dots K - 1\} \quad (3.58)$$

where $\rho = \lambda\mu$ is the queue load.

The probability of having at least one packet in the queue is then

$$q = 1 - \pi_0 \quad (3.59)$$

And the blocking probability is

$$\pi_K = 1 - \frac{1}{\pi_0^d + \rho} \quad (3.60)$$

To specify the service time distribution using results of section 3.2.1 we need to identify the packet availability probability q . In the same time, to specify the packet arrival probability from the queueing analysis we need to identify the service time distribution!

To resolve this problem, given an input rate λ and a queue length $K - 1$, we use a recursive algorithm to estimate the corresponding arrival probability q . Starting with an initial guess q_{in} on the arrival probability, we derive the service time distribution, then we use the queueing analysis to identify the produced arrival probability q_{out} (Eq. 3.59). If the difference between the input probability q_{in} and the output probability q_{out} is greater than a threshold, q_{in} is replaced with q_{out} and the operation is repeated. Otherwise the search is stopped.

Convergence is ensured since the case of $q_{out} > q_{in}$ (respectively $q_{out} < q_{in}$) means that even with a lower estimate of arrival probability q_{in} , and so a lower estimate of the service time, the system is more loaded which indicates that the search must continue on the direction of q_{out} (respectively, even with an upper estimate of the service time the system is less loaded so the search must also continue in the direction of q_{out}).

The average queue length can then be expressed as

$$N = \sum_{k=0}^{K-1} k\pi_k \quad (3.61)$$

The mean packet service time (including MAC delay) by

$$W = \frac{N(\rho + \pi_0^d)}{\lambda} \quad (3.62)$$

And the end-to-end throughput as

$$Thrp_e = n\lambda(1 - \pi_K)(1 - p_{drop}) \quad (3.63)$$

3.6 Simulation results

In this section we validate our analytical results with NS2 (Network Simulator) simulations. We use the same parameters as previously, the queue length is taken equal to 50 and we consider now the RTS/CTS access mode. The optimal constant window in this case is 363 slots. In Fig. 3.13, we plot the achieved throughput under BEB and OCB schemes vs. data arrival rate. First, we observe that results from analytical model are almost equal to that from simulations which validates, not only our queueing model, but also our non-queueing models and our delay statistics model. Second, we can see that BEB performances are close to that of OCB which means that even if BEB collision probability is higher than that of OCB, the penalty in throughput is very small since collision duration is reduced by the use of RTS/CTS handshaking. Fig. 3.14 depicts the corresponding mean packet

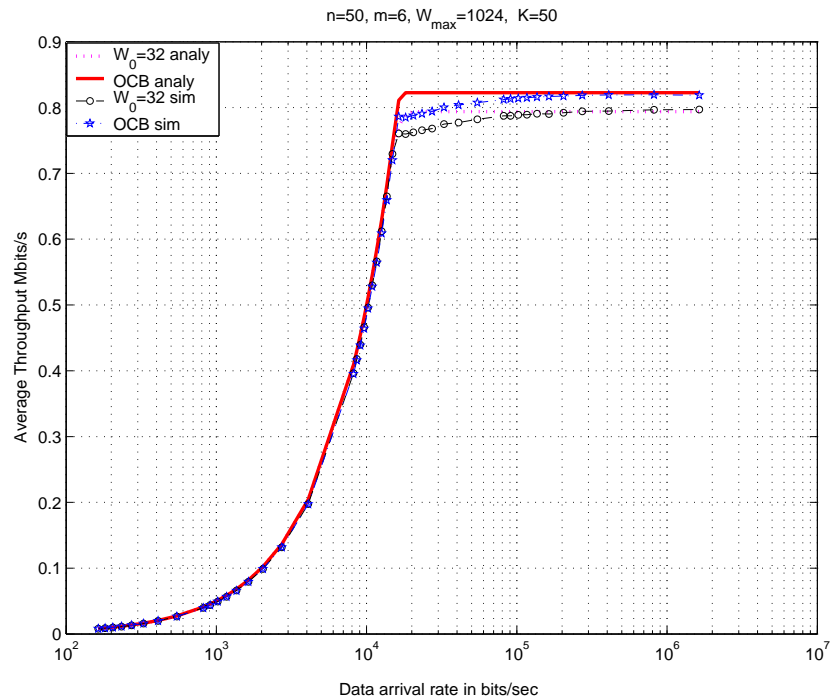


Figure 3.13: Queueing model throughput Vs. simulation

service time (including queueing delay) and shows clearly the existence of the three operating modes (no-backoff, transition and saturation regimes).

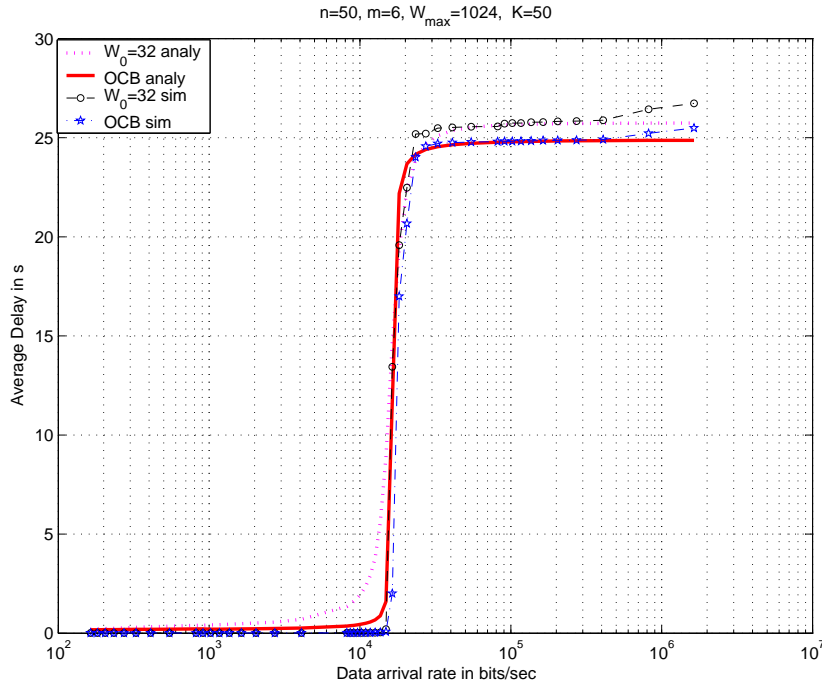


Figure 3.14: Queuing model delay Vs. simulation

In fig. 3.15, we plot the delay Jain's fairness index Vs. packet arrival rate. We observe again that during the no-backoff regime the two schemes are fair, at transition regime the two schemes are less fair and finally at saturation, the two schemes becomes again fair which is different from our previous observation when we analyze the delay fairness. This is due to the fact that, at saturation, the queuing delay is the same for all packets, and it is much more significant than the MAC delay. To illustrate the short-term unfairness of the BEB scheme, we plot in fig. 3.16 the throughput Jain's fairness index using the sliding window method [38]. The data arrival rate is taken equal to $20Kbits/s$, the network is then in saturation regime. We observe that OCB is relatively fair even at short time horizon, and is much fairer than BEB.

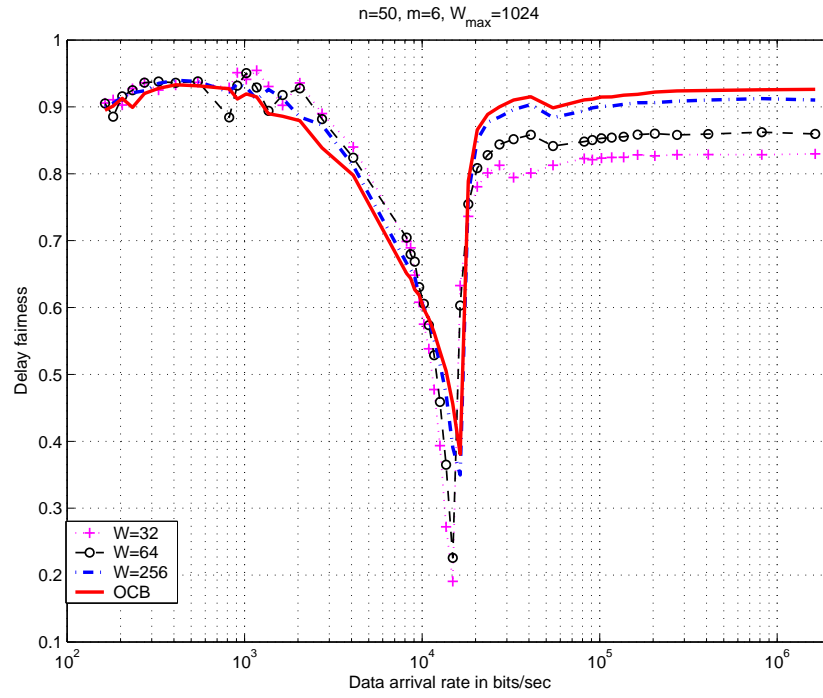


Figure 3.15: Delay fairness

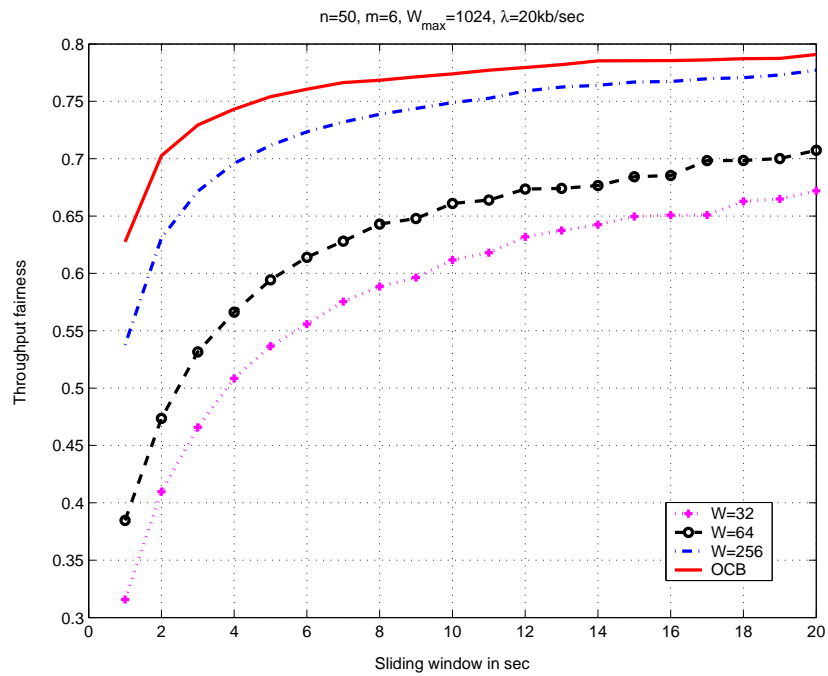


Figure 3.16: Throughput short-term fairness

3.7 Conclusion

In this chapter, we investigated the performance of the IEEE 802.11 DCF multiple access scheme under general load conditions in single-hop configurations and we proposed a backoff scheme enhancement that is blind and quasi-optimal under all traffic conditions. First, we presented a Markov chain model to analyze finite load situations without considering queuing at nodes buffers from which we derived an accurate delay statistics model. We derived then the size of the optimal constant window for a network in saturation regime, we then used this window for all traffic loads and we proved that the system operate nearly optimally independently from the load. When we compared the performance of the two backoff schemes, we found that OCB performs better than BEB both in term of throughput and short-term fairness. We have extended then the study to consider finite queueing capacity at nodes buffers and we have developed a recursive algorithm to alleviate the complexity of the analysis. Finally, we validated our results by NS2 simulations where we show clearly the superiority of OCB over BEB.

In the next chapter of the thesis, we will focus on protocol enhancement and backoff scheme optimization of DCF in multihop configuration. The optimal backoff scheme in this case is no more blind as it needs information about the topology of the network. We then propose a distributed algorithm, built only upon local information, to drive the system to optimal operating conditions.

Part II

Multiple Hop Networks

Chapter 4

IEEE 802.11 DCF Protocol: Enhancement & Optimization

4.1 Introduction

Due to power limitations, nodes in ad hoc networks are not always in the transmission range of each others. In this case, nodes may be requested to act as temporal relays in order to ensure the connectivity of the network. The multiple access control issue becomes then more complicated as new problems occurs, mainly, the hidden node problem. The hidden node problem arise whenever a transmitter node and its corresponding receiver do not share the same neighboring environment.

The hidden node problem was first identified in [30], and numerous techniques have been then proposed to cope with it [54]. For CSMA networks, the general idea of these protocols was to implement a mechanism to protect the receiver reception. Since the busy tone [54] technique requires a complex modem, the adopted solution was then to perform small control-packets handshaking (RTS/CTS) to reserve the medium before the data transmission [55]. Before a data-packet transmission can actually start, the sender broadcasts an RTS packet containing in its control fields both the intended destination of the ensuing data packet and the amount of channel time re-

quired for its transmission. If the RTS packet arrives successfully at the intended receiver, the latter broadcasts a CTS packet, containing also the channel time required for the new packet, to inform the sender of the RTS of the acceptance of the transmission and to inhibit neighboring stations from interfering during that period. Of course, a station is only allowed to send an RTS packet if none of its neighbors are transmitting and the station has not heard a CTS covering the time instant when it wants to transmit.

As the hidden node problem is basically related to power limitation constraints, power control and multiple access control are highly correlated in multihop networks. The problem of power control is complex since the choice of the power level fundamentally affects many aspects of the operation of the network:

- The transmit power level affects the physical layer performance as it determines the quality of the received signal and the magnitude of interferences on/from others transmissions.
- It determines the performance of medium access control since the contention for the medium depends on the number of other nodes within range.
- It affects the network layer as it determines the ranges of transmissions and so the routing.
- It affects the transport layer because interference causes congestion
- The choices of power levels affect the connectivity of the network, and consequently the ability to deliver a packet to its destination.

Transmit power control is therefore a cross layer design problem affecting all layers of the protocol stack from physical to transport, and affecting several key performance measures, including the throughput, delay and energy consumption.

The direct impact of power control on the MAC performance is of determining the transmission and reception range of each node. It determines then the level of contention in the neighboring of each user, and more generally determines the spatial reuse of the multiple access channel. In CSMA based network, the power control determines also the carrier sensing range which is of great importance on the achievable performance of the system. This last point have been especially addressed in the literature as a way to improve

performance of IEEE 802.11 protocol in multihop networks, by tuning the reception thresholds and/or the transmitted powers [56–62].

In this thesis, we have focused only on MAC protocols design and optimization for multihop networks. Our main motivations were first, to yet well understand the impact of the MAC protocol on the performance of multihop networks, and how to design good handshaking and contention mechanisms in this context, only from scheduling point of view. The second reason is that since the introduction of the notion of channel capacity [63] that is closely related, among others, to the transmitted signal power, power control has been extensively addressed in the literature, mainly in the context of cellular systems [64–68] by information theory formalism. The resulting joint power control and scheduling strategies have been shown to improve the performance of the network but require a central controller to be implemented. The transposition of these cross layer optimization problems into ad hoc networks is then a challenging task in term of modeling, solving, and adapting the produced solutions into easy-to-implement distributed algorithms.

The IEEE 802.11 has integrated the RTS/CTS handshaking with CSMA operation as a secondary access scheme to cope with the hidden node problem, i.e., physical carrier sensing and backoff mechanisms to determine channel access rights and exchange of RTS and CTS messages to avoid the hidden terminal problem. The RTS/CTS handshaking acts as a virtual carrier sensing mechanism to reserve the medium in the range of both transmitter and receiver.

A station that wants to transmit a packet waits until the channel is sensed idle for a DIFS, follows the backoff rules explained in the basic access mode (chap. 3), and then, instead of the packet, preliminarily transmits a special short frame containing the RTS message. When the receiving station detects an RTS frame, it responds, after a SIFS, with a CTS frame. The transmitting station is allowed to transmit its packet only if the CTS frame is correctly received. The frames RTS and CTS carry the information of the length of the packet to be transmitted. This information can be read by any listening station, which is then able to update a network allocation vector (NAV) containing the information of the period of time in which the channel will remain busy. Therefore, when a station is hidden from either the transmitting or the receiving station, by detecting just one frame among the RTS and CTS frames, it can suitably delays further transmission, and thus avoid collision.

Since 802.11 employs virtual carrier sensing to reserve the medium prior to packet transmission, the relative size of the spatial region it reserves for

the impending traffic significantly affects the overall network performance. We distinguish two transmission ranges according to the reception threshold used for CS or data reception. The first range is the Transmission Range (TR), which is the range within which a transmission is strong enough to be decoded reliably in the absence of collision. The second range is the Carrier Sense Range (CSR), which is the range within which the signal strength of a transmission will exceed the carrier sense threshold. In general, the CSR is larger than the TR and both are a function of the transmitted power (among other factors). Thus, the CSR determines the size of the region reserved by the RTS/CTS handshaking. Prior research has noted the impact of carrier sense range on the aggregate throughput. That is, the smaller the carrier sense range, the better the spatial reuse of the channel; but higher is the collision probability. Inversely, the larger is the carrier sensing range, the smaller is the collision probability; but lower is the spatial reuse.

We observe then that the CSR has similar impact on system performance as the backoff window length.

The RTS/CTS handshaking does not perform correctly in multihop configuration and may achieve worse performance than the basic CSMA in some cases [69], mainly because nodes are not able to get full access to all signaling messages on the medium (the masked node problem [70]). Thus, reliable and efficient control signaling is still needed to guarantee the correct operation of the scheme. Many work in the literature have addressed the RTS/CTS effectiveness and proposed modification to the basic handshaking scheme to improve its operation [69, 71–73].

4.1.1 Contribution

In this chapter, we introduce a modified RTS/CTS handshaking scheme to deal with the hidden node problem and to guarantee full protection of ongoing transmissions in IEEE 802.11 DCF protocol. Then, we analyze the performance of the resulting protocol in arbitrary network topology, and we propose a distributed algorithm based on stochastic approximations theory to control the backoff window length of each node in order to maximize the network throughput. The resulting algorithm is fully distributed and asynchronous. However, it is not completely blind as it requires some measurement of channel activity. In order to allow each node to collect relevant information about the state of the system in an autonomous manner, we derive the system condition for maximum throughput operation, and we project

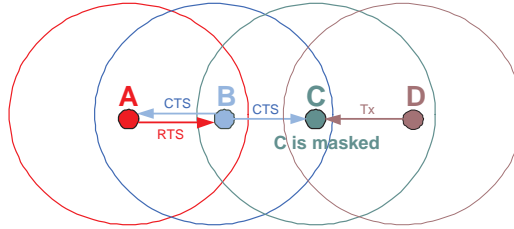


Figure 4.1: Illustration of the masked node problem

it into simple and easy-to-estimate parameters. The estimation process can be done independently by each node, so it avoids the need of users cooperation.

4.2 Effectiveness of RTS/CTS Handshaking in IEEE 802.11 DCF

4.2.1 The Masked Node Problem

The RTS/CTS mechanism can prevent DATA packet collisions when every node in the vicinity of the sender and the receiver hears at least one control packet and defers transmission appropriately. In ad hoc networks, this assumption does not hold, in general. Neighboring nodes are often unable to receive the control packets because they are masked by ongoing transmissions from other nodes near them. This means that the RTS/CTS mechanism does not generally prevent DATA packet collisions, even if the RTS/CTS handshake is performed successfully between a sender and a receiver [70]. Since DATA packet collisions reduce throughput and increase delay, masked nodes may significantly affect network performance.

In Fig. 4.1, node C is masked from node B as it can not receive its CTS message because node D is already transmitting in its range.

Fig. 4.2 illustrates the two possible situations of data packet collision caused by masked nodes. We observe that in the two cases, collision is caused by a neighboring node of the receiver, hidden from the transmitter, which did not correctly receive the CTS message (node E).

In fact, if some node in the neighboring of the sender does not correctly receive the RTS message due to collision, it must delay its future transmission attempt for EIFS time. The EIFS duration is larger than the time needed

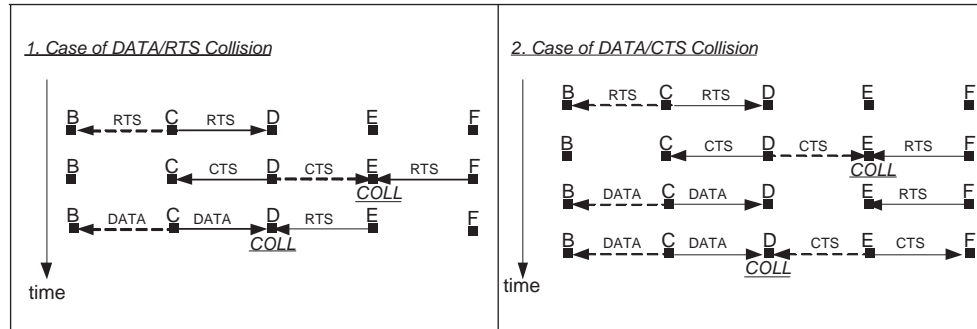


Figure 4.2: DATA collision caused by masked nodes

by the sender to, eventually, receive the CTS message, and to start the data transmission. After EIFS, the masked node performs carrier sensing. In case of data transmission, it will delay its channel access; otherwise, it is free to initiate its handshaking.

At the receiver side, unless the use of busy tone to prevent masked node for accessing the channel, we need to improve the protocol in order to ensure reliable transmission of the CTS message.

In order to limit the impact of the masked node problem, The CSR is made in general much higher than the transmitting range. Hence, even if a CTS message is not correctly received by some masked nodes, the probability that they may sense the DATA packet transmission, and so delay their transmissions, is higher. This may reduce the impact of the masked node problem but at the expense of lower spatial reuse.

4.2.2 The False Blocking Problem and its Propagation

In IEEE 802.11 DCF, a node that initiates RTS/CTS handshaking inhibits all its neighboring nodes from transmitting until the end of its transmission. This rule is designed to ensure that the acknowledgment (ACK) packet can be received by the sender without any collision. However, due to this rule, nearby nodes that successfully received the RTS message may become prohibited from transmitting even if the sender of RTS did not succeed its handshaking. We refer to this situation as the false-blocking problem [72]. This problem cause wasting of the channel utilization in the range of the failing sender, and may propagate into the networks as falsely-blocked nodes can not answers RTS request from their neighbors. Thus, these neighbors do

not succeed their handshaking procedure and may falsely-block their corresponding neighbors and so...!

The false blocking problem may not only propagate throughout a network, but it might also give rise to deadlock situations, at least for temporary periods. Once such a deadlock takes place, the throughput of the nodes involved in the deadlock goes down to zero. However, this deadlock is expected to be broken eventually as packets are dropped after a certain number of back-off attempts.

4.3 Protocol Enhancement: The RTS/R-CTS Handshaking

In order to guarantee correct and efficient operation of the RTS/CTS handshaking, we must protect the reception of CTS and DATA packets at the receiver, and avoid the false blocking problem.

The impact of the geometrical distribution of nodes in a network on transmission and CS ranges may not be manageable even if reception thresholds or transmitted powers are tuned accordingly, this mainly due to constraints on power emissions and correct decoding conditions. Thus, hidden node problem and the resulting masked node problem are unavoidable.

One possible solution to overcome the masked node problem is to constraint each node that senses a transmission on the channel but was unable to correctly decode it, to be silent for time duration greater than the duration of successful transmission (CTS/DATA). This will effectively protect data reception at the receiver, but it is efficient only in case where the uncoded transmission corresponds to at least one CTS message. Otherwise, this will cause high wasting of channel utilization.

As the receiver has no guarantee that its CTS message would be correctly received by all its neighbors, the only way it has to ensure reliable signaling in its range is to periodically retransmit the CTS message. In accordance with the IEEE 802.11 specifications, the period of retransmission must be less or equal to EIFS-2SIFS to guarantee that masked nodes will be kept silent even if they did not receive the repeated CTS messages. The DATA packet is then divided into multiple mini-packets, each of duration EIFS. Each retransmitted CTS contains a field that indicates the remaining amount of time needed to accomplish the transmission. Under this procedure, the re-

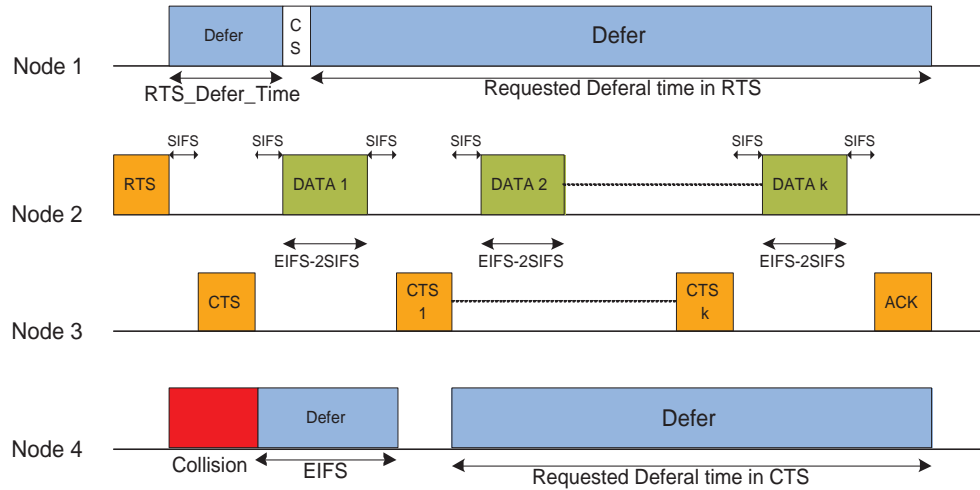


Figure 4.3: The RTS/R-CTS handshaking

ception of DATA packet is protected, and collisions caused by masked nodes are avoided. In order to minimize the signaling overhead caused by the multiple retransmissions of CTS messages, the EIFS duration and/or the DATA packets duration need to be adequately specified.

To resolve the false blocking problem, we integrate the RTS-Validation mechanism proposed in [72] into our RTS/Repeated CTS (RTS/R-CTS) handshaking.

False blocking is a consequence of the fact that every node that receives an RTS inhibits itself from transmitting. However, if a node is false blocked, then the corresponding DATA packet transmission does not take place while the node defers. Therefore, it follows that if a node assesses the channel to be idle during the expected DATA packet transmission period following an RTS, then the node must be false blocked. The RTS Validation solution is based on this observation. A node that uses RTS Validation, upon overhearing an RTS packet defers until the corresponding DATA packet transmission is expected to begin and then assesses the state of the channel. If the channel is found idle, then it defers no longer, otherwise it continues deferral. Specifically, when a node receives an RTS that is not destined for it, it defers for next RTS Defer Time. The RTS Defer Time is set to $CTS+2SIFS$ so that the DATA packet transmission is expected to begin at the end of this period. After this deferral period, the node assesses the channel for next Clear-Channel

Assessment Time (CCA Time) while continuing deferring (The CCA Time is the time required to assess the state of the channel [13]). If the channel is assessed to be busy, the node defers for an additional period so that the total deferral time equals to Requested Defer Time, i.e., the duration of deferral requested by the RTS; otherwise it defers no longer.

Fig. 4.3 illustrates examples of the operation of this handshaking mechanism that we call RTS/Repeated-CTS handshaking (RTS/R-CTS).

4.4 Performance Analysis

We consider an arbitrary network of size N . The network topology is characterized by a connectivity matrix M with binary entries 0, 1. component $M(i, j) = 1$ represents the fact that nodes i and j are in the transmission range of each others, otherwise, $M(i, j)$ is set to 0 ($M(i, i) = 1$). The transmission range is assumed equal to the carrier sensing range (M is symmetric). This choice is motivated by the effectiveness of our RTS/R-CTS handshaking scheme in avoiding the hidden node problem. So, we do not need to set the CS range greater that the TR to reduce the impact of the masked node problem.

As in the single-hop case, we assume that all nodes use a time-normalizing mechanism to produce signaling and DATA packets of equal durations.

Each node i generates a data packet (including forwarded packets) destined to node j in its transmission range, with probability $f_{i,j}$. $\sum_{j \in N_i} f_{i,j} = q$, where q is the probability that the node buffer is not empty, and N_x denotes the set of nodes that are neighbor to x , $N_x = \{i \in \{1, \dots, N\}, i \neq x | M(i, j) = 1\}$.

We consider the IEEE 802.11 DCF protocol using the RTS/R-CTS handshaking with constant window backoff scheme. The hidden node problem and the associated masked node problem are then avoided. Thus, each node that succeeds to send RTS request and receive the CTS grant is guaranteed to success its transmission. This behavior of DCF with RTS/R-CTS in multihop network is then similar to the operation of DCF in single hop network. So, we can use the analytical model introduced in chapter (3), the Markov chain model without queueing) to model the behavior of each node x in the network.

Let τ_x denotes the probability that node x transmit RTS request (τ_x corresponds to transmission probability τ in the single-hop model). In case it

receives a CTS grant, it will send periodically the mini-packets forming the DATA packet, until reception of the acknowledgment (ACK) packet. So τ_x represent the probability that node x access the channel as transmitter.

Now, in case where x receives successfully a RTS request destined to it, it will send a first CTS grant to inform the transmitter of the acceptance of the request. Then it will periodically retransmit CTS to protect the DATA packet reception. We denote by r_x the probability that a node x access the channel as receiver.

The unit-time of the Markov chain is equal to the average duration of events on the channel in the range of node x . This unit-time is an average of the four possible time-slot durations that correspond to successful transmission, successful reception, busy, or idle, weighted by their probability of occurrence:

$$T_x = P_{i_x}\sigma + s_xT_s + r_xT_r + (1 - P_{i_x} - s_x - r_x)B_x \quad (4.1)$$

Where P_{i_x} , s_x , and r_x denote respectively the idle slot probability, the transmission success probability, and the reception success probability.

According to the RTS/R-CTS scheme, we have

$$T_s = RTS + k.CTS + 2kSIFS + ACK + L + EIFS \quad (4.2)$$

$$T_r = k.CTS + 2kSIFS + ACK + L + EIFS \approx T_s \quad (4.3)$$

$$\sigma = EIFS \quad (4.4)$$

Where L is the DATA packet duration, and k is the repetition factor, $k = \frac{L}{EIFS - 2SIFS}$. Without loss of generality we suppose that k is integer. B_x represents the average time duration seen by node x in passive state (idle or backoff). This quantity is difficult to evaluate in multihop configuration so we do not express it¹.

From chapter (3), we have

$$\tau_x = \frac{1 - P_x^{m+1}}{1 - P_x} \pi_{0,0}^x \quad (4.5)$$

Where

$$\pi_{0,0}^x = \left[\frac{(W_0^x + 1 - 2P_x)[1 - P_x^{m+1}]}{2(1 - P_x)^2} + (1 - q) \left[\frac{P_x(W_0^x - 1)}{2(1 - P_x)} + \frac{1}{q} \right] \right]^{-1} \quad (4.6)$$

¹We will see later that this value can be measured by channel activity sensing for optimization purpose

P_x is the busy slot probability seen by node x in passive state. It is given by

$$P_x = 1 - \prod_{i \in N_x} (1 - \tau_i - r_i) \quad (4.7)$$

Pi_x , the idle slot probability, is given by

$$Pi_x = (1 - \tau_x - r_x) \prod_{i \in N_x} (1 - \tau_i - r_i) \quad (4.8)$$

And the successful reception probability r_x is

$$r_x = (1 - \tau_x - r_x) \sum_{i \in N_x} f_{i,x} \tau_i \prod_{j \in N_x - \{i\}} (1 - \tau_j - r_j) \quad (4.9)$$

where we can see that as soon as any node i transmits successfully its RTS message to node x , the DATA packet is also successful.

For ease of notation, we define the following variables

$$G_x = \tau_x + r_x \quad (4.10)$$

$$\alpha_x = \prod_{i \in N_x} (1 - G_i) \quad (4.11)$$

$$\alpha_x^i = \prod_{j \in N_x - \{i\}} (1 - G_j) = \frac{\alpha_x}{1 - G_i} \quad (4.12)$$

$$\alpha_i^{x,+} = (1 - G_i) \alpha_i^x \quad (4.13)$$

$$\beta_x = \sum_{i \in N_x} f_{i,x} \tau_i \alpha_x^i \quad (4.14)$$

The transmission success probability is defined as

$$s_x = \tau_x \gamma_x \quad (4.15)$$

$$\text{where } \gamma_x = \sum_{i \in N_x} f_{x,i} \alpha_i^{x,+} \quad (4.16)$$

While the reception success probability can be rewritten now as

$$r_x = (1 - G_x) \beta_x \quad (4.17)$$

We define the node throughput S_x as the ratio of time node x spent in transmitting successfully data packet over the average slot duration

$$S_x = \frac{s_x T_s}{T_x} = \frac{\tau_x \gamma_x L}{\alpha_x^+ \sigma + (\tau_x \gamma_x + (1 - G_x) \beta_x) T_s + \left(1 - \alpha_x^+ - (\tau_x \gamma_x + (1 - G_x) \beta_x)\right) B_x} \quad (4.18)$$

Similarly, we define the node reception throughput R_x as the ratio of time node x spent in receiving successfully data packet over the average slot duration

$$R_x = \frac{r_x T_s}{T_x} = \frac{(1 - G_x) \beta_x T_s}{\alpha_x^+ \sigma + (\tau_x \gamma_x + (1 - G_x) \beta_x) T_s + \left(1 - \alpha_x^+ - (\tau_x \gamma_x + (1 - G_x) \beta_x)\right) B_x} \quad (4.19)$$

Finally we define the node total throughput as the sum of the two last quantities

$$Z_x = S_x + R_x \quad (4.20)$$

4.5 Backoff Window Optimization

For optimization purpose, we have to solve first a very complex system of non linear equations to express the different system parameters, then we have to find the extremum of some objective function with respect to the window length W_0 . This is evidently a hard problem to resolve.

The optimal control problem of the MAC protocol for wireless networks could be divided into two parts:

1. *What is the relevant information we have to check in order to measure our actual deviation, (distance) from the optimal system's performance?*
(The ternary feedback, the backlog state...?)
2. *How to act optimally on the basis of this information to reach the optimal system's performance?*
(How much the retransmission probability or the backoff window should be increased or decreased?)

Usually in wireless network, MAC protocols are modeled as Markov chains, and nodes are asked to optimize some common objective function J (maximize the throughput, minimize the delay, minimize the power consumption...) with respect to some control parameters vector θ (retransmission

probability, backoff window, transmission powers....). Very often, as for our problem above, it is difficult to characterize analytically the optimal performance points (derivation of steady-state probabilities and the extremum of the objective function). For implementation issues, we require in addition that these optimal points be available for distributed calculation or observation from all nodes. As the optimization concern a common performance objective, it will depend naturally on some parameters of all nodes making the availability of distributed information and implementation hard to achieve.

The direct way to optimize the objective function J is to calculate its gradient G with respect to the control parameters $G(\theta) = \partial L(\theta)/\partial \theta$, and look for its extremums. However, even if we obtain an analytical expression for the optimal values of the control parameters, the remarks above about the availability of distributed information and implementation remain a problematic. When we transpose our control problem into stochastic optimization theory [74], we obtain immediate answers to our two fundamental questions, i.e., our distance from the optimal system's performance is given by the gradient of the performance with respect to the control parameters, and the optimal action we have to take is to align our parameter to some value with a descent gradient direction.

In the absence of analytical expression of the optimal control parameter θ^* , the most common approach to determine θ^* is based on iterative schemes of the general form

$$\theta(k+1) = \Pi \left[\theta(k) + \alpha_k \hat{G}(\theta(k)) \right] \quad (4.21)$$

Where Π is a projection into the feasible set of θ , \hat{G} is some estimate of a descent direction of G , and α_k is referred to as the step-size or gain or learning rate.

We distinguish two families of stochastic approximation (SA) algorithms: gradient-based family known as Robins-Monro (RM) [75] and gradient-free family known as Kiefer-Wolfowitz (KW) [76].

The gradient-based algorithms rely on the a priori knowledge or the direct measurements of the gradient of objective function with respect to parameters being optimized. In the absence of a priori knowledge of $G(\theta)$, the measurements typically yield an estimate of the gradient $G(\theta)$ in the stochastic setting. In the case where no analytical expression of G is available, we are still able to obtain appropriate gradient estimate by using the underlying

system input-output model (transition probabilities), examples are the likelihood ratio (LR) method [77, 78] and the infinitesimal perturbation analysis (IPA) [79, 80].

In the gradient-free setting, the optimization is done without the need of a system analytical model [76, 81]. It is just required that measurements of objective function $J(\theta)$ are available at various values of θ . No direct measurements (either with or without noise) of $G(\theta)$ are assumed available.

Under a number of conditions on the set of admissible control parameter vectors, the step-size sequence, and the estimates of the gradient, convergence w.p.1 of the sequence $\{\theta_k\}$ to the optimal θ^* can be established for the basic scheme (4.21). Generally, the (RM) algorithms yield convergence rate in order of $O(1/n^{\frac{1}{2}})$, higher than those of (KW) ones ($O(1/n^{\frac{1}{3}})$).

Convergence to the optimal control parameter θ^* is normally established by allowing the step-size sequence α_k to go to zero over time. If however, (4.21) is used online as an adaptive control mechanism, then the scheme can obviously not respond to statistical changes in the operating environment when the step-size value is near zero. One possible solution to this problem is to lower bound the step-size value to permit the control vector to track various changes online, usually at the expense of some oscillatory behavior around the steady state value of the optimal objective function J^* .

The implementation issue gives rise to a number of additional problems. In wireless ad hoc network, and in absence of central controller, it is highly desirable to develop distributed control algorithms, whereby all the necessary computation is carried out locally at each node. In the scheme (4.21), the main computational burden involve the gradient estimation process. One of our goals, therefore, is to have each node n_i locally evaluate an estimate of the gradient of J with respect to its local control parameter θ_i ; $G_i(\theta) = \partial L(\theta)/\partial \theta_i$. Once the gradient estimates are evaluated, the simplest approach for executing an update in (4.21) is to have a central controller who collects all estimates and performs control's parameters update. Even in the presence of such a central controller, this approach requires significant coordination among nodes, as well as the transfer of state information; this involves substantial communication overhead and delay which render the state information useless. In the absence of such a central controller, we allow each node to separately update its own control parameter. In a fully synchronized control scheme, this will be exactly equivalent to the centralized control version. In the asynchronous case however, parameter's updates occur at random in-

starts which will increase uncertainty in the local gradient estimates.

In our optimization problem, we aim to develop a fully decentralized and asynchronous stochastic approximation algorithm to maximize the overall network throughput. Further, we do not consider additional signaling between nodes for this purpose.

In order to reduce the impact of asynchronism on the consistence of the local gradient estimates, we consider local objective functions, where each node is responsible of maximizing a local objective function with respect to its control parameter, rather than one common objective function (the network throughput in our case).

Intuitively, if each node in the network tries to maximize only its own throughput then this will lead to an aggressive behavior of nodes as they will naturally decrease their backoff window to increase their access rate. This result has been shown for slotted networks with game theory formalism [82]. However, we can ask from each node to not only increase its throughput (transmission throughput), but also its reception throughput. In doing so, each node will implicitly increase its throughput as well as other nodes throughput (reception at some node corresponds to transmission from another node).

Each node x in the network is then asked to optimize its Z_x with respect to W_0^x . For ease of derivation, we begin by calculating the gradient of Z_x with respect to τ_x , then it is easy to relate it to W_0^x .

First, we have

$$G_x = \tau_x + r_x = \tau_x + (1 - G_x)\beta_x = \frac{\tau_x + \beta_x}{1 + \beta_x} \quad (4.22)$$

$$\implies \frac{\partial G_x}{\partial \tau_x} = \frac{1}{1 + \beta_x} \quad (4.23)$$

We can then express $\partial S_x / \partial \tau_x$ as follows

$$\begin{aligned} \frac{\partial S_x}{\partial \tau_x} &= \frac{\gamma_x T_s}{T_x^2} \left(T_x - \tau_x \left[-\frac{\alpha_x}{1 + \beta_x} (\sigma - B_x) + \left[\alpha_x - \frac{\beta_x}{1 + \beta_x} \right] (T_s - B_x) \right] \right) \\ &= \frac{\gamma_x T_s}{T_x^2} \left[\frac{\alpha_x}{1 + \beta_x} (\sigma - B_x) + \frac{\beta_x}{1 + \beta_x} (T_s - B_x) + B_x \right] \\ &= \frac{\gamma_x T_s}{T_x^2} \left[\frac{\alpha_x^+}{1 - \tau_x} (\sigma - B_x) + \frac{r_x}{1 - \tau_x} (T_s - B_x) + B_x \right] \\ &= \frac{1}{T_x^2} \left[\frac{s_x T_s}{\tau_x} \frac{1}{1 - \tau_x} \left[\alpha_x^+ (\sigma - B_x) + r_x (T_s - B_x) + B_x \right] - \frac{s_x T_s B_x}{1 - \tau_x} \right] \quad (4.24) \end{aligned}$$

For R_x we obtain

$$\begin{aligned}
 \frac{\partial R_x}{\partial \tau_x} &= -\frac{\beta_x T_s}{T_x^2} \left(\frac{T_x}{1 + \beta_x} + (1 - G_x) \left[-\frac{\alpha_x}{1 + \beta_x} (\sigma - B_x) + \left[\alpha_x - \frac{\beta_x}{1 + \beta_x} \right] (T_s - B_x) \right] \right) \\
 &= -\frac{\beta_x T_s}{(1 + \beta_x) T_x^2} [\gamma_x (T_s - B_x) + B_x] \\
 &= -\frac{1}{T_x^2} \left[\frac{r_x T_s}{(1 - \tau_x)} \frac{1}{\tau_x} [s_x (T_s - B_x) + B_x] + \frac{r_x T_s B_x}{1 - \tau_x} \right] \tag{4.25}
 \end{aligned}$$

Then, the gradient of the user total throughput is

$$\frac{\partial Z_x}{\partial \tau_x} = \frac{\partial S_x}{\partial \tau_x} + \frac{\partial R_x}{\partial \tau_x} \tag{4.26}$$

In order to obtain efficient estimation of the gradient, we can project the different terms that appears in Eqs. (4.24,4.25) into simple quantities that each node may compute independently. Thus, $\frac{\partial S_x}{\partial \tau_x}$ could be rewritten as follows

$$\begin{aligned}
 \frac{\partial S_x}{\partial \tau_x} &= \frac{1}{T_x^2} \left[\frac{s_x T_s}{\tau_x} \frac{1}{1 - \tau_x} [\alpha_x^+ (\sigma - B_x) + r_x (T_s - B_x) + B_x] - \frac{s_x T_s B_x}{1 - \tau_x} \right] \\
 &= \frac{1}{T_x^2} \left[\frac{s_x T_s T_{pas}}{\tau_x} - \frac{s_x T_s B_x}{1 - \tau_x} \right] \\
 &= \frac{1}{T_x^2} [\bar{s}_x T_s T_{pas} - s_x T_s \bar{B}_x] \tag{4.27}
 \end{aligned}$$

where $\bar{B}_x = \frac{B_x}{1 - \tau_x}$ represents the conditional busy duration when node x is in passive state.

$\bar{s}_x = \frac{s_x}{\tau_x}$ represents the conditional transmission success rate when node x is in active state (transmitting).

And $T_{pas} = \frac{1}{1 - \tau_x} [\alpha_x^+ (\sigma - B_x) + r_x (T_s - B_x) + B_x]$ represents the mean slot duration when node x is in passive state (idle, successful reception, or busy).

Similarly, $\frac{\partial R_x}{\partial \tau_x}$ could be expressed as

$$\begin{aligned}
 \frac{\partial R_x}{\partial \tau_x} &= -\frac{1}{T_x^2} \left[\frac{r_x T_s}{(1 - \tau_x)} \frac{1}{\tau_x} [s_x (T_s - B_x) + B_x] + \frac{r_x T_s B_x}{1 - \tau_x} \right] \\
 &= -\frac{1}{T_x^2} \left[\frac{r_x T_s}{(1 - \tau_x)} T_{act} + \frac{r_x T_s B_x}{1 - \tau_x} \right] \\
 &= -\frac{1}{T_x^2} [\bar{r}_x T_s T_{act} + r_x T_s \bar{B}_x] \tag{4.28}
 \end{aligned}$$

Where now $T_{act} = \frac{1}{\tau_x} [s_x(T_s - B_x) + B_x]$ represents the mean slot duration when node x is in active state (successful transmission or collision).

And $\bar{r}_x = \frac{r_x}{1-\tau_x}$ represents the conditional reception success rate when node x is in passive state.

Then, $\frac{\partial Z_x}{\partial \tau_x}$ becomes

$$\frac{\partial Z_x}{\partial \tau_x} = \bar{s}_x T_{pas} - \bar{r}_x T_{act} - (s_x + r_x) \bar{B}_x \quad (4.29)$$

In [83], a decentralized and asynchronous stochastic approximation algorithm using fixed learning rate was shown to converge in case where the objective function can be decomposed into multiple local functions. Each node in the network can then update asynchronously the overall control parameters to optimize its local function. This is obviously a distributed computation problem, where the asynchronism reduces the consistency of the local gradient estimates. Our problem is less constraining as each component is limited to update only its local control parameter.

Once we have derived a distributed and simple estimation scheme of the gradient of $\frac{\partial Z_x}{\partial \tau_x}$, we can use a distributed stochastic approximation algorithm, in the spirit of [83], with fixed learning rate to optimize the transmission and reception throughput of each node locally. For lack of time, we are unable to provide results of this scheme. Obviously, we have just made the basis of the optimization process. However, the proposed model could be simply extended to consider joint power control and backoff optimization. This is one of our main directions in future works, where we will deeply address the subject (choice of the step size, proof of convergence, etc).

4.6 Conclusion

In this chapter, we introduced a modified RTS/CTS handshaking scheme to combat the hidden node problem and to guarantee full protection of ongoing transmissions in IEEE 802.11 DCF protocol. The proposed handshaking is mandatory for the correct operation of the protocol in multihop configurations. However, it reduces the efficiency of the scheme as it requires multiple transmission from the receiver of the CTS message to protect its reception. We then analyze the performance of the resulting protocol in arbitrary network topology, and we propose a distributed algorithm based on stochastic approximations theory to control the backoff window length of each node

in order to maximize the network throughput. The resulting algorithm is fully distributed and asynchronous. Nevertheless, it is not completely blind as it requires some measurement of channel activity. In order to allow each node to collect relevant information about the state of the system in an autonomous manner, we have defined the node total throughput as the sum of its transmission and reception throughput. This allowed us to obtain distributed conditions on the maximum total throughput of each node. These conditions are then measured at each node by projecting them into simple and easy-to-estimate parameters. The estimation process can be done independently by each node, so it avoids the need of users' cooperation.

Chapter 5

Design & Optimization of MAC protocol for Multi-channel Networks

5.1 Introduction

The use of multiple channels in wireless ad hoc networks may provide some performance advantages by reducing collisions and enabling more concurrent transmissions, and thus better bandwidth usage and spatial reuse even with the same aggregate physical capacity as in single channel networks. The multiple channels may be obtained through frequency division multiple access (FDMA) and code division multiple access (CDMA) (frequency hopping, time hopping, and direct sequence spread spectrum) techniques.

Research on wireless network capacity has typically considered wireless networks with a single channel [1–3], although the results are applicable to a wireless network with multiple channels as well, provided that at each node there is a dedicated interface per channel. With a dedicated interface per channel, a node can use all the available channels simultaneously. However, the number of available channels in a wireless network can be fairly large, so it is expensive to have a dedicated interface per channel at each node. When

nodes are not equipped with a dedicated interface per channel, then capacity degradation occurs, compared to using a dedicated interface per channel.

In [4], it has been shown that in a random network of size n with up to $O(\log n)$ channels, even with a single interface per node, there is no capacity degradation. This implies that it may be possible to build near capacity-optimal multi-channel networks with few channels and one interface per node.

To take benefit of channelized system, the multiple access protocol has to address additional design problems. Especially, the multiples channel assignment issue. Early in the 80's, Sousa and Silvester [84] analyzed the throughput of some code's assignment schemes such as transmitter-based, receiver-based, or transmitter-receiver-based. The channel assignment problem is trivial when the network size is small; it becomes inefficient to assign a unique channel to each transmitter or receiver when the network size grows or the topology changes. Moreover, we have seen in the last chapter that efficient reservation scheme in multihop network suffers from the masked node problem. Thus, if we further permit signaling of control messages to take place over multiple channels the problem is aggravated. For this reason, the widely adopted technique is to reserve one common channel for the exchange of control messages while the others channel serve for data transfer.

In [85], a protocol that assigns channels dynamically, in an on-demand style, is proposed. This protocol, called Dynamic Channel Assignment (DCA), maintains one dedicated channel for control messages and other channels for data. Each host has two transceivers, so that it can listen on the control channel and the data channel simultaneously. RTS/CTS packets are exchanged on the control channel, and data packets are transmitted on the data channel. In RTS packet, the sender includes a list of preferred channels. On receiving the RTS, the receiver decides on a channel and includes the channel information in the CTS packet. Then, DATA and ACK packets are exchanged on the agreed data channel. As in Dual busy tone protocol [54], the ability of each node to continuously listen to the control channel permit to avoid the hidden terminal problem.

In [86], a protocol called Multi-Channel MAC (MMAC), and requiring only one transceiver was proposed. In MMAC, periodically transmitted beacons divide time into beacon intervals. Each host maintains a preferred channel list (PCL) with a high, medium, or low preference attached to every channel. A small window called the ad-hoc traffic indication message (ATIM) is placed at the start of each beacon interval. During the ATIM window, senders and

receivers switch to the common channel and negotiate channels access using a three-way handshake messaging that indicates also their respective PCLs. At the end of an ATIM window, all hosts switch to their respective selected channel and begin normal RTS-CTS-data-ACK cycles for data transmission. The control channel is also used for data transmission outside the ATIM window. The main drawbacks of the scheme are its requirement of global network synchronization, and the inefficient negotiation mechanism due to the masked node problem.

In order to protect ongoing data transmissions over the data channels, many MAC proposals have integrated carrier sensing functionality into their schemes. In [87], a multi-channel CSMA protocol with "soft" channel reservation is introduced. If there are N available data channels, the protocol assumes that each host can perform carrier sensing on all N channels concurrently. A host wanting to transmit a packet searches for an idle channel and transmits on that idle channel. Among the idle channels, the one that was used for the last successful transmission is preferred. In [88] the protocol is extended to select the best channel based on signal power observed at the sender. A similar scheme was proposed in [89] but selects the best channel according to the channel condition at the receiver side. The protocol achieves some throughput improvements by intelligently selecting the data channel. These protocols require N transceivers for each host, which is very expensive. In addition, carrier sensing in CDMA systems may be not physically feasible¹.

Another family of protocol, requiring no code assignment have been proposed in [90,91]. In [90], Hop Reservation Multiple Access is a multi-channel protocol for networks using slow frequency hopping spread spectrum (FHSS). The hosts hop from one channel to another according to a predefined hopping pattern. When two hosts agree to exchange data by an RTS/CTS handshake, they stay in a frequency hop for communication. Other hosts continue hopping, and more than one communication can take place on different frequency hops. Receiver Initiated Channel-Hopping with Dual Polling [91] takes a similar approach, but the receiver initiates the collision avoidance handshake instead of the sender. Transmitter-initiated schemes (TIS) perform better at low loads as collision probability is small and they are naturally adapted to the network load, while receiver-initiated schemes (RBS) are better suited for high loads but need to be adapted to the network load to perform well.

¹for example, CS in time hopping systems requires synchronization!!

Another difference among the two schemes is their signaling overhead and energy consumption. In TIS idle nodes must continuously listen to the channel while in RBS only nodes with packet to transmit have to listen the channel waiting invitation messages from receivers.

The schemes in [90, 91] can be implemented using only one transceiver for each host, but they require global network synchronization, and apply only to frequency hopping networks, so they cannot be used in systems using other channel division mechanisms.

5.1.1 Contribution

In this chapter we present an Aloha like MAC protocol for multi-channel multihop ad-hoc network and we derive its performances in multihop configuration. The proposed protocol is fully distributed, channel assignment free, and does not need global network synchronization, the multihop analysis is based on a Markov chain model and it is limited to a homogenous spatial distribution of nodes. Section 5.2 deals with the description of the protocol and the fundamental design choices behind it. In section 5.3, the analytical model is presented and then used to derive the protocol's saturation throughput and the corresponding optimal retransmission backoff window. The analysis is then extended to consider general load conditions. We again show that it is sufficient to use the optimal saturation window under all load to achieve near maximal throughput. Conclusion and directions of future works are given in section 5.4.

5.2 Protocol Description

The basic philosophy of the developed scheme is to reduce as much as possible signalization overhead and avoid global network synchronization due to the difficulties related to its practical realization in multihop networks. All nodes are given the same responsibility (i.e flat architecture), thus, single points of failure are avoided and the protocol is topology transparent. Only local synchronization is performed between each transmitter and its intended receiver and eventually maintained for data transfer. To relieve the channel assignment problem, a common channel (CC) is dedicated for broadcasting initial signalization message RTS (Request To Send), while other channels are used randomly (uniformly selected) by all nodes to complete communi-

cations setup and eventually for data transfers. This simplifies the channel assignment functionality since no inter-node collaboration is needed.

Access to the CC is pure Aloha, as soon as a node has a packet, it sends a RTS message. The RTS message consists on a synchronization sequence, source identifier (ID), destination ID and a channel ID randomly chosen at each RTS message transmission. The synchronization sequence allows the listening nodes to detect the transmission of the RTS message and get synchronized with its sender in order to be able to correctly receive its message. The source and destination IDs permit nodes identification. The data channel (DC) denoted in the RTS message is used later by the corresponding receiver for sending CTS (Clear To Send) message and then eventually for data transfer and acknowledgment.

As for the basic Aloha scheme, in case of communication failure; i.e., collision on the CC, receiver not available or collision on the DC; the transmitter must backoff for a random delay before making new attempts. We do not make any limit on the number of retransmissions. Each node is equipped with a single half-duplex transceiver, but may switch on all channels.

Virtual carrier sensing is not considered due to the masked node problem. The RTS/CTS handshaking is employed only to reserve the DC, i.e., the RTS message is used by the transmitter to inform the receiver about the ID of the DATA channel, while the CTS message is sent by the receiver to acknowledge the transmitter that the RTS message was correctly received, and that it is ready to receive its DATA packet on the chosen DC. Physical carrier sensing is also avoided, even on data channels. On the CC, because it is of no interest since the RTS message is of small duration, and as each node may operate only on a single channel at time, sensing all data channels may be time consuming so that information collected during the sensing phase may be out-of-date at the end of the sensing operation.

5.2.1 State Diagram

We define the system states as follow (Fig. 5.1):

- *Idle state*: A node is said to be in the *Idle state* when it has no activity. If it receives a packet to transmit, it sends directly a RTS message on the CC and becomes Ready Transmitter (RT): *RTS state*. Otherwise, if it correctly setup communication with a RT who has a packet designated to it, it moves to the *COM state*.

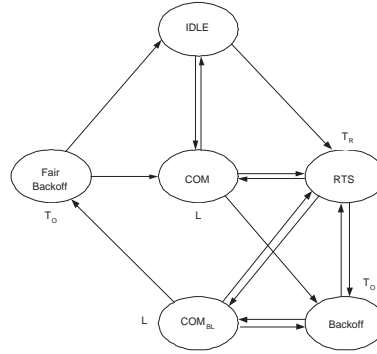


Figure 5.1: State diagram

- *RTS state*: A node is said to be in the *RTS state* when it is sending RTS message and waiting for CTS reply. If it succeeds to initiate a communication it moves to the *COM state*, otherwise it moves to the *Backoff state*.
- *Backoff state*: If a RT does not receive a CTS reply, it backoff its future attempt for a random period of mean T_o . During the backoff period, it can be involved in other communications as receiver, in this case, it moves to the *COM_{BL} state*. Otherwise, at the end of its backoff delay, it sends a new RTS message and moves to the *RTS state*.
- *COM state*: A node is said to be in the *COM state* when it is transmitting or receiving DATA packet. In case of collision on the data channel, the receiver goes back to *Idle state* while the RT moves to the *backoff state*. Otherwise, at the end of the communication, both the receiver and the RT move to the *Idle state*.
- *COM_{BL} state*: During backoff period, a backlogged node (BN) could be involved in a communication as receiver with a RT node, the two nodes are then said to be in *COM_{BL} state*. In case of a collision on the DATA channel, the RT moves to the *Backoff state* and the BN moves directly to the *RTS state*. Otherwise, at the end of the communication, the BN moves to the *RTS state* and RT passes to the *Fair Backoff state*; As it was served by a BN, the RT node will backoff its eventual future transmission to reduce contention on the CC, hence, the BN node has a greater probability of no collision on the CC. This is mainly a fairness

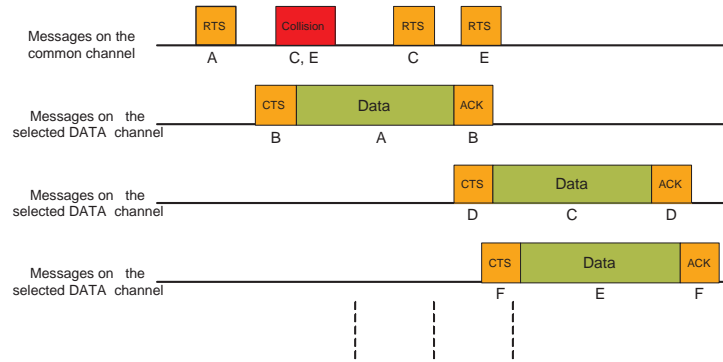


Figure 5.2: Case of no collision

measure and it differs greatly from classical backoff technique. We can say that the RT node gets indirectly information about the CC's load and then prevent itself from accessing the CC immediately. Note also that we have added the COM_{BL} state to correctly represent the fact that the MAC protocol handles only one packet at time until its successful transmission. So at the end of a communication, the BN node moves to The RTS state and not to the Idle state, this permit to us to keep track of backlogged packets, and so to separate without ambiguity backlogged traffic and new traffic.

- *Fair Backoff state:* As seen before, is the state of a RT node who has just been successfully served by a BN.

Fig. (5.2) illustrates an example of the protocol operation.

5.3 Delay-Throughput Analysis

The main difficulty that we face when analyzing MAC protocol in multihop configuration is how to model the fact that every node has its own range, which is generally different from other nodes ranges and partially hidden for some nodes in its range. In this case, unless using deterministic topologies or simplifying assumptions about interactions between regions in the network, it is difficult to analyze the performance of a part or the entire network since every node behave differently depending on its neighboring environment.

To avoid the need of analyzing the complex behavior of a group of nodes, we

consider a symmetric network model where each node, *on average*, evolves in the same environment, has the same capabilities and the same requests. Hence, it's possible by analyzing the performance of only one node to deduce the mean network performance.

This is an intermediate problem between the single hop case and the real multihop configuration. We mainly seek to show that the use of multiple channels permits to obtain asymmetric data packet duration and RTS packet collision durations. As in IEEE 802.11 DCF, this permits to use the optimal saturation backoff window under all load to achieve quasi-maximal throughput. This result is valid even in multihop network as the protocol is insensitive to the hidden node problem.

We use then an equilibrium point analysis, i.e, we approximate the stationary probability distribution of the other nodes' states by a unit impulse located at a point in the state space where the system is in equilibrium. Then, this stationary distribution will be used and explicitly calculated when deriving the single node performance.

Thus, the multihop symmetric network model allows us to obtain closed-form expression of system's performances so that we can derive some optimal retransmission mechanism as in single hop topology. In the same time, it permits to take into account the effect of multihop topology on system's performances. In the following, we show the correctness of this approach and we use it analyze the protocol.

5.3.1 Saturation Throughput Analysis

To construct a symmetric network model, we take the following assumptions:

- Channel Model: The physical layer offers $(D+1)$ orthogonal and identical channels (D for data and one for signalization). Only one transmission at time is allowed on every channel. Propagation delays and channel switching delays are neglected. The elementary time unit is taken equal to the duration of the RTS+CTS messages T_r (we take $T_r = 1$). Random retransmission delay is exponentially distributed with mean $T = T_o(T_r)$ ($T_o \geq T_r$). Packets are assumed to be of fixed duration $L(T_r)$.
- Topological structure: we consider some arbitrary network where each node has N neighbors. We further assume that the network is fully

connected.

Many topological models have been introduced in the literature:

1. Regular structure: Nodes are considered to be located in some regular pattern on the (n -dimensional hyper-plane). The advantage of this approach is that we can make assumptions that all nodes are statistically equivalent, which greatly simplifies the (analytical) problem.
2. Continuum of Nodes: In this model, nodes are considered to be continuously present throughout the space of interest (typically the infinite plane). This continuum of nodes is then considered to generate traffic at some rate per unit area. The advantage here is that we can assume the existence of a node at any convenient location.
3. Random Locations: Nodes are considered to be randomly distributed in the space of interest (again typically the infinite plane or some finite subset). This complicates matters in that assumptions about homogeneity are a little harder to swallow, but the Poisson assumption often allows closed-form solutions. The Poissonian model was widely used in the literature. For slotted ALOHA systems, the interference level (network topology) was assumed to be independent from slot to slot so that the obtained results may be applied to a network with dynamically changing topology or to obtain the average performance results for a collection of random networks [92, 93],

For our continuous-time protocol where the users are asynchronous, it is too difficult to consider the probabilistic performance of the MAC protocol over the random topologies. This is because there is no way to define the time instants when topology may change without affecting the protocol operation (we are not interested in analyzing the more complex case of mobile network).

The random topology in this case is not appropriate as we seek to obtain statistically a symmetric network in order to facilitate the equilibrium point analysis. For this reason, we consider some arbitrary network where each node has N neighbors (ring, infinite 2D grid...)

- Traffic model: Nodes traffic is uniform over the whole network. We

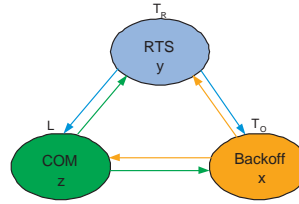


Figure 5.3: State diagram in saturation conditions

do not address the routing problem, we focus only on the single hop performance of the MAC layer.

In saturation conditions, nodes in Idle state get instantaneously packets to transmit. The corresponding state machine in this case is reduced to the one given in figure (5.3).

The resultant system can be modeled as a closed network of queues with network's state dependent transition rates. In fact, there is no queueing in every state (queue) and the system is simply a delay model (infinite server queues). Insensitivity propriety of this type of queues [94,95] makes their average performances depend only on mean service time and mean transition probabilities. As the state space is finite (finite S and λ) and the chain is irreducible, the chain has unique stationary distribution. Thus, we use this stationary distribution to specify the mean transition rates. Furthermore, if we apply mean value analysis technique to our infinite server system, we find that: $Q_N(i) = N \cdot Q_1(i)$, Where $Q_N(i)$ denotes the mean number of customers in queue i where there is N customers in the system.

This permits us to simply analyze the behavior of one node and then to deduce other nodes performances. To recapitulate, we can say that we have assimilated the complex analysis of the entire network of nodes by the analysis of one isolated node evolving in equilibrium state of the rest of the network².

Transition Rates

We suppose that in the stationary regime every node is in the state $X_e = \{\text{backoff, RTS, COM}\}$ with probability x, y, z , where x is the probability of being in Backoff state (BN), y the probability of being in the RTS state (RT) and z the probability of being in the COM_{BL} state (COM).

²We use the same technique to analyze performance of IEEE 802.11 DCF. Here is a queueing theory argument of its validity.

- A node in the Backoff state transits to the COM_{BL} state and begin to receive if and only if there is only one RTS message sent in it's range, the BN is the destination of the RTS message and there are no other transmission on the DATA channel chosen for communication setup in the range of the RT (for the correct reception of CTS message). The probability that RTS message does not collide with other RTS messages in the range of the BN is $(1-y)^{2(N-1)}$ because RTS packet may collide with a packet in the two slots that overlap with its transmission time.

$$\begin{aligned}
P(\text{only one RTS in the range of the BN}) &= yN(1-y)^{2(N-1)} \\
P(\text{BN is the destination of RTS}) &= \frac{1}{N} \\
P(\text{The chosen DATA channel is free}) &= 1 - \frac{zN}{2D}
\end{aligned}$$

So

$$P(\text{Backoff} \rightarrow COM_{BL}) = y(1-y)^{2(N-1)} \left(1 - \frac{zN}{2D}\right) \quad (5.1)$$

- A node in the RTS state transits to the COM_{BL} state and begin to transmit if and only if it succeeds to initiate communication with its destination's node, the corresponding probability is

$$P(RTS \rightarrow COM) = x(1-y)^{2(N-1)} \left(1 - \frac{zN}{2D}\right) \quad (5.2)$$

A node in the COM_{BL} state transits to the RTS state or to the Backoff state if and only if a collision occurs on the used data channel or in the contrary case the communication finishes successfully. In the two cases, it stays in the Com_{BL} state for the duration of the DATA packet transmission and acknowledgment .

$$P(COM \rightarrow RTR) = P(COM \rightarrow RTT) = \frac{1}{2} \quad (5.3)$$

The global balance equations with the normalizing equation are given as follows

$$x \left[y(1-y)^{2(N-1)} \left(1 - \frac{zN}{2D} \right) \left(1 - \frac{1}{T_o} \right) + \frac{1}{T_o} \right] = \frac{y}{T_r} \left[1 - x(1-y)^{2(N-1)} \left(1 - \frac{zN}{2D} \right) \right] + \frac{z}{2L} \quad (5.4)$$

$$\frac{y}{T_r} = \frac{x}{T_o} \left[1 - y(1-y)^{2(N-1)} \left(1 - \frac{zN}{2D} \right) \right] + \frac{z}{2L} \quad (5.5)$$

$$\frac{z}{L} = 2xy(1-y)^{2(N-1)} \left(1 - \frac{zN}{2D} \right) \quad (5.6)$$

$$1 = x + y + z \quad (5.7)$$

The scheme uses pure ALOHA protocol to access the CC and the DATA channel. As it uses no reservation mechanisms, the analysis of symmetric multihop network where each node has N neighbors is valid also for single hop network of size $N + 1$.

As the probabilities of a node to transmit or receive a packet are equals, the probability that a node is currently transmitting is then

$$\frac{z}{2} = \frac{xy(1-y)^{2(N-1)}DL}{xy(1-y)^{2(N-1)}NL + D} \quad (5.8)$$

However, transmission success probability is reduced by collisions on DATA channels. A collision on a currently used DATA channel occurs if a communication is successfully setup on it, in the range of the receiver during the reception of DATA packet, and in the range of the transmitter during the reception of ACK packet. Thus, the probability of no collision on a currently used DATA channel is

$$P_{NCD} = \left[1 - \frac{xy(1-y)^{2(N-1)}}{D} \right]^{L+1} \quad (5.9)$$

We define the user channels utilization U_{cu} as the ratio of time a node spend in transmitting successfully DATA packets

$$U_{cu} = \frac{xy(1-y)^{2(N-1)}DL}{xy(1-y)^{2(N-1)}NL + D} \left[1 - \frac{xy(1-y)^{2(N-1)}}{D} \right]^{L+1} \quad (5.10)$$

and we define network local channels utilization N_{cu} as the sum of U_{cu} in the range of any node normalized over the total number of channels used by the system

$$N_{cu} = \frac{N+1}{D+1} U_{cu} \quad (5.11)$$

We define optimal retransmission delay T_o^* as the value of T_o that maximizes the U_{cu} (symmetric network). From eq. (5.10) we find that the U_{cu} is maximal

for $y^* = \frac{1}{2N-1}$. In this case, the system steady-state probabilities and the corresponding optimal retransmission delay are given as follows

$$y^* = \frac{1}{2N-1} \quad (5.12)$$

$$z^* = \frac{D(\alpha L + 1) + \alpha NL \left(1 - \frac{1}{2N-1}\right) - \sqrt{D^2(\alpha L + 1)^2 + \left(\alpha \left(1 - \frac{1}{2N-1}\right) NL\right) \left[\alpha \left(1 - \frac{1}{2N-1}\right) NL - 2D(\alpha L - 1)\right]}{2\alpha NL} \quad (5.13)$$

$$x^* = 1 - y^* - z^* \quad (5.14)$$

$$T_o^* = \frac{2x^* \left[1 - y^*(1 - y^*)^{2(N-1)} \left(1 - \frac{z^* N}{2D}\right)\right] L}{2y^* L - z^*} \quad (5.15)$$

$$\text{Where } \alpha = \frac{1}{2N-1} \left(1 - \frac{1}{2N-1}\right)^{2(N-1)} \quad (5.16)$$

$y^* = 1/(2N-1)$ corresponds to a mean utilization of the common channel in any transmitter range equal to $e^{-1}/2$ (large N) which is the capacity of pure ALOHA protocol. So optimally designing the retransmission delay T_o permits us to achieve the common channel capacity and consequently the maximal channels utilization. The performances of the protocol depend then mainly on the performances of the common channel.

$T_o < T_o^* \Rightarrow$ high collision probability \Rightarrow Common channel is saturated \Rightarrow Access rate to CC above its capacity \Rightarrow Access rate to data channel is very small \Rightarrow Loss in throughput is high.

$T_o > T_o^* \Rightarrow$ low collision probability \Rightarrow Common channel is lightly used \Rightarrow Access rate to CC below its capacity \Rightarrow As idle duration is small compared to the data packet duration, small success rate on the CC corresponds to sufficiently high success rate on the data channel \Rightarrow Loss in throughput is small \Rightarrow Saturation retransmission delay may be used at all load without significant loss in throughput (Sec. 5.3.2).

This optimization is possible under the following constraint ($T_o \geq T_r$)

$$L \geq \frac{D(2N-3)(2N-1)}{\alpha[2D(2N-1) - (2N-3)N]} \quad (5.17)$$

Fig. 5.4 shows optimal values of T_o Versus node degree for DATA packet length 100 and 10, DATA channels number 4 and 10. We observe that T_o^* increase only linearly with node degree.

Fig. 5.5 shows the corresponding network channels utilization. We observe that while the U_{cu} decreases with increasing node degree, the N_{cu} increases and saturates for high values of N . This is a desirable feature and means that the MAC protocol can schedule successfully an increasing number of

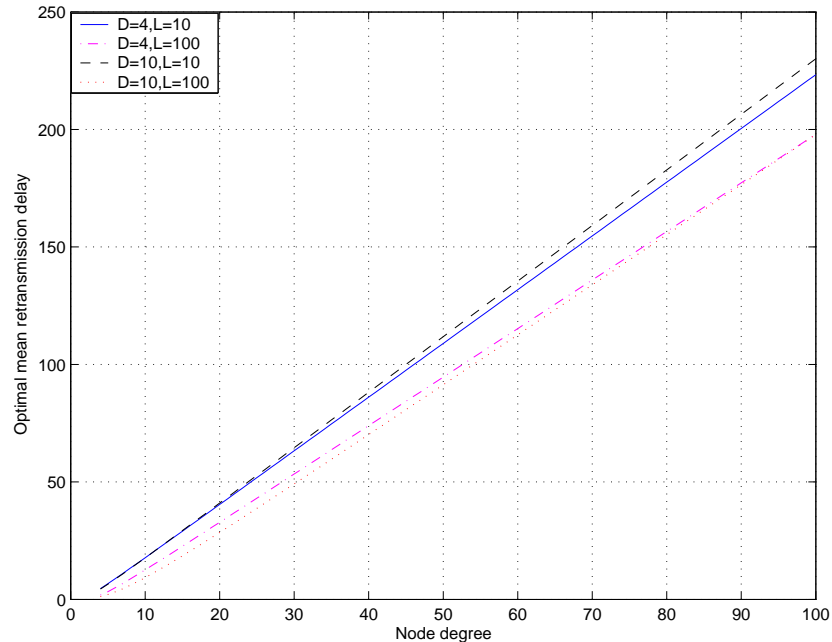


Figure 5.4: Optimal Retransmission Delay To

users with increasing global efficiency. We explain this as follow, while the retransmission scheme keeps the access rate to the common channel at it's optimal level, the increase in the number of users increase the probability that the RT node find its destination in the Backoff state. Remember that these are lower performances as we have upper-bounded the hidden area. We observe also that for each value of N , there exist an optimal choice of the number of DATA channel to be employed with a given DATA packet duration L .

To show this, we plot in Figs. (5.6,5.7) the achieved network throughput for $N = 10, 50$ vs. the number of DATA channels D for different packet duration L . We observe first that the network throughput increases with increasing L at the expense of higher packet delay. Second, we can see then clearly the existence of an optimal choice of D depending on N and L . From a capacity study point of view [4], it is sufficient to set $D = \log(N)$ to achieve the system capacity. for $N = 10, 50$ this suggest to take $D = 2, 3$. However, from the figures, we can see that this is true for small values of L (10), but not for larger values (100,500, and 1000).

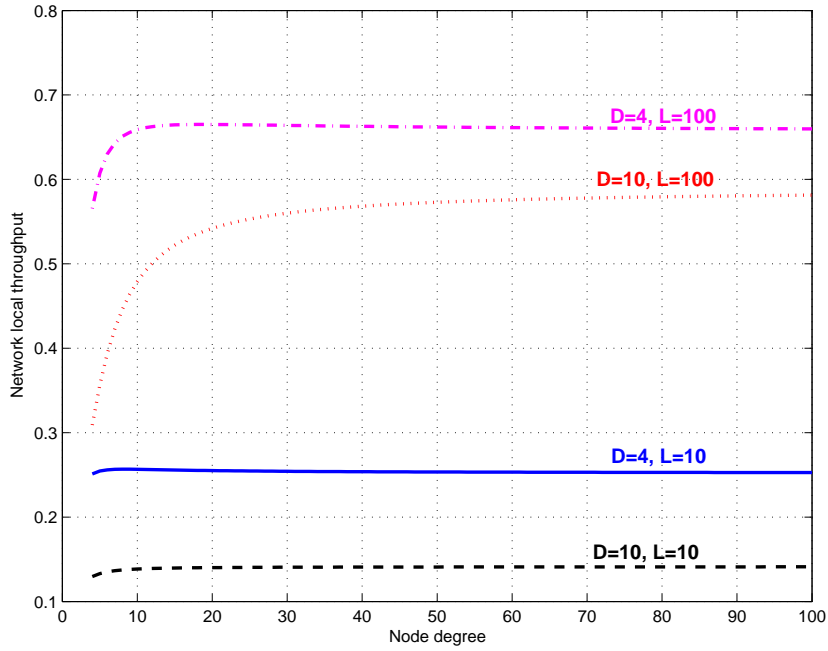


Figure 5.5: Network Throughput

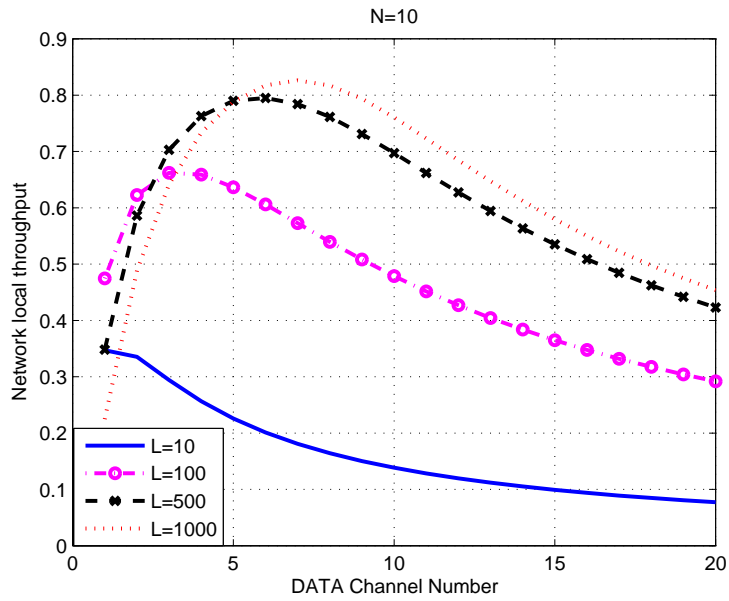


Figure 5.6: Network Throughput vs. Packet duration L for $N = 10$

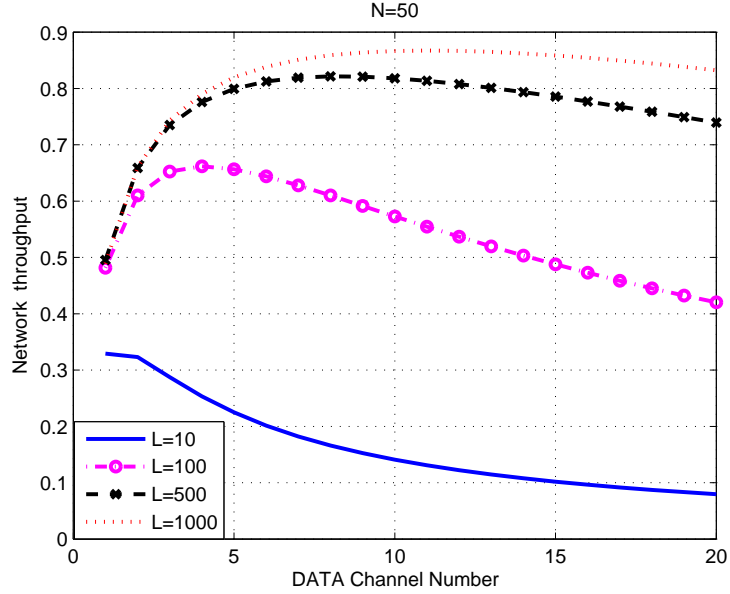


Figure 5.7: Network Throughput vs. Packet duration L for $N = 50$

5.3.2 General Load Analysis

In this section, we extend the analyze of the protocol to general load conditions. We model the packet arrival as poisson process with rate η . To keep the analysis tractable, we assume that only one packet at time is handled by the MAC protocol (no queueing). The truncation of the packet arrival process does not give us a precise idea of the real packet arrival rate seen by the MAC. In our case, the real arrival rate can be written as :

$$R = L.\eta.P(\text{node is in Idle state}) \text{ packet}/\text{packet time} \quad (5.18)$$

Using the same analytical model as for the saturation throughput, we find the following numerical results (detailed derivation of the transition probabilities is given in appendix 5.A.1) for the case of $N = 20$, $D = 10$ and $l = 100$. In fig. 5.8 we plot the values of the real load R seen by the MAC protocol and the values of the Optimal retransmission delay T_o versus the mean packet arrival rate η . We can observe that for η below the saturation throughput Th_{sat} , the rate seen by the MAC is almost the same as η and this mean that the MAC is able to handle each packet arrival without any excessive backoff delay (the very small loss is due only to signalization overhead).

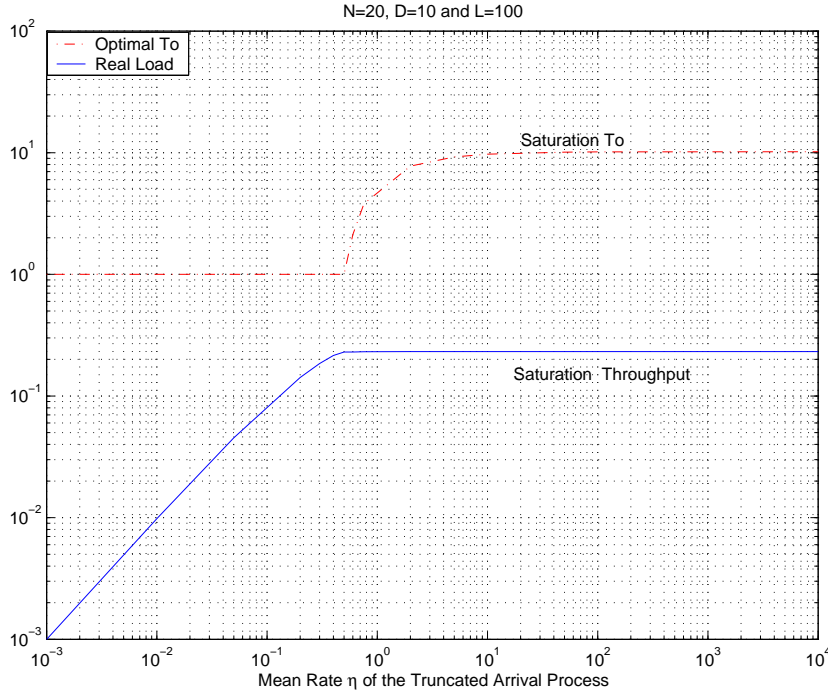


Figure 5.8: Optimal Retransmission Delay and Real Load R Vs Mean Arrival rate η

To see this, observe that the optimal retransmission delay T_o is 1 which mean that the common channel is lightly used and that there is no need to backoff users. For η above the Th_{sat} , we see that R is kept almost constant and equal to Th_{sat} while optimal retransmission delay T_o increase exponentially to the optimal saturation retransmission delay ST_o . This mean that for values of R approaching the Th_{sat} , the protocol turn very quickly from a lightly regime to a saturated regime which explains the exponential increase of optimal T_o .

Given the last observation, we want to measure the effect of using the optimal saturation retransmission delay ST_o , independently from the packet arrival rate, on the general performances. Fig.(5.9) depicts the achievable user throughput versus R for optimal T_o and optimal saturation ST_o and the corresponding normalized delay. We can see that the achievable performances are almost the same except a relative bigger difference in delay for values of R approaching Th_{sat} . To explain this, we note that below the Th_{sat} ,

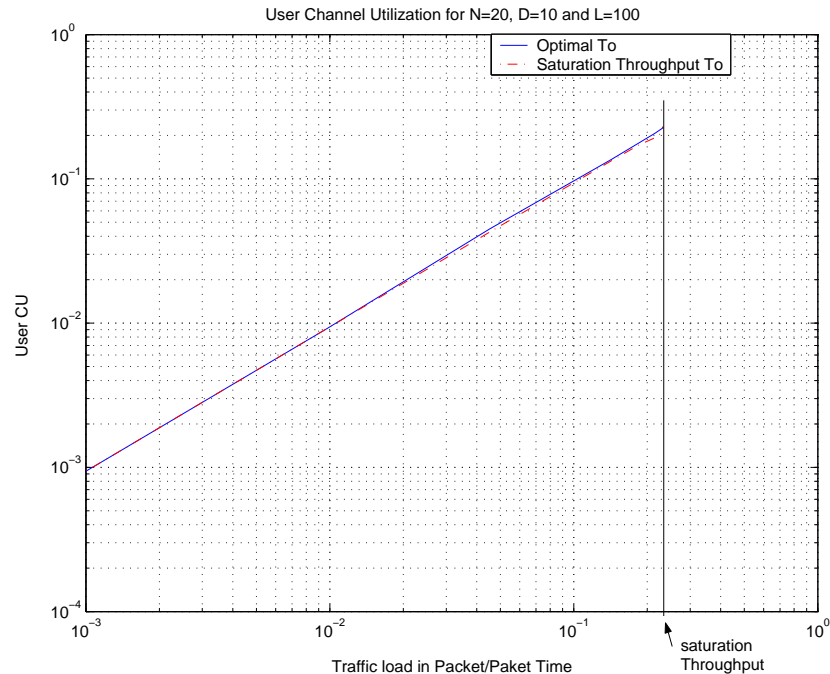


Figure 5.9: User Channels Utilization in General Load Conditions

there is no need to backoff users. In the transition phase, the use of the CC is driven below its capacity and nodes succeed their transmission but with a relative bigger delay. Finally, above the Th_{sat} the protocol is optimally operating.

5.4 Conclusion

In this work, we have presented a realistic Aloha-like MAC protocol for multi-channel multihop ad hoc network. Global network synchronization is avoided and no carrier sensing is performed. To resolve the channel assignment problem, a dedicated common channel is used in Aloha manner to broadcast RTS message. The RTS message contains an ID of a randomly data channel to be used to complete the communication setup. A simple and exact queueing network model is then used for the analysis of the protocol in symmetric multihop environment and in saturation conditions. Then, an optimal retransmission delay is derived depending only on the node degree. We use

then the saturation optimal retransmission delay under all traffic loads and we show that the achieved performance are quasi-optimal. This result is similar to the one obtained by the IEEE 802.11 DCF in single hop configuration. Thus, the asymmetry property in events duration (idle and collision durations for DCF, and RTS collision duration and data packet duration for multi-channel ALOHA) is determinant in achieving high system performance. Our multi-channel ALOHA protocol achieve this property without carrier sensing and even in multihop situation, while DCF use carrier sensing to achieve it.

5.A Appendix

5.A.1 Transition Rates For General Load

Let $(x, y, z, \alpha, \beta, \gamma)$ be respectively the probability of node being in (Backoff, RTS, COM_{BL} , Idle, Fair backoff, COM) state. Under the assumption of no packet forwarding and following the same argumentation as before, the system transition rates are given as follow: An Idle node (IN) transits to the COM state if it receives successfully RTS message designated to it, the corresponding transition rate is then

$$T_{I.C} = y(1-y)^{2(N-1)} \left(1 - \frac{(z+\gamma)N}{2D}\right) \quad (5.19)$$

Otherwise, the IN moves to the RTS state with rate:

$$T_{I.R} = \eta \left[1 - y(1-y)^{2(N-1)} \left(1 - \frac{(z+\gamma)N}{2D}\right)\right] \quad (5.20)$$

A RT moves to the COM state if it successfully setup communication with a destination node in the Idle or Fair Backoff state:

$$T_{R.C} = (\alpha + \beta)(1-y)^{2(N-1)} \left(1 - \frac{(z+\gamma)N}{2D}\right) \quad (5.21)$$

And moves to the COM_{BL} state if the destination is in the Backoff state:

$$T_{R.CB} = x(1-y)^{2(N-1)} \left(1 - \frac{(z+\gamma)N}{2D}\right) \quad (5.22)$$

Otherwise, it moves to the Backoff state:

$$T_{R.B} = \left[1 - (x + \alpha + \beta)(1-y)^{2(N-1)} \left(1 - \frac{(z+\gamma)N}{2D}\right)\right] \quad (5.23)$$

At the expiration of the retransmission delay T_o , the BN moves to the RTS state with rate:

$$T_{B.R} = \frac{1}{T_o} \left[1 - y(1-y)^{2(N-1)} \left(1 - \frac{(z+\gamma)N}{2D}\right)\right] \quad (5.24)$$

Transitions from Backoff state to COM_{BL} state and from Fair Backoff state to COM state are similar to (5.19), and transition from fair Backoff state to Idle state is similar to (5.24).

In case of collision on the DC not involving a BN, the RT nodes moves to the Backoff state while the receiver moves to the Idle State:

$$T_{C.B} = \frac{2 - P_{NCD}}{2L} \quad (5.25)$$

$$T_{C.I} = \frac{P_{NCD}}{2L} \quad (5.26)$$

In case of collision on the DC involving a BN, The RT node moves to Backoff state. Otherwise, it moves to the Fair Backoff state:

$$T_{CB.FB} = \frac{P_{NCD}}{2L} \quad (5.27)$$

$$T_{CB.B} = \frac{1 - P_{NCD}}{2L} \quad (5.28)$$

In the two cases, the BN moves to the RTS state:

$$T_{CB.R} = \frac{1}{2L} \quad (5.29)$$

Part III

Case study: Ultra-Wideband Networks

Chapter 6

Time Delay estimation of UWB Signals

An ultra-wideband (UWB) signaling scheme is defined as any wireless technology that occupies a bandwidth of more than 500 MHz and/or has fractional bandwidth greater than 20%. The fractional bandwidth is defined as $f_{frac} = 2(f_H - f_L)/(f_H + f_L)$, where f_H and f_L are respectively the upper and lower frequency at $-10dB$.

Recently, UWB signaling has grown in popularity since the Federal Communications Commission (FCC) regulations in the United States [6] have defined emission masks for UWB signals. The FCC ruling allows for coexistence with traditional and protected radio services and enable the potential use of UWB transmission without allocated spectrum. This is achieved by constraining UWB transmission systems to operate at a very low spectral density, sensibly equal to the power spectral density of thermal noise at the receiver. Thus, interference from UWB transmitters to others UWB users as well as other wireless systems with overlapping spectrum bandwidth resembles thermal noise. As result, scarce spectrum transmitter may be used more efficiently.

Ultra-Wideband (UWB) signaling is an example of transmission technology that may be used to provide channelized systems. The widely used form of UWB signaling is based on impulse radio (IR) [10]. IR-based UWB (IR-

UWB) technology employs pulses of very short durations ($\leq ns$) with very low spectral densities. It is resistant to channel multipath and has very good time-domain resolution allowing for location and tracking applications, and is relatively low-complexity and low-cost. Due to low power density, duty cycle transmission, and dense UWB multipath channel [10, 11], very fine synchronization is required for reliable transmission in UWB systems.

In this chapter, we address the performance of some coherent and no-coherent time-delay estimation schemes of IR-UWB signals. This issue is crucial for the deployment of ad hoc based UWB solutions as the synchronization task of sub nanosecond signals appears to be a critical issue. In addition to their communication capabilities, future UWB networks are also expected to provide some interesting extra-features such as localization and ranging. This may help system designer in exploiting valuable information for power control, multiple access, and routing purposes.

We are specially interested in deriving lower and upper bounds on the mean square error (MSE) obtained by these schemes, and giving an idea about the time they need to reach these bounds (the upper bounds).

Many works have addressed this issue and derived different Cramer Rao lower bounds (CRLB) [16, 96] to set a limit on the attainable MSE of the estimation procedure [97–100].

It is well known that the CRLB applies only to unbiased estimates and yields accurate answers only for large signal-to-noise ratios (SNR) [101]. As UWB systems are expected to operate at low SNR, CRLB represents a very pessimistic performance limit. This motivates our choice to use the improved Ziv-Zakai lower bound (IZZLB) [14] rather than the CRLB to address the time-delay estimation performance for IR-UWB signals.

The IZZLB applies to biased estimators, is valid under all SNR regimes, and includes explicitly the dependence on the a priori interval. It was applied for time delay estimation in broadband acoustic channel [102, 103], bearing estimation [104], and harmonic retrieval [105].

We apply the IZZLB to the case of IR-UWB signal where receiver has perfect 2nd. order statistics information about the received signal.

When applying conventional coherent structures for UWB receivers, the optimal exploitation of the pulse timing accuracy is only possible with extremely high-frequency clocks on the order of tens of gigahertz, which are capable of sampling sub nanosecond time windows. The fine delay resolution, guaranteed by the large signal bandwidth, provides a high robustness in dense multipath environments [106]. On the other hand, to fully exploit the chan-

nel diversity, a conventional coherent Rake receiver must be able to capture and track the energy associated with a high number of multipath replicas. In [107, 108], it is shown that the number of paths to be considered to reach a significant part of the overall energy is large. Due to complexity constraint, only a small subset of the received replicas is expected to be selected and combined, a fact that justifies the performance loss illustrated in [106, 109, 110], for various selection combining methods. In addition, the radiation and propagation process can act on the transmitted pulse as a filter whose characteristics vary from path to path. Therefore, the received signal can be seen as a train of distorted waveforms, that often show little resemblance to the transmitted pulse [96, 111]. Thus, the presence of pulse distortion increases the complexity of the channel estimation algorithm [112].

A different approach to overcome all the abovementioned disadvantages is based on the use of non-coherent reception techniques [110, 113]. These techniques do not require channel side information and allow capturing a large amount of the received energy, despite distortions and multipath propagation.

For these reasons, we are interested in studying practical synchronization schemes that are based on imperfect or no information about the channel state. When studying sub-optimal estimators, we are interested in characterizing upper bounds on their performance, which in addition serve as general upper bounds on the MSE of an optimal estimator.

To characterize the performance of sub-optimal estimators, we give first a new upper bound on signal parameter estimation suited to characterize imperfect estimation schemes. The upper bound is similar to the IZZLB in the sense that it is based also on the performance of a binary hypothesis detector, which uses the same imperfect likelihood-like function as the considered estimator.

We analyze then mis-matched maximum likelihood (ML) estimator based on the knowledge of noisy second order statistics of the channel, and estimator with no information performing only equal gain combining (EGC) of the received signal (we do not discuss implementation aspect of these schemes). The last estimator we review is for great interest for practical implementation, i.e, it is based on a simple discrete-time energy detector that requires no information about the channel state. The performance of the different estimators are then compared and show that practical schemes would achieve good performance if estimation is performed over a sufficiently large interval of observations.

6.1 System Model

Let $s(t) = \sqrt{\frac{E_p}{T_p}}p(t)$ be the transmitted IR-UWB single-pulse one-shot signal, with E_p been the pulse energy, $p(t)$ is the transmitted pulse of duration T_p with $\int_0^{T_p} p(t)^2 dt = 1$, and $W_b = 1/T_p$ the signal bandwidth. Propagation studies for IR-UWB signals have shown that they undergo dense multipath environment producing large number of resolvable paths [11]. A typical model for the impulse response of a multipath channel is given by

$$h(t) = \sum_{i=1}^L h_i \delta(t - \tau_i) \quad (6.1)$$

Where τ_i is the i -th path delay and h_i is random variable modeling signal attenuation at τ_i , $\sum_{i=1}^L E[|h_i|^2] = 1$.

The received signal during an observation period of duration T_f can then be written as

$$r(t) = \begin{cases} y(t - \theta_0) + n(t) & t \in [\theta_0, \theta_0 + T_d], \\ n(t) & t \in [0, \theta_0] \cup [\theta_0 + T_d, T_f] \end{cases} \quad (6.2)$$

Where θ_0 is the time delay parameter to be estimated, T_d the channel delay spread, $n(t)$ complex is Gaussian noise process with zero mean and power spectral density N_o , and

$$\begin{aligned} y(t) &= s(t) * h(t) \\ &= \sqrt{\frac{E_p}{T_p}} \sum_{i=1}^L h_i p(t - \tau_i) \end{aligned} \quad (6.3)$$

Since each component of y is a combination of many significant random variables we model it as non-stationary circular complex Gaussian process. The autocorrelation function of y is given as

$$K_y(t, u) = \frac{E_p}{T_p} \sum_{i=1}^L E[|h_i|^2] p(t - \tau_i) p(u - \tau_i)$$

6.2 Lower Bound on Mean Square Estimation Error

6.2.1 The Improved Ziv-Zakai Lower Bound

The Ziv-Zakai formulation of the lower bound is based on the probability of deciding correctly between two possible values (θ) and ($\theta + x$) of the signal delay θ_0 . The derivation of this bound relies on result from detection theory [114]. An optimal detection scheme which minimizes the probability of error performs a likelihood ratio test between the two hypothesized delays. On the other hand, a suboptimal procedure will be to apply, first, some estimation procedure to estimate the delay $\hat{\theta}_0$ of the received signal then decide between the two hypothesis by comparing $\hat{\theta}$ with $\theta + x/2$ (the algebraic mean of θ and $\theta + x$).

By comparing the performance the two schemes, one obtains the improved Ziv-Zakai lower bound (IZZLB) [14] on mean square error of the delay estimate

$$E[(\hat{\theta}_0 - \theta_0)^2] \geq \int_0^{T_f - T_d} x dx \int_0^{T_f - T_d - x} \frac{P_d(\theta, \theta + x)}{T_f - T_d} d\theta \quad (6.4)$$

Where $P_d(\theta, \theta + x)$ denotes the probability of error of the likelihood ratio test when deciding between θ and $\theta + x$.

In cases where $P_d(\theta, \theta + x)$ is independent of θ_0 , the expression in (6.4) becomes

$$E[(\hat{\theta}_0 - \theta_0)^2] \geq \int_0^{T_f - T_d} x \frac{T_f - T_d - x}{T_f - T_d} P_d(x) dx \quad (6.5)$$

Detailed Derivation of the IZZLB is given in Appendix (6.A.1).

6.2.2 Case of perfect 2nd. order statistics information

Single-frame observation

The received signal during the observation interval $[0, T_f]$ is given by

$$r(t) = \begin{cases} y(t - \theta_0) + n(t) & t \in [\theta_0, \theta_0 + T_d], \\ n(t) & t \in [0, \theta_0] \cup [\theta_0 + T_d, T_f] \end{cases}$$

We assume that the receiver has perfect information about the second order statistics K_y of the received signal $y(t)$. The binary detection error probability is independent from the arrival time θ_0 , we use inequality (6.5) to express the lower bound on the time-delay estimation error of UWB signal. Let $\theta_1 = 0$ and $\theta_2 = x$ denote the two hypothesized delays, $x \in]0, T_f - T_d]$. We get then

$$r(t) = \begin{cases} y(t) + n(t) & t \in [0, T_d] \\ n(t) & t \in [T_d, T_f] \end{cases} \Big|_{H_1} \quad (6.6)$$

$$r(t) = \begin{cases} y(t-x) + n(t) & t \in [x, x+T_d] \\ n(t) & t \in [0, x] \cup [T_d+x, T_f] \end{cases} \Big|_{H_2} \quad (6.7)$$

When the distance between the two hypothesized delays is greater than the duration of the signal, the two hypotheses can be rewritten to obtain a symmetric-hypothesis detection problem

$$r(t) = \begin{cases} y(t) + n(t) & t \in [0, T_d] \\ n(t) & t \in [x, x+T_d] \end{cases} \Big|_{H_1} \quad (6.8)$$

$$r(t) = \begin{cases} y(t-x) + n(t) & t \in [x, x+T_d] \\ n(t) & t \in [0, T_d] \end{cases} \Big|_{H_2} \quad (6.9)$$

For $x \leq T_d$, the two hypothesis are no more symmetric. The observation interval could be reduced to cover only the region where the signal is present under at least one of the two hypotheses. The two hypotheses becomes then

$$r(t) = \begin{cases} y(t) + n(t) & t \in [0, T_d] \\ n(t) & t \in [T_d, x+T_d] \end{cases} \Big|_{H_1} \quad (6.10)$$

$$r(t) = \begin{cases} y(t-x) + n(t) & t \in [x, x+T_d] \\ n(t) & t \in [0, x] \end{cases} \Big|_{H_2} \quad (6.11)$$

In this cases, projecting the signal in term of its covariance matrix on each observation interval ($[0, T_d]$ and $[x, x+T_d]$) leads to singularities in the covariance matrix of the resulting coordinates.

For this reason, we will use Fourier basis, common to the two hypotheses, to obtain our sufficient statistics from the received signal.

Case of $x > T_d$: External Bound

The two observation intervals are disjoint, the received signal over each observation interval is projected on a corresponding Fourier basis as follows

$$r(t) = \sum_{i=1}^N R_i^1 \psi_i^1(t) \quad R_i^1 = \int_0^{T_d} r(t) \psi_i^1(t) dt \quad (6.12)$$

$$\psi_i^1(t) = \frac{1}{\sqrt{T_d}} e^{-\frac{j2\pi i t}{T_d}} \quad \text{for } t \in [0, T_d] \quad (6.13)$$

$$r(t) = \sum_{i=1}^N R_i^2 \psi_i^2(t) \quad R_i^2 = \int_x^{x+T_d} r(t) \psi_i^2(t) dt \quad (6.14)$$

$$\psi_i^2(t) = \frac{1}{\sqrt{T_d}} e^{-\frac{j2\pi i (t-x)}{T_d}} \quad \text{for } t \in [x, x+T_d] \quad (6.15)$$

Where $N = 2W_b T_d$, and $j = \sqrt{-1}$.

Let $R^1 = [R_1^1, \dots, R_N^1]^T$, $R^2 = [R_1^2, \dots, R_N^2]^T$ and $R = [R^{1T} \ R^{2T}]^T$.

Under H_1 , R is zero mean circular complex Gaussian process with covariance matrix ${}_1K_x$ whose elements are given by

$$E[R_i^1 R_k^{1\dagger} | H_1] = E \left[\frac{1}{T_d} \int_0^{T_d} \int_0^{T_d} r(t) r(u)^\dagger \psi_i^1(t) \psi_k^{1\dagger}(u) dt du \right] \quad (6.16)$$

$$= \frac{N_0}{2} \delta_{i,k} + \frac{1}{T_d} \int_0^{T_d} \int_0^{T_d} K_y(t, u) e^{-\frac{j2\pi(i t - k u)}{T_d}} dt du \quad (6.17)$$

$$E[R_i^2 R_k^{2\dagger} | H_1] = E \left[\frac{1}{x+T_d} \int_0^{x+T_d} \int_x^{x+T_d} r(t) r(u)^\dagger \psi_i^2(t) \psi_k^{2\dagger}(u) dt du \right] \quad (6.18)$$

$$= \frac{N_0}{2} \delta_{i,k} \quad (6.19)$$

$$E[R_i^1 R_k^{2\dagger} | H_1] = E \left[\frac{1}{T_d} \int_0^{T_d} \int_0^{T_d} r(t) r(u)^\dagger \psi_i^1(t) \psi_k^{2\dagger}(u) dt du \right] \quad (6.20)$$

$$= 0 \quad (6.21)$$

Similarly, under H_2 , R is zero mean circular complex Gaussian process with covariance matrix ${}_2K_x$ whose elements are given by

$$E[R_i^2 R_k^{2\dagger} | H_2] = E \left[\frac{1}{T_d} \int_x^{x+T_d} \int_x^{x+T_d} r(t-x) r(u-x)^\dagger \psi_i^2(t) \psi_k^{2\dagger}(u) dt du \right] \quad (6.22)$$

$$= \frac{N_0}{2} \delta_{i,k} + \frac{1}{T_d} \int_0^{T_d} \int_0^{T_d} K_y(t, u) e^{-\frac{j2\pi(i t - k u)}{T_d}} dt du \quad (6.23)$$

$$E[R_i^1 R_k^{1\dagger} | H_2] = \frac{N_0}{2} \delta_{i,k} \quad (6.24)$$

$$E[R_i^1 R_k^{2\dagger} | H_2] = 0 \quad (6.25)$$

The log-likelihood ratio function is defined as

$$L(x) = \ln \left\{ \frac{P(R|H1)}{P(R|H2)} \right\} = R^\dagger Q_x R \quad (6.26)$$

$$\text{Where } Q_x = {}_1K_x^{-1} - {}_2K_x^{-1} \quad (6.27)$$

The two hypothesis are then compared according to the decision rule

$$L(x) \underset{H_2}{\overset{H_1}{\geq}} 0 \quad (6.28)$$

As the two hypotheses are symmetric, the resulting binary detection error probability is

$$P_d(x) = P(Z > 0 | H_1 \text{ is correct}) \quad (6.29)$$

Where $Z = R^\dagger Q_x R$.

Z is a quadratic form on complex Gaussian random variables. In appendix 6.A.2, we give a general technique to decompose Z and derive its distribution.

Case of $x \leq T_d$: Internal Bound

The observation interval is reduced to cover only the region where the signal is present under at least one of the two hypotheses; So the received signal during the interval $[0, x + T_d]$ is projected on a Fourier basis, common to the two hypotheses, as follows

$$r(t) = \sum_{i=0}^N R_i \psi_i(t) \quad (6.30)$$

$$R_i = \int_0^{x+T_d} r(t) \psi_i(t) dt \quad (6.31)$$

$\psi_i(t) = \frac{1}{\sqrt{x+T_d}} e^{-\frac{j2\pi it}{x+T_d}}$ are elements of the Fourier basis defined in the interval $[0, x + T_d]$, $N = 2W_b(x + T_d)$, and $j = \sqrt{-1}$.

R_i are circular complex Gaussian variables with zero mean. Under H_1 their covariance matrix is given as

$$\begin{aligned} {}_1K_x(i, k) &= E[R_i R_k^\dagger | H_1] \\ &= E \left[\frac{1}{x+T_d} \int_0^{x+T_d} \int_0^{x+T_d} r(t) r(u)^\dagger \psi_i(t) \psi_k^\dagger(u) dt du \right] \\ &= \frac{N_0}{2} \delta_{i,k} + \frac{1}{x+T_d} \int_0^{T_d} \int_0^{T_d} K_y(t, u) e^{-\frac{j2\pi(it-ku)}{x+T_d}} dt du \end{aligned} \quad (6.32)$$

Similarly, under hypothesis H_2 , R_i have a covariance matrix given as

$$\begin{aligned}
{}_2K_x(i, k) &= E[R_i R_k^\dagger | H_2] \\
&= \frac{N_0}{2} \delta_{i,k} + \frac{1}{x + T_d} \int_x^{x+T_d} \int_x^{x+T_d} K_y(t-x, u-x) e^{-\frac{j2\pi(it-ku)}{x+T_d}} dt du \\
&= \frac{N_0}{2} \delta_{i,k} + \frac{e^{-\frac{j2\pi x(i-k)}{x+T_d}}}{x + T_d} \int_0^{T_d} \int_0^{T_d} K_y(t, u) e^{-\frac{j2\pi(it-ku)}{x+T_d}} dt du \\
&= e^{-\frac{j2\pi x(i-k)}{x+T_d}} K_1(i, k)
\end{aligned} \tag{6.33}$$

The resultant log-likelihood ratio function is then

$$L(x) = \ln \left\{ \frac{P(R|H_1)}{P(R|H_2)} \right\} = R^\dagger Q_x R - D_x \tag{6.34}$$

$$\text{Where } Q_x = {}_1K_x^{-1} - {}_2K_x^{-1} \tag{6.35}$$

$$D_x = [\ln \det({}_1K_x) - \ln \det({}_2K_x)] = 0 \tag{6.36}$$

The two hypothesis are then compared according to the decision rule

$$L(x) \underset{H_1}{\overset{H_2}{\geq}} 0 \tag{6.37}$$

The resulting probability of detection error is

$$P_e(x) = \frac{1}{2} [P(Z > 0 | H_1 \text{ is correct}) + P(Z < 0 | H_2 \text{ is correct})] \tag{6.38}$$

Where $Z = R^\dagger Q_x R$.

Multiframe observation

In this case, the transmitted signal is repeated over N_f frames. In order to compare fairly with the single frame scheme, the transmitted signal energy over each frame is divided over N_f . The receiver signal during the observation interval $[0, N_f T_f]$ is then

$$r(t) = \begin{cases} y_m(t - \theta_0) + n(t) & , t \in [mT_f, mT_f + T_d], m = 0 \dots N_f - 1 \\ n(t) & \text{elsewhere} \end{cases} \tag{6.39}$$

$$\text{Where } y_m(t) = s(t) * h(t) = \sqrt{\frac{E_p}{N_f T_p}} \sum_{i=1}^L h_i p(t - \tau_i) \tag{6.40}$$

Internal Bound

The received signal during the observation interval $\cup_{m=0}^{N_f-1} [mN_f, mN_f+x+T_d]$ is now projected on N_f Fourier basis as follows

$$r(t) = \sum_{m=0}^{N_f-1} \sum_{i=1}^N R_i^m \psi_i^m(t) \quad (6.41)$$

$$R_i^m = \int_{mN_f}^{mN_f+x+T_d} r(t) \psi_i^m(t) dt \quad (6.42)$$

$$\psi_i^m(t) = \frac{1}{\sqrt{x+T_d}} e^{-\frac{j2\pi it}{x+T_d}}, \quad t \in [mT_f, mT_f+x+T_d] \quad (6.43)$$

Following the same processing as in sec.(6.2.2, Internal Bound), the detection error probability is

$$P_e(x) = \frac{1}{2} [P(Z_f > 0 | H_1 \text{ is correct}) + P(Z_f < 0 | H_2 \text{ is correct})] \quad (6.44)$$

Where now $Z_f = \sum_{m=0}^{N_f} R^{m\dagger} Q_x R^m$; $R^m = (R_1^m, \dots, R_N^m)^T$ and Q_x is defined as in sec.(6.2.2, Internal Bound).

External Bound

The received signal during the observation intervals $[mN_f, mN_f+T_d]$ and $[mN_f+x, mN_f+x+T_d]$, $m = 0 \dots N_f$, is now projected on the corresponding $2N_f$ Fourier basis. The same processing as in sec.(6.2.2, External Bound) can be done to obtain the resulting detection error probability.

6.2.3 Numerical Results

For numerical purpose, we assume the knowledge of a degenerate kernel of the second order statistics $K_y(t, u)$ characterized by a finite number of eigenmodes. We take a equi-spaced multipath channel with power delay profile $E[|h_i|^2] = \exp -\alpha \frac{T_i}{T_d}$, with α defined as the power decay factor (PDF).

In Fig. 6.1, we plot the obtained IZZLB on the root mean square error (RMSE) for different delay spread durations T_d vs. Average transmitted SNR. The pulse is of duration $T_p = 1ns$, the observation period is of length $T_f = 100ns$, and the PDF is 2. The average SNR is defined as $SNR = \frac{E_p T_p}{T_f N_0}$. As predicted by the bound, we observe three different operating regions:

1. The full ambiguity region corresponding to a very small SNR, in this region the receiver see the signal as noise and the error in this case is uniformly distributed over the a priori interval $[0, T_f - T_d]$.

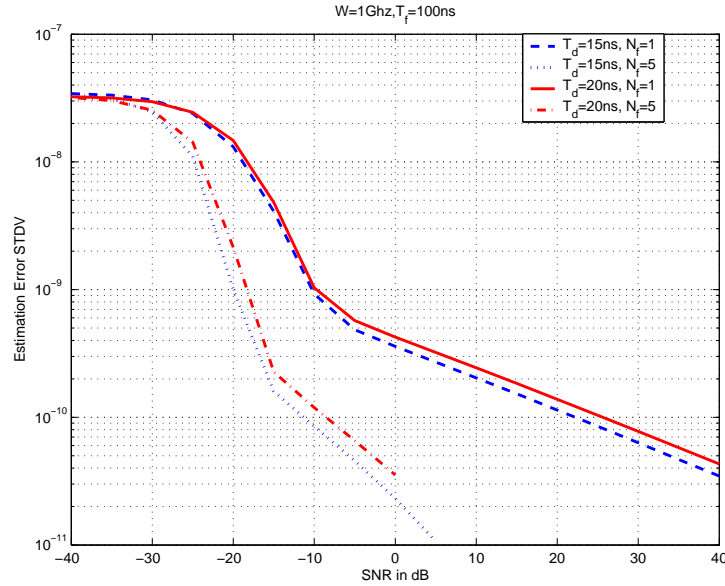


Figure 6.1: IZZLB on RMSE of single frame and multiframe estimators Vs. average SNR, and $T_d=15\text{ns}$, 20ns

2. The Cramer-Rao region corresponds to a high SNR, in this case the receiver succeeds to match well the signal with very small uncertainty. We observe also that for increasing delay spread T_d , and for the same pulse energy, the increase in error variance is small even if the energy is more spread.
3. The threshold region is located just between the two regions cited above. The estimation error in this case exceeds the CRLB by a large factor and describes more precisely the limit of the estimation error. It is then more realistic bound, especially for UWB systems that are supposed to operate on this range of SNR.

We observe also that the multiframe scheme outperforms greatly the single frame one even with a small number of repetitions.

In order to study the impact of the observation interval length on estimation performance, we plot in Fig. 6.2 the RMSE achieved for signal of delay spread $T_d = 20\text{ns}$ Vs. varying observation interval length T_f , and different SNRs. To fairly compare, the transmitted power is adequately adapted for each value of T_f in order to obtain unique average SNR. We observe then that

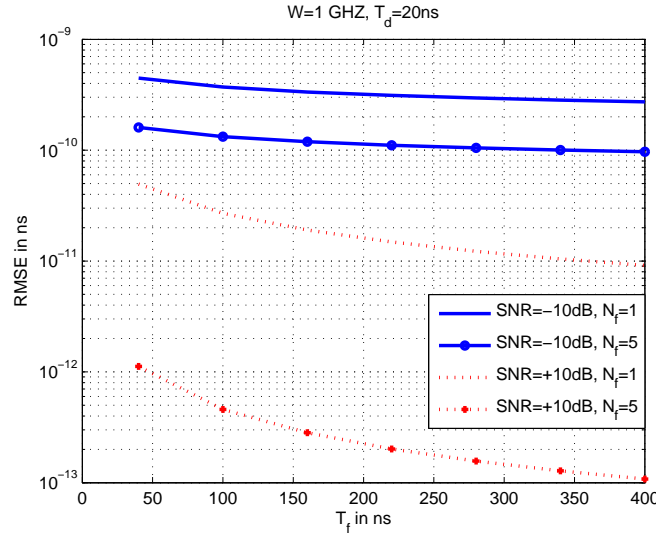


Figure 6.2: IZZLB on RMSE of single frame and muliframe estimators Vs. observation length T_f , and $SNR=-10\text{dB}$, $+10\text{dB}$

the RMSE decreases with increasing T_f , which means that the ML estimator performs better with increasing signal power even if the search interval is larger.

6.3 Performance of Sub-optimal estimators

When dealing with sub-optimal estimation schemes, we are interested in deriving upper-bounds on the MSE obtained by these schemes, which serve in addition as general upper bounds on the MSE of an optimal estimator. Existing upper bound on MSE [115,116] apply only for maximum likelihood estimator, and are difficult to evaluate.

In the spirit of the IZZLB, we derive a new upper bound on the MSE achieved by any continuous-time estimator, by comparing its performance to a discrete-time estimator, then to a binary detector scheme that use the same likelihood-like function. The resulting bound is easy to derive and its accuracy may be improved by increasing the numbers of testing points in the discrete time estimator.

6.3.1 Upper Bound on Mean Square Estimation Error

Let θ_0 denotes a continuous signal's parameter uniformly distributed over the interval $[0, T_f - T_d]$, and $r(t) = s(t, \theta_0) + n(t)$ the received signal where $n(t)$ is a circularly complex Gaussian noise process.

Let E_c be a continuous-time estimator of θ_0 built upon the information function f (the likelihood-like function). The estimate obtained by E_c is defined as

$$\hat{\theta}_c = \arg_{\theta \in [0, T_f - T_d]} \max f(\theta) \quad (6.45)$$

A sub-optimal estimation scheme E_d , based on the same information function f , is obtained by discretizing the observation interval into N intervals of equal lengths Δ . It then tests the function f at some chosen points of each interval, say the points at the middle of each interval. The estimator in this case is

$$\hat{\theta}_d = \bar{i}\Delta \quad \text{Where} \quad \bar{i} = i + \frac{1}{2}, \quad i = \arg_{i \in \{0, 1, \dots, N-1\}} \max L(\bar{i}\Delta) \quad (6.46)$$

For large SNR, we expect that the estimation error will be distributed uniformly in an interval of length Δ . The choice of Δ can then be driven from what target precision do we want to achieve.

Let $P_{ed}(x) = P(\hat{\theta} - \theta_0 = x)$ denotes the estimation error probability of the estimator E_d . A desirable property of E_d is to yield a decreasing estimation error probability $P_{ed}(x)$ with increasing $|x|$ ($|x|$ denotes absolute value of x). This can be expected since for positive SNR (in dB), parameter at distance $|x|$ from θ_0 miss more and more significant signal components with increasing $|x|$. For negative SNR, the noise process dominates the signal so that the inverse may be true. However, because of the high ambiguity in the received signal, performance may be identical at different distances x from θ_0 .

In the following, we suppose that our estimator E_d possesses this property. We define now $P_d(x)$ as the detection error probability achieved when using, again, the same information function f as above to decide between two hypothesis parameters θ_1 and θ_2 at distance x from each others. We assume also that $P_d(x)$ is independent from θ_0 .

Define MSE_c and MSE_d as, respectively, the mean square error of the continuous-time estimator E_c and the discrete-time one E_d . We then have the following result:

Theorem 6.3.1 MSE_c and MSE_d are upper-bounded as follows

$$MSE_c \leq MSE_d \leq \frac{\Delta^2}{12} \left[1 + \frac{2}{N} \sum_{j=1}^N (12j^2 + 1)(N - j)P_d(j\Delta) \right] \quad (6.47)$$

Detailed proof of the theorem 6.3.1 is given in Appendix 6.A.3.

In the following, we use this bound to evaluate performances of sub-optimal time-delay estimation schemes of UWB signals.

6.3.2 Mis-Matched Maximum Likelihood Estimator

Now we consider the case where the receiver has only an estimate \hat{K}_y of the true covariance matrix of the received signal K_y . This estimate is based on a finite number K of i.i.d realizations of the received signal Y .

$$\hat{K}_y(t, u) = \frac{1}{K} \sum_{i=1}^K Y_i Y_i^\dagger = K_y(t, u) + \Delta K_y(t, u) \quad (6.48)$$

According to [117], for sufficiently large K , ΔK_y is zero mean complex Gaussian random matrix with covariance matrix given as

$$E[\Delta K_y (\Delta K_y)^\dagger] = 2 \frac{K_y \otimes K_y}{K} \quad (6.49)$$

Where \otimes denotes Kronecker product.

Internal Bound

We project the received signal during the observation interval $[x, x + T_d]$ on a Fourier basis. We follow the same derivation as in Sec. (6.2.2, Internal Bound). The resulting error probability is then

$$P_d(x) = \frac{1}{2} [P(Z_n > 0 | H_1 \text{ is correct}) + P(Z_n < 0 | H_2 \text{ is correct})] \quad (6.50)$$

Where $Z_n = R^\dagger Q_x^n R$.

R is the vector of resulting projections and $Q_x^n = {}_1K_x^{-1} - {}_2K_x^{-1}$, where now

$$\begin{aligned} {}_1K_x(i, k) &= \frac{N_0}{2} \delta_{i,k} + \frac{1}{x + T_d} \int_0^{T_d} \int_0^{T_d} \hat{K}_y(t, u) e^{-\frac{j2\pi(i t - k u)}{x + T_d}} dt du \\ {}_2K_x(i, k) &= e^{-\frac{j2\pi x(i - k)}{x + T_d}} {}_1K_x(i, k) \end{aligned} \quad (6.51)$$

The external bound can be derived in a similar way as in sec. (6.2.2, external bound) and just changing K_y by \hat{K}_y in the hypothesis. Extension to multiple-frame observation is straight forward by following the same derivation as in section (6.2.2)

6.3.3 Case of No 2nd Order Statistics Information: Equal Gain Combining (EGC)

Here we suppose that the receiver has no knowledge about the 2nd order statistics of the received signal. The detection is then based on an equal gain combining scheme, which means that the received signal is supposed to be a stationary Gaussian process with covariance matrix

$$\hat{K}_y(t, u) = \left(\frac{E_s}{T_d} + \frac{N_0}{2} \right) \delta(t - u) \quad (6.52)$$

$$(6.53)$$

Internal Bound

We project the received signal during the observation interval $[x, x + T_d]$ on a Fourier basis. We follow the same derivation as in Sec. (6.2.2, Internal Bound). The resulting error probability is then

$$P_d(x) = \frac{1}{2} [P(Z_e > 0 | H_1 \text{ is correct}) + P(Z_e < 0 | H_2 \text{ is correct})] \quad (6.54)$$

Where $Z_e = R^\dagger Q_e^n R$.

R is the vector of resulting projections and $Q_x^e = {}_1K_x^{-1} - {}_2K_x^{-1}$, where now

$$\begin{aligned} {}_1K_x(i, k) &= \frac{N_0}{2} \delta_{i,k} + \frac{E_s}{T_d(x + T_d)} \int_0^{T_d} e^{-\frac{j2\pi t(i-k)}{x+T_d}} dt du \\ {}_2K_x(i, k) &= e^{-\frac{j2\pi x(i-k)}{x+T_d}} {}_1K_x(i, k) \end{aligned} \quad (6.55)$$

The external bound can be derived in a similar way as in sec. (6.2.2, external bound) and just changing $K_y(t, u)$ by $\frac{E_s}{T_d} \delta(t - u)$ in the hypothesis. Extension to multiple-frame observation is straight forward by following the same derivation as in section (6.2.2)

6.3.4 Discrete Time Estimation by Energy Maximization

Single-frame estimation

In this section, we present and analyze a discrete time energy detection based estimator of the time delay. The energy detector scheme is shown in fig. (6.3).

The received signal $r(t)$ during an observation period $[0, T_f]$ is first filtered by an ideal band pass filter and then squared and integrated over a time

interval T_d to produce a measure of the received energy. The output of the integrator is then sampled at rate δ . The produced samples will act as the test statistics of the time delay estimator.

According to the sampling theorem, the filtered signal can be expressed as

$$\hat{r}(t) = \sum_{i=-\infty}^{+\infty} r_i \text{sinc}(2W_b t - i) \quad (6.56)$$

Where $r_i = r(\frac{i}{W_b})$.

The output of the integrator can be then approximated as [118,119]

$$g(t) = \frac{1}{W_b} \sum_{i=\lfloor W_b t \rfloor}^{\lfloor W_b(t+T_d) \rfloor - 1} \|r_i\|^2 \quad (6.57)$$

Where $\lfloor x \rfloor$ denotes integer part of x .

The produced integrator samples at rate Δ can be written as

$$G_k = \frac{1}{W_b} \sum_{i=W_b \bar{k} \Delta}^{W_b(\bar{k} \Delta + T_d) - 1} \|r_i\|^2, \quad k \in \{0, \dots, N - M - 1\} \quad (6.58)$$

Where $\bar{k} = k + \frac{1}{2}$, $N = \frac{T_f}{\delta}$, and $M = \frac{T_d}{\Delta}$; without loss of generality, we take ΔW_b , M , and N as integers. We construct then our test as :

$$L(k) = \frac{1}{N_0} G_k = \sum_{i=W_b \bar{k} \Delta}^{W_b(\bar{k} \Delta + T_d) - 1} \|R_i\|^2, \quad k \in \{0, \dots, N - M - 1\} \quad (6.59)$$

Where $R_i = \frac{r_i}{\sqrt{W_b N_0}}$.

The time delay estimate is then defined as

$$\hat{\theta}_0 = \bar{k}_0 \Delta \quad \text{Where } k_0 = \underset{k \in \{0, \dots, N - M - 1\}}{\text{arg max}} L(\bar{k}) \quad (6.60)$$

Using the bound in theorem 6.3.1, the MSE of this estimator is upper-bounded as

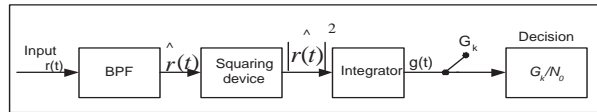


Figure 6.3: Discrete Time Energy Detector

$$MSE_d \leq \frac{\Delta^2}{12} \left[1 + \frac{2}{N} \sum_{j=1}^N (12j^2 + 1)(N - j)P_d(j\Delta) \right] \quad (6.61)$$

As P_d is independent from the arrival delay θ_0 , we get

$$P_d(\bar{j}\Delta) = \frac{1}{2} [P(L(\bar{0}\Delta) < L(\bar{j}\Delta)) | \theta_0 = \bar{0}\Delta) + P(L(\bar{0}\Delta) > L(\bar{j}\Delta)) | \theta_0 = \bar{j}\Delta]$$

Where

$$P(L(\bar{i}\Delta) < L(\bar{j}\Delta)) | \theta_0 = \bar{i}\Delta) = \begin{cases} P \left(\sum_{k=2\Delta\bar{i}}^{2\Delta\bar{j}-1} \|y_k\|^2 + \|n_k\|^2 < \sum_{k=2\Delta(\bar{i}+M)}^{2\Delta(\bar{j}+M)-1} \|n_k\|^2 \right) & \text{for } 0 < (j - i)\Delta \leq T_d \\ P \left(\sum_{k=2\Delta\bar{i}}^{2\Delta\bar{j}-1} \|n_k\|^2 > \sum_{k=2\Delta(\bar{i}+M)}^{2\Delta(\bar{j}+M)-1} \|y_k\|^2 + \|n_k\|^2 \right) & \text{for } 0 < (i - j)\Delta \leq T_d \\ P \left(\sum_{k=1}^{2\Delta(M)-1} \|y_k\|^2 + \|n_k\|^2 < \sum_{k=2\Delta\bar{j}}^{2\Delta\bar{j}+M-1} \|n_k\|^2 \right) & \text{for } (j - i)\Delta > T_d \end{cases} \quad (6.62)$$

6.3.5 Numerical Results

In Fig. 6.5 we plot upper bounds on the RMSEs achieved by the mis-matched ML estimator, the EGC, and the energy maximization estimator, and we compare them to the IZZLB. The signal is of duration $T_d = 20ns$, $W_b = 1GHz$, $T_f = 100ns$, $N_f = 1$, PDF $\alpha = 2$, and discretization step for the upper bound and the energy detector is $\Delta = 0.5ns$. The mis-matched ML estimator builds its information on K_y by observing $K = 10$ realizations of the signal.

We observe then that the Mis-matched ML perform nearly as the perfect ML, taking into account that the gap in the performances of the two schemes is due also to the fact that we are considering an upper bound for the mis-matched ML. The EGC estimator achieves the worst performance while the energy detector begin to really approaches the lower bound for SNR greater than 20dB. In Fig .6.5 we plot the same performance, except the perfect ML for which we plot its upper bound, for $N_f = 10$. We observe then clearly that the mis-matched ML approaches the ML, and that the energy detector scheme exploits better the signal repetition than the EGC estimator. However, even with 10 frames repetition, the gain in the performance is not too significant. To investigate on the impact of the integration window length of the energy detection scheme, we plot in Fig. 6.6 the achieved RMSE vs SNR for various

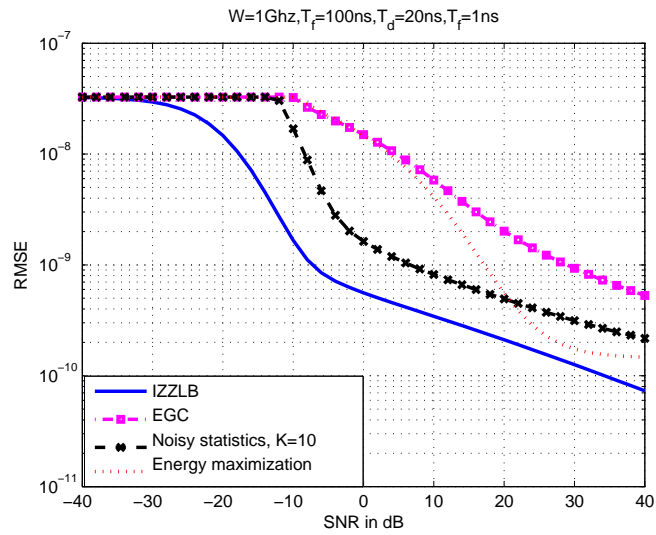


Figure 6.4: IZZLB and upper bounds on RMSE of single frame estimators Vs. average SNR

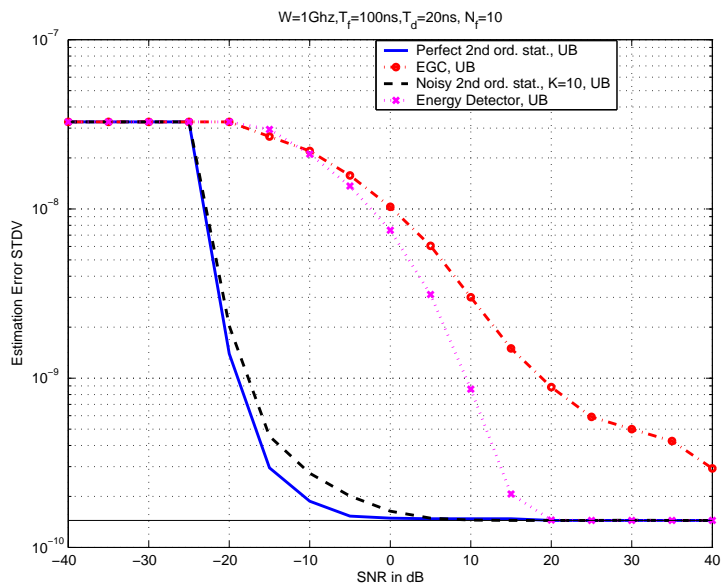


Figure 6.5: Upper bounds on RMSE of multiframe estimators Vs. average SNR

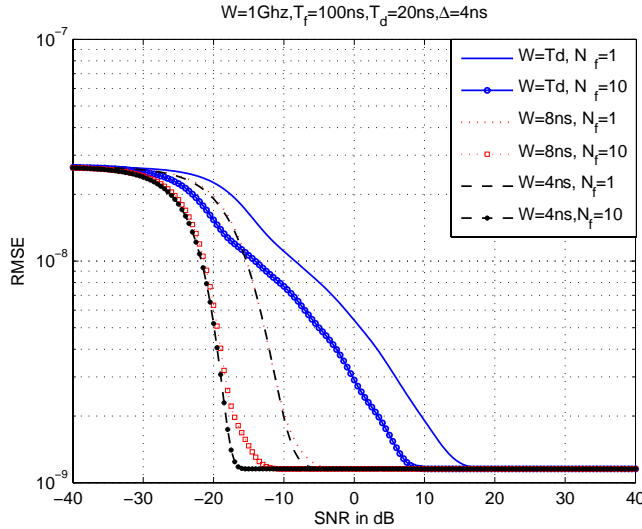


Figure 6.6: Upper bound on RMSE of the energy maximization scheme Vs. SNR for various integration window lengths and PDF $\alpha = 2$

value of the integration window W . The discretization step for the upper bound is again $\Delta = 0.5ns$. In this case, the estimator function is given as

$$L(k) = \frac{1}{N_0} G_k = \sum_{i=W\bar{k}\Delta}^{W(\bar{k}\Delta+W)-1} \|R_i\|^2, \quad k \in \{0, \dots, N - M - 1\} \quad (6.63)$$

We observe then that estimation error decreases significantly for decreasing window length W . We can see also that for $W = 4$ and $W = 8$, the error achieved in single frame (one shot) estimation is similar to that achieved by the multiframe one. This means that the energy detector scheme can provide precise estimation of the signal delay without a reliable estimation procedure. This is a desirable result for ranging or localization applications that may be offered by UWB networks as extra features.

Given the last result, we look now on the impact of the power decay factor on the choice of the integration window length. Fig. 6.7 illustrates the RMSE of energy maximization estimator vs. integration window length W , for various discretization step Δ , various power decay factor α , $T_f=100ns$, $T_d=20ns$, and $SNR=-10dB$. We then observe a tradeoff behavior where the optimal integration depends on the value of the decay factor. Indeed, for W greater than the optimal window length, loss is due to the fact that the integrator

collect no more significant signal components. While in the contrary case, the integrator misses significant signal components.

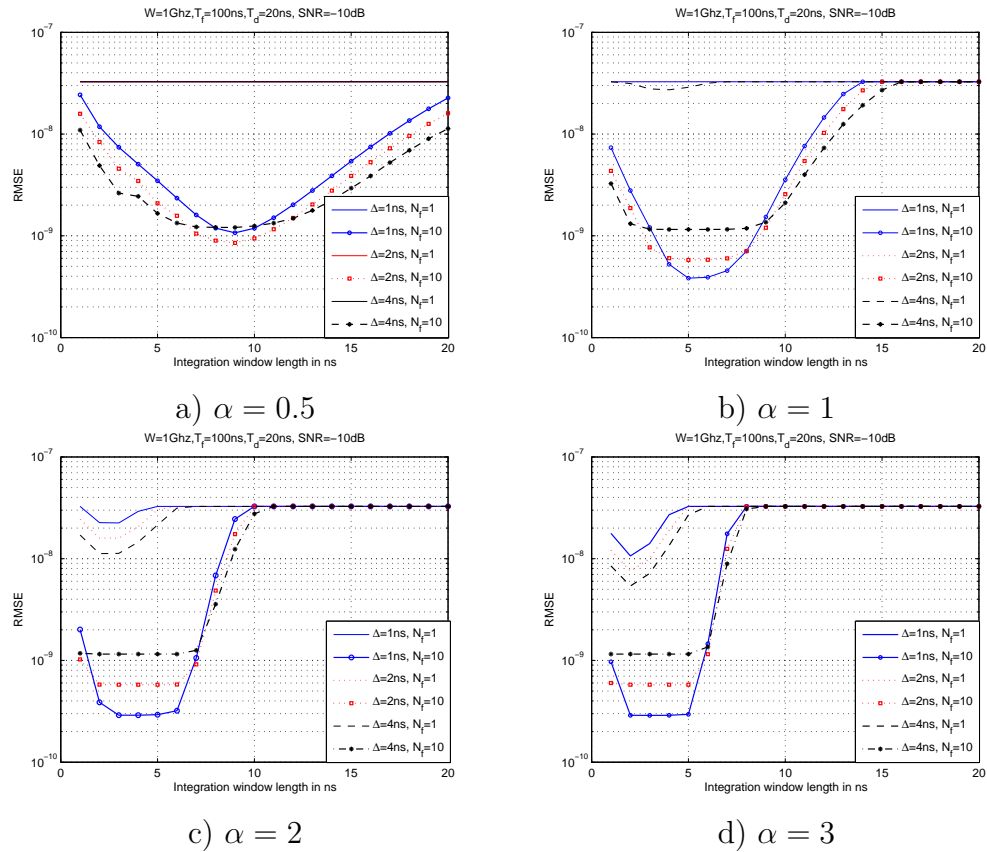


Figure 6.7: RMSE of energy maximization estimator Vs. integration window length, for various integrating step Δ , various power decay factor α , $T_f=100\text{ns}$, $T_d=20\text{ns}$, and $\text{SNR}=-10\text{dB}$

6.4 Conclusion

In this chapter, we give fundamental limitations on the performance of some coherent and non-coherent time-delay estimation schemes of UWB signals. For this purpose, we use the IZZLB to express the lower bound and we derive a new upper bound suited for sub-optimal estimators. The upper bound is simple to derive, and was shown to provide good indications of estimation

performances.

The IZZLB was then used to set a lower bound of a ML estimator based on the 2nd. order statistics information, and performance of sub-optimal schemes was given by the upper bounds.

The obtained estimation results of the energy detection scheme are motivating to consider the same procedure for reception purpose. Nevertheless, the obtained performance account only for single user transmission, so the multi-user case is still to be investigated.

6.A Appendix

6.A.1 Derivation of the Improved Ziv-Zakai Lower Bound

The Ziv-Zakai formulation of the lower bound is based on the probability of deciding correctly between two possible values (θ) and ($\theta + x$) of the signal delay. For our purposes it is the signal arrival time θ_0 . The derivation of this bound relies on result from detection theory [114, 120, 121].

A detection scheme which minimizes the probability of error simply forms the likelihood ratio test (LRT) between the two hypothesized delays. Consider now the following suboptimal detection procedure based on some arbitrary estimate $\hat{\theta}_0$ of θ_0

$$|\hat{\theta}_0 - \theta| \stackrel{\theta_0 = \theta + x}{\underset{\theta_0 = \theta}{\geq}} |\hat{\theta}_0 - \theta - x| \quad (6.64)$$

The decision is therefore made to the favor of θ if $|\hat{\theta}_0 - \theta| < |\hat{\theta}_0 - \theta - x|$ and $\theta + x$ otherwise. If the two hypothesized delays are equally likely to occur, the probability of error for this suboptimal detection scheme is given by

$$\frac{1}{2}P(\hat{\theta} - \theta > x/2|\theta) + \frac{1}{2}P(\hat{\theta} - \theta - x \leq -x/2|\theta + x) \quad (6.65)$$

Let $P_d(\theta, \theta + x)$ denotes the minimum attainable probability of detection error (associated with the LRT). It immediately follows that

$$P_d(\theta, \theta + x) \leq \frac{1}{2}P(\hat{\theta} - \theta > x/2|\theta) + \frac{1}{2}P(\hat{\theta} - \theta - x \leq -x/2|\theta + x) \quad (6.66)$$

Let the a priori domain of θ_0 by $[0, T_f - T_d]$. Since inequality (6.66) holds for any pre-selected θ and x , it certainly holds for all combinations of θ and x such that $\theta, x \in [0, T_f - T_d]$, or equivalently

$$0 \leq \theta \leq T_f - T_d - x \quad 0 \leq x \leq T_f - T_d \quad (6.67)$$

Let $\epsilon = \hat{\theta} - \theta_0$. Integrating (6.66) with respect to θ over $[0, T_f - T_d - x]$ one obtains

$$\begin{aligned}
& \int_0^{T_f - T_d - x} P_d(\theta, \theta + x) d\theta \\
\leq & \frac{1}{2} \int_0^{T_f - T_d - x} [P(\epsilon > x/2|\theta) + P(\epsilon - x \leq -x/2|\theta + x)] d\theta \\
= & \frac{1}{2} \int_0^{T_f - T_d - x} P(\epsilon > x/2|\theta) d\theta + \frac{1}{2} \int_x^{T_f - T_d} P(\epsilon - x \leq -x/2|\theta) d\theta \\
\leq & \frac{1}{2} \int_0^{T_f - T_d} P(|\epsilon| \geq x/2|\theta) d\theta \tag{6.68}
\end{aligned}$$

Now define

$$F(x) = \frac{1}{T_f - T_d} \int_0^{T_f - T_d} P(|\epsilon| \geq x|\theta) d\theta \tag{6.69}$$

$F(x)$ can therefore be regarded as the average of $P(|\epsilon| \geq x|\theta)$ where θ is uniformly distributed in $[[0, T_f - T_d]$. In terms of $F(x)$ the inequality in (6.68) reads

$$\int_0^{T_f - T_d - x} P_d(\theta, \theta + x) d\theta \leq \frac{T_f - T_d}{2} F(x/2) \tag{6.70}$$

Multiplying both sides of (6.70) by $2x/(T_f - T_d)$ and integrating with respect to x over $[0, T_f - T_d]$ one obtains

$$\begin{aligned}
\frac{1}{T_f - T_d} \int_0^{T_f - T_d} x dx \int_0^{T_f - T_d - x} P_d(\theta, \theta + x) d\theta &= 4 \int_0^{\frac{T_f - T_d}{2}} x F(x) dx \leq 4 \int_0^{T_f - T_d} x F(x) dx \\
&= 2x^2 F(x)|_0^{(T_f - T_d)^+} - 2 \int_0^{T_f - T_d} x^2 F(x) dx \tag{6.71}
\end{aligned}$$

One can always assume that $F((T_f - T_d)^+) = 0$ (otherwise the estimate can be improved by an obvious modification). One further observes that

$$\bar{\epsilon}^2 = - \int_0^{T_f - T_d} x^2 F(x) dx \tag{6.72}$$

Where $\bar{\epsilon}^2$ is, by definition, the MSE when θ_0 is uniformly distributed in $[0, T_f - T_d]$. Substituting (6.72) into (6.71) one immediately obtains

$$E[(\hat{\theta}_0 - \theta_0)^2] \geq \int_0^{T_f - T_d} x dx \int_0^{T_f - T_d - x} \frac{P_d(\theta, \theta + x)}{T_f - T_d} d\theta \tag{6.73}$$

This is the improved version of the Ziv-Zakai bound derived in [14]. Assuming that $P_d(\theta, \theta + x) = P_e(x)$ is independent of θ_0 , the expression in (6.4) becomes

$$E[(\hat{\theta}_0 - \theta_0)^2] \geq \frac{1}{T_f - T_d} \int_0^{T_f - T_d} x(T_f - T_d - x) P_d(x) dx \quad (6.74)$$

6.A.2 Derivation of the detection error probability

We begin by making a Karhunen-Loeve decomposition of R in the basis of its covariance matrix.

$$K_0 = U\Lambda U^\dagger \quad (6.75)$$

where Λ is a diagonal matrix with eigenvalues of K_0 as diagonal elements, and U is a unitary matrix formed by the corresponding eigenvectors.

R can be written then as

$$R = U\Lambda^{\frac{1}{2}}\dot{R} \quad \text{where} \quad \dot{R} = \Lambda^{-\frac{1}{2}}U^\dagger R \quad , \quad K_{\dot{R}} = I \quad (6.76)$$

So we get

$$Z = \dot{R}^\dagger \dot{Q}_x \dot{R} \quad \text{with} \quad \dot{Q}_x = \Lambda^{\frac{1}{2}}U^\dagger Q_x U\Lambda^{\frac{1}{2}} \quad (6.77)$$

As ${}_1K_{\theta_1,x}$ and ${}_2K_{\theta_1,x}$ are Hermitian, \dot{Q}_x is also Hermitian and can be decomposed also as VMV^\dagger where V is an orthonormal matrix of eigenvectors of \dot{Q}_x and M is a diagonal matrix of corresponding eigenvalues μ_x^i . We can thus write

$$Z = (V^\dagger \dot{R})^\dagger M (V^\dagger \dot{R}) = \sum \mu_x^i \|\ddot{R}_i\|^2 \quad (6.78)$$

Where

$$\ddot{R} = V^\dagger \dot{R} = V^\dagger \Lambda^{-\frac{1}{2}} U^\dagger R \quad , \quad K_{\ddot{R}} = V K_{\dot{R}} V^\dagger = I \quad (6.79)$$

As R_i are circular complex Gaussian random variables $CN(0, 1)$, the random variables U_i defined as $U_i = 2\|\ddot{R}_i\|^2$ are independent chi-square random variables with two degrees of freedom $\chi(2)$. We have thus expressed Z as weighted sum of N independent Chi-square random variables.

The eigenvalues $\{\mu_x^i\}$ are not necessary equals nor distinct, the closed form

expression of the distribution of Z is not tractable. However, a linear combination of chi-square variables can be well approximated by a Gamma distributed variable [105, 122] that have the same first and second moments.

We split the set of eigenvalues as $a_x^i = \{\mu_x^i, \mu_x^i \geq 0\}$ and $b_x^i = \{|\mu_x^i|, \mu_x^i < 0\}$. Z can then be given as

$$Z = Z_1 - Z_2 \quad \text{Where} \quad Z_1 = \sum \frac{a_x^i}{2} U_i \quad Z_2 = \sum \frac{b_x^i}{2} U_i \quad (6.80)$$

And the probability of decision error becomes

$$P_d(x) = \frac{1}{2} [P_{H_1}(Z_1 - Z_2 > 0) + P_{H_2}(Z_1 - Z_2 < 0)] \quad (6.81)$$

We approximate then Z_1 and Z_2 as a gamma distributed variables $G_1(\alpha_1, \beta_1)$ and $G_2(\alpha_2, \beta_2)$.

The first two moments of V_1 and V_2 are

$$E[V_1] = m1 = \sum a_x^i \quad , \quad E[(V1 - m1)^2] = \sigma_1 = \sum (a_x^i)^2 \quad (6.82)$$

$$E[V_2] = m2 = \sum b_x^i \quad , \quad E[(V2 - m2)^2] = \sigma_2 = \sum (b_x^i)^2 \quad (6.83)$$

By equating the first moments of $\{V_1, G_1\}$ and $\{V_2, G_2\}$ we obtain

$$\alpha_1 = \frac{m1^2}{\sigma_1} \quad , \quad \beta_1 = \frac{\sigma_1}{m1} \quad (6.84)$$

$$\alpha_2 = \frac{m2^2}{\sigma_2} \quad , \quad \beta_2 = \frac{\sigma_2}{m2} \quad (6.85)$$

From [123], we have

$$F(Z_1 - Z_2 \leq 0) = \frac{\beta_1^{\alpha_2} \beta_2^{\alpha_1}}{\alpha_1 B(\alpha_1, \alpha_2) (\beta)^{\alpha}} {}_2F_1 \left(1, \alpha, \alpha_1 + 1, \frac{\beta_2}{\beta} \right) \quad (6.86)$$

$$\text{with} \quad \alpha = \alpha_1 + \alpha_2, \quad \beta = \beta_1 + \beta_2 \quad (6.87)$$

6.A.3 Proof of Theorem 6.3.1

Proof by construction, the continuous-time estimator outperforms the discrete time one.

Consider now the discrete-time estimator, and define $P_{est}(i, a) = P(\hat{a} = \bar{i}\Delta | a_0 = a)$ as the estimation error probability of deciding \hat{a} as equal to $(i + \frac{1}{2})\Delta$ instead of the true parameter value a .

$$P_{est}(i, a) = P(\hat{a} = \bar{i}\Delta | a_0 = a) = \prod_{\substack{j=0 \\ j \neq i}}^{N-1} P(L(\bar{i}\Delta) > L(\bar{j}\Delta) | a_0 = b) \quad \text{for } i, j \text{ in } \{0, \dots, N-1\} \quad (6.88)$$

The distance between the true parameter a_0 and the estimated parameter \hat{a} is then distributed as follows

$$P_{ed}(\epsilon) = P(a_0 - \hat{a} = \epsilon) = \begin{cases} \frac{1}{T_f - T_d} \sum_{i=0}^{N-1-I_\epsilon} P_{est}(i, \bar{i}\Delta - \epsilon) & \text{for } \epsilon \in [-(T_f - T_d), 0] \\ \frac{1}{T_f - T_d} \sum_{i=I_\epsilon}^{N-1} P_{est}(i, \bar{i}\Delta - \epsilon) & \text{for } \epsilon \in [0, T_f - T_d] \end{cases} \quad (6.89)$$

Where $I_\epsilon = \left\lfloor \frac{|\epsilon|}{\Delta} \right\rfloor + 1$; $\lfloor x \rfloor_n$ denotes integer part of x .

The resulting mean square estimation error is then

$$MSE_d = \int_{-D}^D \epsilon^2 P_{ed}(\epsilon) d\epsilon \quad (6.90)$$

The expression in (6.90) is computationally consuming because of the sum in the expression of $P_{ed}(\epsilon)$ and the product in that of $P_{est}(a, a + \epsilon)$. In order to reduce the complexity of $P_{est}(a, a + \epsilon)$ we upper bound the integral in 6.90 to consider only values of ϵ that coincide with the testing points $\{\frac{\Delta}{2}, \frac{3\Delta}{2}, \dots, N\Delta - \frac{\Delta}{2}\}$.

$$\begin{aligned} MSE_d &= \int_{-(T_f - T_d)}^0 \epsilon^2 P_{ed}(\epsilon) d\epsilon + \int_0^{T_f - T_d} \epsilon^2 P_{ed}(\epsilon) d\epsilon \\ &= \int_{-N\Delta}^{-N\Delta + \Delta/2} \epsilon^2 P_{ed}(\epsilon) d\epsilon + \sum_{j=1}^{N-1} \int_{-\bar{j}\Delta}^{-(j-1)\Delta} \epsilon^2 P_{ed}(\epsilon) d\epsilon + \int_{-\Delta/2}^0 \epsilon^2 P_{ed}(\epsilon) d\epsilon \\ &\quad + \int_0^{\Delta/2} \epsilon^2 P_{ed}(\epsilon) d\epsilon + \sum_{j=1}^{N-1} \int_{j-1\Delta}^{\bar{j}\Delta} \epsilon^2 P_{ed}(\epsilon) d\epsilon + \int_{N\Delta - \Delta/2}^{N\Delta} \epsilon^2 P_{ed}(\epsilon) d\epsilon \end{aligned} \quad (6.91)$$

Now using the fact that $P_{ed}(\epsilon)$ is a decreasing function of $|\epsilon|$ we get

$$\begin{aligned}
MSE_d &\leq P_{ed}(-\overline{(N-1)\Delta}) \int_{-\overline{N}\Delta}^{-\overline{(N-1)\Delta}} \epsilon^2 d\epsilon + \sum_{j=1}^{N-1} P_{ed}(-\overline{(j-1)\Delta}) \int_{-\overline{j}\Delta}^{-\overline{(j-1)\Delta}} \epsilon^2 d\epsilon \\
&\quad + P_{ed}(0) \int_{-\Delta/2}^{\Delta/2} \epsilon^2 d\epsilon + \sum_{j=1}^{N-1} P_{ed}(\overline{(j-1)\Delta}) \int_{\overline{j-1}\Delta}^{\overline{j}\Delta} \epsilon^2 d\epsilon + P_{ed}(\overline{(N-1)\Delta}) \int_{\overline{N-1}\Delta}^{\overline{N}\Delta} \epsilon^2 d\epsilon \\
&\leq \frac{\Delta^3}{12} \left[\frac{N}{T_f - T_d} + \sum_{j=1}^N (12j^2 + 1) \left[P_{ed}(-\overline{(j-1)\Delta}) + P_{ed}(\overline{(j-1)\Delta}) \right] \right]
\end{aligned} \tag{6.92}$$

We have now discretized the estimation error to consider only points corresponding to the estimator's testing points. We can then upper bound the estimation error as follows

$$\begin{aligned}
P_{est}(i, \overline{k}\Delta) &= \prod_{\substack{j=0 \\ j \neq i}}^{N-1} P(L(\overline{i}\Delta) > L(\overline{j}\Delta) | a_0 = \overline{k}\Delta) \quad \text{for } i, j \text{ in } \{0, \dots, N-1\} \\
&\leq P(L(\overline{i}\Delta) > L(\overline{k}\Delta) | a_0 = \overline{k}\Delta)
\end{aligned} \tag{6.93}$$

The bound in (6.92) becomes

$$\begin{aligned}
MSE_d &\leq \frac{\Delta^2}{12} \left[1 + \frac{1}{N} \sum_{j=1}^N (12j^2 + 1) \left(\sum_{i=0}^{N-j} P(L(\overline{i}\Delta) > L(\overline{i+j}\Delta) | a_0 = \overline{i+j}\Delta) \right) \right. \\
&\quad \left. \left(\sum_{i=j}^{N-1} P(L(\overline{i}\Delta) > L(\overline{i-j}\Delta) | a_0 = \overline{i-j}\Delta) \right) \right]
\end{aligned} \tag{6.94}$$

If we assume that $P(L(a) > L(b) | a_0 = b)$ is independent from a_0 the inequality (6.94) becomes

$$\begin{aligned}
MSE_d &\leq \frac{\Delta^2}{12} \left[1 + \frac{1}{N} \sum_{j=1}^N (12j^2 + 1) \left(\sum_{i=0}^{N-j} P(L(\overline{i}\Delta) > L(\overline{i+j}\Delta) | a_0 = \overline{i+j}\Delta) \right) \right. \\
&\quad \left. \left(\sum_{i=j}^{N-1} P(L(\overline{i+j}\Delta) > L(\overline{i}\Delta) | a_0 = \overline{i}\Delta) \right) \right]
\end{aligned} \tag{6.95}$$

If we define $P_d(x)$ as the error probability of a binary hypothesis detector deciding between θ_1 and $\theta_1 + x$ (sec.6.2.1)

$$P_d(\bar{i}\Delta, \overline{i+j}\Delta) = \frac{1}{2} [P(L(\bar{i}\Delta) > L(\overline{i+j}\Delta)|_{a_0 = \overline{i+j}\Delta}) + P(L(\bar{i}\Delta) < L(\overline{i+j}\Delta)|_{a_0 = \bar{i}\Delta})] \quad (6.96)$$

Then we obtain

$$MSE_d \leq \frac{\Delta^2}{12N} \left[1 + \frac{2}{N} \sum_{j=1}^N (12j^2 + 1)(N - j)P_d(j\Delta) \right] \quad (6.97)$$

■

Chapter 7

General Conclusion & Perspectives for Future Works

Throughout this work, we have addressed the design, the enhancement, and the optimization of MAC protocols for wireless ad hoc networks. Since the introduction of the ALOHA systems and the associated MAC protocol, this topic has attracted significant research efforts, with the ultimate hope to set a basic theory that would be able to model the diversity of constraints and requirements that characterize it. Meanwhile, different aspects of the problem are addressed continuously by different approaches, enabling more and more advances in the treatment of the subject.

In dealing with MAC protocols for ad hoc networks, we have considered random access schemes, and we have focussed on two fundamental problems that affect their performances: The backoff scheme design and optimization, and the robust handling of the hidden terminal problem.

The first problem is inherent to any random access mechanism as collisions of packets are unavoidable. Thus, the performances of the MAC protocol in this case are mainly governed by the efficiency of its retransmission mechanism.

The second problem is associated to the multihop situations faced in ad hoc networks. It is shown that in this case, known efficient access protocol in single hop network, as the IEEE 802.11 DCF, suffers serious performance

degradation due to the lack of unique broadcasting channel to support efficient signalling schemes.

In the first part of the thesis, we address the optimization of the retransmission schemes for ALOHA and DCF protocols in single hop networks. Optimization is carried out in order to maximize the overall network throughput. Our goal was then to design simple and blind optimal retransmission mechanisms under this configuration. For ALOHA protocol, we find that the optimal retransmission scheme is not blind as it is sensitive to the network load.

For DCF protocol, we first show that the binary exponential backoff scheme is sub-optimal in term of throughput and fairness. We propose then a constant-window backoff mechanism that solves the fairness issue. Then, we derive the optimal backoff window length that brings the system to operate at maximum throughput. As for ALOHA protocol, the optimal window depends, among others, on the network load. However, since in CSMA mechanism the duration of idle slots is small compared to that of collisions, we propose to use the optimal window length of saturated load independently from the exact system load. We have proven then the effectiveness of this choice, and we have extended the analysis to consider the impact of queueing at nodes buffer on the system performance.

Multihop networks were addressed in the second part of the thesis. For DCF protocol, we have shown the weakness of the classical RTS/CTS handshaking in dealing with the hidden/masked node problems. We have then proposed a new handshaking mechanism, RTS/R-CTS, that handles effectively the hidden node problem, but at the expense of increased signalling overhead. The correctness of the proposed mechanism helped us in reusing the analytical model used in the single hop case, to consider arbitrary multihop topology, with little modifications. The Backoff scheme optimization was then addressed by arguing the use of a stochastic approximation (SA) algorithm to compensate the lack of symmetric channel behavior at the users. To avoid the need of cooperation among nodes in building their optimal retransmission mechanism, we have introduced the notion of reception throughput. Each node was then asked to maximize both its transmission and reception throughput. In doing so, we have avoided aggressive behavior of users, and we have limited the dependency of each node on the information of other users. As a result, we succeeded to characterize for each node, its optimal retransmission scheme, by some easy-to-learn parameters of system's activity. In the perspective of using UWB signalling technology for ad hoc networks,

and to take benefit from its multiplexing capabilities, we have introduced a new multi-channel ALOHA-like protocol. To relieve the channel assignment problem, a common channel (CC) was dedicated for broadcasting initial signalization message RTS (Request To Send), while other channels were used randomly by all nodes to complete communications setup and eventually for data transfers. The proposed protocol does not use virtual carrier sensing due to the masked node problem, neither physical carrier sensing. Thus, it is insensitive to the hidden node problem. The performance of the proposed protocol was analyzed in saturation conditions and shown to be very good if the retransmission scheme over the common channel is well designed. The analysis is extended to consider general load conditions. Then, we have shown again that it is sufficient to use the optimal saturation window under all loads to achieve near maximal throughput. This result was possible as a consequence of the asymmetry between idle periods duration on the common channel and data packet durations on the data channels. So we have succeeded to assimilate the behavior of CSMA protocol in a multi-channel multihop system.

In chapter (6), we have studied fundamental performance of time-delay estimation schemes in IR-UWB systems. This issue is crucial for the deployment of ad hoc based UWB solutions as the synchronization task of sub nanosecond signals appears to be a critical issue. In addition to their communication capabilities, future UWB networks are also expected to provide some interesting extra-features such as localization and ranging. This may help system designer in exploiting valuable information for power control, multiple access, and routing purposes.

Fundamental time-delay estimation performances were derived in term of lower and upper bounds on the MSE of different estimators. We have used the IZZLB to express the lower bound and we have derived a new upper bound that apply for any estimator, and that is simple to derive with controllable accuracy.

The bounds were then applied to characterize performance of perfect ML estimator, mis-matched ML estimator, EGC estimator, and energy detector estimator. Different results on estimators' performances were provided that have shown that the simple energy detector performs well with few numbers of signal's repetition and adequate integration window length.

In future works

- We will look for general framework for the analysis of the performance of MAC protocols in general multihop networks. We will especially focus on modeling some additional key cross-layer parameters to provide general treatment of the design and optimization issues.
- We will deeply analyze the use of SA algorithms for the joint backoff scheme optimization and power control of MAC protocols in arbitrary multihop network. We will investigate mainly on some critical aspect of these algorithms such the choice of the step size, the proofs of their convergence, and their robustness to estimation error and variations in network conditions.
- We will investigate on fundamental performance of some optimal and practical time delay estimation procedure in the multi-user setting.
- We will also consider performance of the closely-related issues of localization and ranging and study the integration of efficient mechanisms to exploit the information provided by them in the design of MAC and routing protocols.

Résumé

Les réseaux sans fil ont gagné une immense popularité au cours de ces dernières années. Leur utilisation prédominante a été dans les réseaux simple-bond munis d'infrastructure fixe. Vu le grand succès des systèmes de téléphonie sans fil (GSM, UMTS..) et des normes de réseaux locaux sans fil (WLAN) (IEEE802.11, Bluetooth,..), les utilisateurs/applications mobiles d'avenir exigeront encore une plus grande capacité et flexibilité du réseau comme une évolution naturelle de l'utilisation des technologies de communications vers des accés multimedia n'importe où n'importe quand. Ceci a motivé une activité significative de recherche sur les réseaux ad-hoc sans fil qui peuvent être utilisés en tant que réseaux privés de communication, réseaux de sondes, réseaux ad hoc mobiles, systèmes de communication de secours, etc... On définit comme étant un réseaux ad hoc sans fil toute collection de terminaux mobiles qui communiquent par le canal radio sans présence d'infrastructure fixe. Dans le cas où deux noeuds ne peuvent pas communiquer directement, chaque noeud doit agir en tant que relais, pour acheminer les paquets de données en direction de leurs destinations finales. Les caractéristiques principales de ce type de réseaux, dont les conséquences doivent être soigneusement adressées durant la conception des différents protocoles de communication, sont le manque d'unité centrale de contrôle, la difficulté de synchroniser le réseau, et l'éventuelle topologie multi-bonds.

1 Motivations

Dans les réseaux sans fil, le canal physique disponible est rare, ainsi, son utilisation est de grande importance; Par conséquent, le protocole de contrôle d'accès au canal (CAC) est une partie critique de la pile protocolaire qui détermine l'opération correcte et efficace du réseau. L'objectif principal des protocoles CAC pour les réseaux sans fil est de partager efficacement et équitablement le canal de communication entre les utilisateurs. Ces protocoles diffèrent selon l'environnement en question et les contraintes système à satisfaire. Les protocoles CAC peuvent être classifiés en deux groupes selon leurs stratégies pour déterminer les droits d'accès : protocoles d'accès déterministes et protocoles d'accès aléatoires.

Les protocoles d'accès déterministes assignent à chaque noeud dans le réseau un planing fixe de transmission indiquant dans quel créneau horaire ou dans quel canal de données (fréquences, codes d'étalement ou leurs combinaisons)

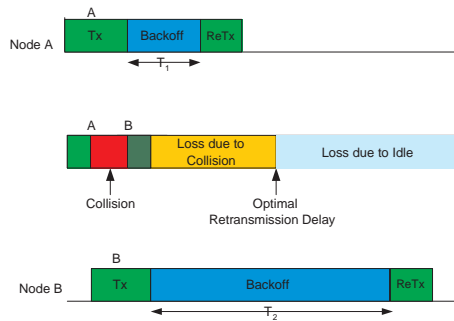


Figure 7.1: Le schema de retransmission

le noeud peut transmettre. Ces protocoles ont un délai de transmission fini mais sont inefficace à faible charge. En plus, en cas de topologie variable, ces protocoles peuvent potentiellement devenir inefficaces et instables puisque le maintien des planings de transmission, dans une topologie multi-bonds, peut monopoliser toute la capacité du réseau.

Les protocoles d'accès aléatoires sont plus appropriés aux architectures ad hoc, assez efficaces sous trafic sporadiques, et n'exigent pas la synchronisation globale du réseau. Cependant, leurs performances sont principalement limitées par leur capacité à gérer efficacement les retransmissions des paquets perdus à cause des collisions.

Dans les réseaux ad hoc sans fil, les noeuds utilisent le canal radio pour communiquer sans présence d'infrastructure fixe. Dans ce cas, l'accès multiple est fondamentalement distribué et aléatoire, et les collisions de paquets sont inévitables. Le défi principal qu'on rencontre donc pour la conception d'un (bon) protocole CAC est de contrôler de façon optimale les retransmissions des paquets perdus en collision. Le schéma de retransmission doit retarder la prochaine tentative de transmission assez longtemps afin d'éviter des collisions à répétition, mais pas trop longtemps pour ne pas gaspiller l'utilisation du canal (Fig. 7.1).

En raison des limitations de puissance, les noeuds dans les réseaux ad hoc ne sont pas toujours à la portée de transmission des uns et des autres. Dans ce cas, des noeuds peuvent être demandés d'agir en tant que relais temporels afin d'assurer la connectivité du réseau. Le contrôle d'accès multiple quant à lui devient plus compliqué puisque de nouveaux problèmes apparaissent, notamment le problème du terminal caché. Le problème du terminal

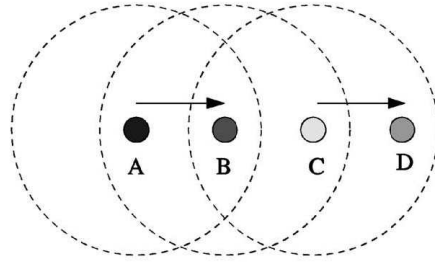


Figure 7.2: le problème du terminal caché

caché ne permet pas une signalisation efficace et complète des messages de signalisation. Il affecte ainsi n'importe quel protocole basé sur l'écoute ou sur la réservation du canal. Pour exemple, on considère un protocole CAC avec écoute de canal (CSMA) opérant dans la topologie de la Fig. 7.2. Dans cette topologie, le noeud C n'entend pas les transmissions du noeud A. Ainsi, le noeud C peut transmettre un paquet au noeud D alors que le noeud A transmet un paquet au noeud B. Ces transmissions simultanées mènent à une collision au noeud B, détruisant le paquet envoyé par le noeud A. Dans ce scénario, le noeud C est désigné comme étant un terminal caché par rapport au terminal A.

L'utilisation des canaux multiples dans les réseaux ad hoc sans fil peut fournir une amélioration de performances en réduisant les collisions et en permettant des transmissions simultanées, augmentant ainsi l'utilisation du canal radio et sa réutilisation spatiale, même avec une capacité physique totale des canaux égale à celle d'un réseau mono-canal. Les canaux multiples peuvent être obtenus par une division du canal dans le domaine fréquentiel (FDMA) ou dans le domaine des codes d'étalement (saut de fréquence, saut temporel, étalement directe du spectre).

La recherche sur la capacité des réseaux sans fil a exclusivement considéré les réseaux mono-canal [1–3]. Cependant, les résultats obtenus sont aussi valides pour des systèmes à canaux multiples, à condition que chaque noeud soit équipé par une interface physique dédiée à chaque canal. Avec une interface dédiée par canal, un noeud peut utiliser tous les canaux disponibles simultanément. Cependant, le nombre de canaux disponibles dans un réseau sans fil eut être assez grand, il se peut donc que ce soit assez coûteux de consacrer une interface par canal.

Dans le cas où les nœuds ne disposent pas d'une interface dédiée par canal, il est possible alors qu'une dégradation de la capacité du réseau se produise. Toutefois dans [4], il a été montré que dans un réseau de topologie aléatoire de taille n , ayant un nombre de canaux de l'ordre $O(\log n)$, même avec une interface simple par nœud, il n'y a aucune dégradation de capacité. Ceci implique qu'il est possible de construire des réseaux multi-canaux à capacité optimale avec peu de canaux et juste une interface par nœud. Ceci indique aussi que le temps est venu pour tirer bénéfice de la panoplie des techniques de multiplexage offertes par les avancées récentes en technologies de transmission dans la conception de protocoles efficaces de CAC.

En effet, en observant les normes existantes pour les réseaux locaux sans fils, nous pouvons constater que les protocoles CAC ne sont pas conçus pour exploiter pleinement les caractéristiques spécifiques des technologies de transmission.

Par exemple, les standards IEEE 802.11b et IEEE 802.11a définissent les normes de la couche physique (PHY) qui sont plus rapides que celle du standard IEEE 802.11. Dans IEEE 802.11b, il peut y avoir 3 canaux de PHY en service, alors que dans IEEE 802.11a, il peut y avoir 8 canaux. Cependant, les deux normes emploient le protocole CAC de l'IEEE 802.11 ou IEEE 802.11e¹ indépendamment des caractéristiques de la couche physique. Dans les normes courantes d'IEEE 802.11/11b/11a, les différents canaux de PHY sont principalement utilisés pour séparer les réseaux dans l'espace.

Afin de mieux exploiter les systèmes multi-canaux, le contrôle d'accès multiple doit adresser des problèmes additionnels de conception. En particulier, comment distribuer efficacement les demandes d'accès sur les différents canaux ?

La signalisation à très large bande (UWB) est un exemple de technologie de transmission qui peut être employée pour fournir des systèmes multi-canaux. Récemment, la signalisation UWB a gagné beaucoup d'intérêt depuis la publication des réglementations du (FCC) [6] qui définissent les masques des puissances d'émission des signaux UWB. Les règles du FCC autorisent la coexistence des nouveaux systèmes UWB avec d'autres services radio traditionnels protégés, et permettent l'utilisation potentielle de la transmission UWB sans assignement de spectre. Ceci est réalisé en contraignant

¹IEEE 802.11e [5] est une extension de l'IEEE 802.11 pour une garantie de qualité de service

les systèmes UWB à fonctionner avec une faible densité spectrale de puissance, approximativement au niveau de puissance du bruit thermique. Ainsi, l'interférence des émetteurs UWB aux autres utilisateurs UWB et aux autres systèmes sans fil ressemble à du bruit thermique. Comme résultat, le précieux spectre radio peut être (re)utilisé plus efficacement.

Les domaines d'application de la signalisation UWB sont beaucoup, s'étendant des systèmes d'imagerie (radar, systèmes médicaux et systèmes de surveillance) aux systèmes véhiculaires de radar, systèmes de communications et systèmes de mesure. La technologie offre aussi un fort potentiel pour le déploiement des futurs systèmes de communication personnels à courte portée (WPAN)

Dans l'IEEE, deux groupes de travail ont été créés pour étudier l'application de la technologie UWB. Le premier est le groupe 3a (TG3) [7] qui est chargé de la définition d'une couche physique alternative pour la norme IEEE 802.15.3 basée sur la signalisation UWB. Le PHY nouvellement défini répondra à la demande des consommateurs dans le domaine de la distribution multimédia et fonctionnera avec le CAC déjà existant [8]. Le second est le TG4 [9] qui travaille sur une norme pour les systèmes à basse puissance-bas débit, avec des capacités de localisation.

La forme la plus répandue de signalisation UWB est la technique d'impulsion radio (IR) [10]. La technologie IR-UWB utilise des signaux de très courtes durées ($\leq ns$) ayant des densités spectrales de puissance très basses. Elle est résistante aux propagations multi-trajets, a une très bonne résolution temporelle qui permet d'appliquer des algorithmes de localisation, et elle est relativement moins complexe et peu coûteuse. En raison de sa grande résolution temporelle [10, 11], une synchronisation très fine des signaux IR-UWB est obligatoire pour garantir des transmissions fiables dans les systèmes UWB.

Dans les réseaux ad hoc utilisant une signalisation UWB (aucune station de base pour effectuer la synchronisation), la synchronisation devient cruciale puisque que chaque émetteur et récepteur doivent se synchroniser avant chaque transmission. Ainsi, des schémas de synchronisation robustes doivent être conçus, et les informations sur leurs performances (statistiques de l'erreur de synchronisation) doivent être prises en considération durant la construction de la pile protocolaire.

Par exemple, si le temps de synchronisation nécessaire pour atteindre un niveau acceptable d'erreur est haut, alors on doit penser à un noeud central pour synchroniser tout le réseau. Par conséquent, le protocole CAC

et le protocole du routage doivent s'y adapter. Ou par exemple, si le temps nécessaire à la synchronisation est court, la taille des paquets de données doit aussi s'y adapter afin d'obtenir une bonne utilisation du canal.

En outre, la capacité des systèmes UWB à fournir des informations sur la localisation peuvent être de grand intérêt pour le contrôle de puissance, le CAC et le routage dans les réseaux ad hoc.

Les problèmes de la synchronisation et de la localisation des signaux UWB sont étroitement liés au problème de l'estimation du temps d'arrivée des signaux UWB. En effet, la synchronisation consiste en deux phases : une première phase d'acquisition approximative du signal qui correspond à une estimation de son temps d'arrivée, suivie d'une deuxième phase d'acquisition fine et de maintien du signal. L'information sur la localisation est également établie sur la base de l'estimation du temps d'arrivée du signal.

2 Contributions

Dans cette thèse, nos principales objectifs sont la conception, l'analyse et l'optimisation de protocoles CAC existants ou nouveaux pour les réseaux ad hoc sans fil, et l'étude des limites fondamentales de l'estimation du temps d'arrivée des signaux IR-UWB.

2.1 Réseaux Simple-Bond

Pour les réseaux simple-bond, nous nous concentrons sur la dérivation de schémas de retransmissions optimaux qui maximisent la capacité totale du réseau. Nous nous intéressons spécialement aux schémas quasi-aveugles qui nécessitent juste une information sur la taille du réseau. En effet, les schémas existants se basent soit sur l'estimation du nombre des paquets en attente de retransmission, soit sur d'autres informations obtenues par la mesure de l'activité du canal. L'information sur la taille du réseau est plus simple à obtenir dans les réseaux simple-bond. Nous considérons alors spécialement le protocole ALOHA synchronisé [12] et le protocole CAC du standard IEEE 802.11 connu sous le nom DCF [13].

2.1.1 Protocole ALOHA, Analyse & Optimisation

Historiquement, ALOHA pur [17] est le premier protocole CAC aléatoire. Il a été employé pour la première fois dans le système ALOHA, un réseau

d'accès simple-bond développé en 1970 l'université d'Hawai, utilisant la commutation par paquets sur canal radio. Pur ALOHA permet à chaque utilisateur de transmettre quand il désire. Si l'émetteur reçoit une confirmation par le récepteur de la bonne réception du paquet au cours d'un certain délai, alors il sait qu'aucun conflit ne s'est produit. Autrement, à la fin de ce délai, il suppose qu'une collision s'est produite, il doit donc retransmettre le paquet. Afin d'éviter la répétitions des conflits d'accès, le délai de retransmission est tenu aléatoire, évitant ainsi que les utilisateurs retransmettent au memes instants. Une version synchronisée de ALOHA [12], est obtenue en divisant le temps en intervalles de durées égales à la durée de transmission d'un paquet. Chaque utilisateur est synchronise alors sa transmission avec le debut des intervalles. Quand deux paquets se heurtent, ils se recouvrent complètement plutôt que partiellement, fournissant une augmentation de la l'utilisation du canal. En raison des conflits et du temps de canal non utilisé, la capcite obtenue par ALOHA est seulement de 18% pour pur ALOHA et de 36% pour ALOHA synchronisé. La version synchronisée est certe plus efficace, mais dans les réseaux multi-bonds, la synchronisation peut être très compliquée et couteuse à réaliser.

Une des caractéristiques dynamiques importante des réseaux ALOHA est qu'ils possèdent, statistiquement, deux points stables d'équilibre, un dans une région souhaitable de court délai (faible nombre des paquets en attente de retransmission), et l'autre dans une région indésirable de long délai (grand nombre des paquets en attente de retransmission). Puisque la stabilité est seulement statistique en nature, ALOHA oscille entre ces deux points, alors que les performances du système sont principalement régies par les probabilités à l'état stationaire [18, 19]. Dans [20], les auteurs ont prouvé la stabilité des schémas de retransmission où les probabilités de retransmission dépendent du nombre exacte des paquets en attente. Plusieurs travaux ont alors proposé des procédures dynamiques de contrôle des retransmissions pour maintenir ALOHA dans un régime stable et à faible délai [20–22]. Cependant, ces schémas ne peuvent pas être mis en application d'une façon distribuée. Des stratégies décentralisées de retransmission, comme celles présentées dans [22, 23] sont sous-optimales car elles se basent seulement sur une estimation du nombre de paquets en attente [23], ou sur une évaluation de certaines métriques de performances obtenues par la mesure de l'activité du canal. [22].

Dans le chapitre 2, on passe en revue les performances de ALOHA synchronisé dans les réseaux simple-bond et on discute sa bi-stabilité. On utilise une

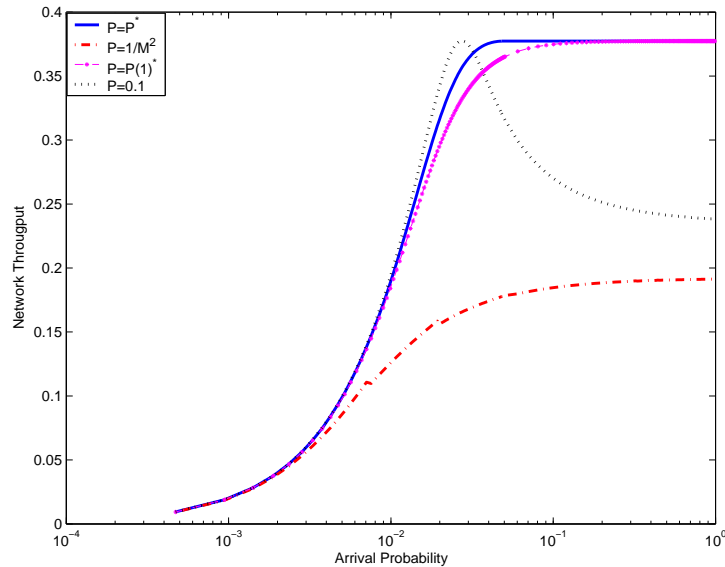


Figure 7.3: Débit obtenu par ALOHA dans un réseau de taille $n=20$ sous différents choix de probabilités de retransmission

analyse en point d'équilibre pour obtenir un schéma de retransmission optimal qui ne depend pas du nombre des paquets en attente de retransmission. Le schéma obtenu est stable mais pas quasi-aveugle puisqu'il dépend en plus de la taille du réseau, de la charge du trafic.

Afin d'obtenir un schéma quasi-aveugle, on utilise le schéma optimal de retransmission obtenu en saturation de trafic sous toutes les charges du réseau. Sous ce choix, ALOHA atteint un débit quasi-optimal et un délai relativement quasi-optimal, Fig. (7.3, 7.4).

2.1.2 Protocole IEEE 802.11 DCF, Analyse & Optimisation

Peut-etre l'amélioration principale dans la conception des protocoles CAC était l'introduction de la technique de l'accès multiple avec écoute de canal (CSMA) par Kleinrock et Tobagi [30]. CSMA réduit le niveau d'interférences provoquées par les collisions des paquets en permettant à chaque terminal d'écouter au préalable le canal et de détecter donc les éventuelles transmissions en cours. En se basant sur l'information de l'état du canal (occupée ou libre), chaque terminal prend une mesure prescrite par le protocole associé à CSMA (persistant, non-persistant, etc.). En particulier, chaque terminal ne

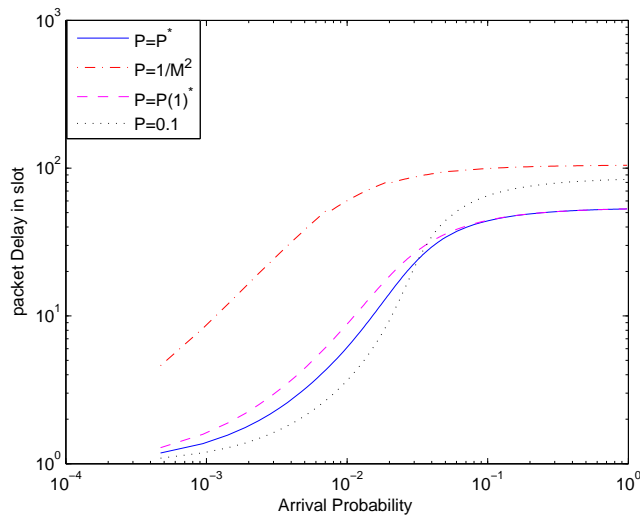


Figure 7.4: Délai obtenu par ALOHA dans un réseau de taille $n=20$ sous différents choix de probabilités de retransmission

peut jamais transmettre quand le canal est occupé. Dans des réseaux simple-bond où tous les noeuds partagent le même canal, les protocoles CSMA peuvent atteindre de très bonnes performances si leurs schémas de retransmission sont bien conçus.

Dans le standard IEEE802.11 populaire est largement répandue pour les réseaux locaux sans fils [13], le protocole CAC principal est le protocole DCF (fonction distribuée de coordination). DCF est un schéma d'accès multiple avec écoute de canal et un mécanisme de retransmission à fenêtres exponentielles binaires (BEB). Le mécanisme BEB a l'avantage d'être simple et n'exige pas la coopération des utilisateurs ou n'importe quelle information sur l'état du canal. Il essaie d'adapter aveuglément la fenêtre de compétition au niveau de congestion du canal en se basant seulement sur son expérience, c.à.d., la fenêtre de compétition est agrandie en cas de collision, et elle est remise à sa valeur initiale en cas de succès. Ses performances cependant s'avèrent sous-optimales, en terme de débit puisqu'il a besoin de plusieurs tentatives pour trouver la meilleure taille de la fenêtre de compétition, et également en terme d'équité à court terme puisqu'il favorise le premier utilisateur à réussir sa transmission à entrer encore en concurrence pour le canal, avec la plus petite fenêtre de compétition, contre d'autres utilisateurs qui eux

ont éventuellement des fenêtres plus grandes. L'amélioration de BEB a été largement adressée dans la littérature, les schémas proposés peuvent être divisés en deux classes :

1. schémas aveugles: comme dans BEB, il n'y a aucun besoin de mesurer l'activité du canal ; le changement de la longueur de la fenêtre de compétition s'effectue suite aux collisions ou succès mais d'une autre façon que dans BEB ([40] MILD, FCR [41], [42] d'EIED pour citer peu) afin d'améliorer le débit et/ou l'équité à court terme.
2. : schémas cohérents: ici l'optimisation est faite afin d'adapter dynamiquement la fenêtre de compétition pour conduire le système à atteindre un certain état d'optimalité. La distance par rapport à l'état optimal est obtenue en mesurant certaines métriques à partir de l'état du canal d'accès. Ces schémas modifient donc certains paramètres pour réduire la distance entre l'état actuel et l'état optimal [43–46]. Même si ces schémas identifient et essaient d'atteindre un point optimal de fonctionnement du système, leurs façons de changer les paramètres clés pour atteindre l'optimalité n'est elle pas optimale comme dans les schémas aveugles.

Dans le chapitre 3, nous donnons d'abord une analyse détaillée des performances du protocole IEEE802.11 DCF dans des conditions de trafic générales. Nous dérivons les statistiques du délai du protocole, et nous prouvons la non-équité à court terme du schéma de retransmission BEB. Nous présentons alors un schéma optimal de retransmission, et nous montrons qu'il est suffisant d'employer la fenêtre optimale de la saturation sous toutes les charges du réseau pour atteindre un débit et un délai quasi-optimal, Fig. (7.5,7.6), et une équité à court terme améliorée, Fig. (7.7). Ce choix paraît très judicieux pour les systèmes à écoute de canal puisque la durée des périodes sans activité du canal est petite comparée à la durée des collisions. Ainsi, la perte infligée par l'emploi de la fenêtre optimale de saturation (la plus grande pour une taille donnée du réseau) sous toutes les charges est petite. Notre schéma est donc quasi-aveugle.

Afin de considérer l'effet des files d'attente sur les performances de DCF, on propose un nouveau algorithme récursif qui utilise les statistiques du délai de DCF pour les intégrer dans un modèle de file d'attente de type M/G/1/K. Les résultats obtenus par ce dernier modèle sont comparés aux résultats de simulation de DCF sous le simulateur NS2, Fig. (7.8, 7.9).

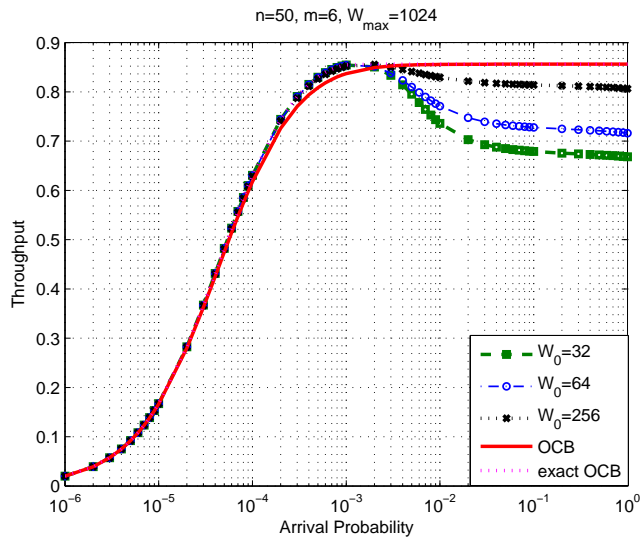


Figure 7.5: Débit d'un réseau de taille $n=50$

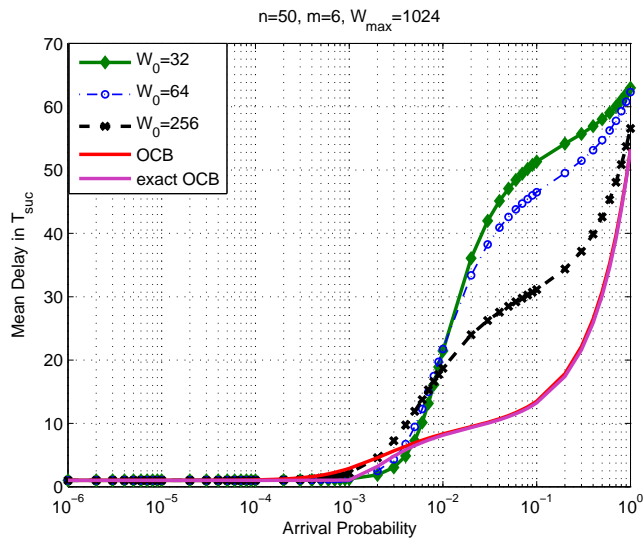


Figure 7.6: délai normalisé d'un réseau de taille $n=50$

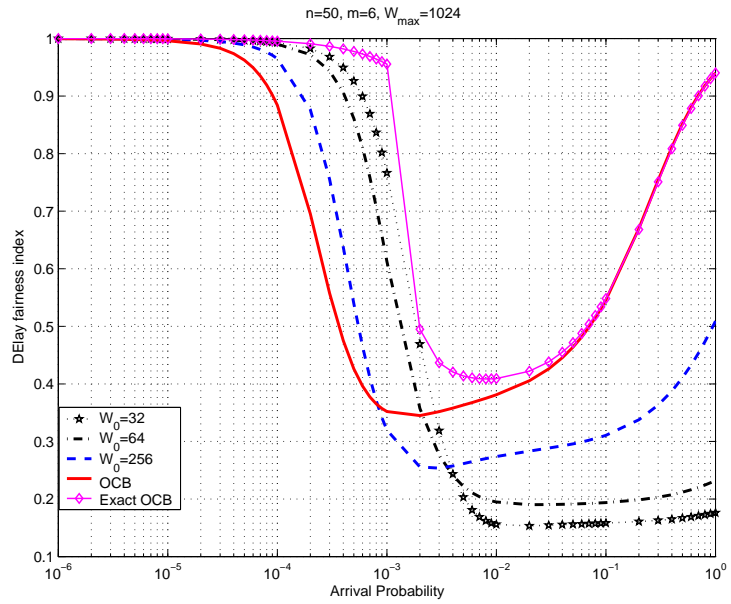


Figure 7.7: Indice d'équité de Jain sur le délai d'un réseau de taille $n=50$

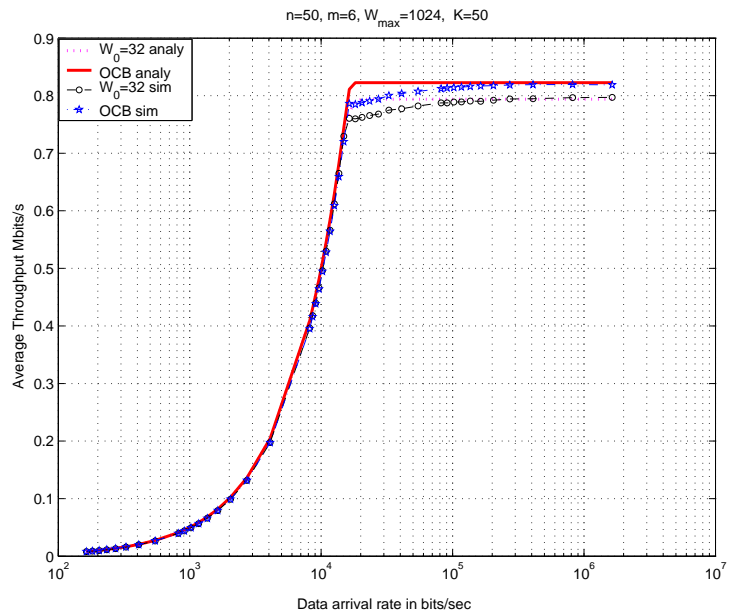


Figure 7.8: Débit du modèle théorique vs. simulation

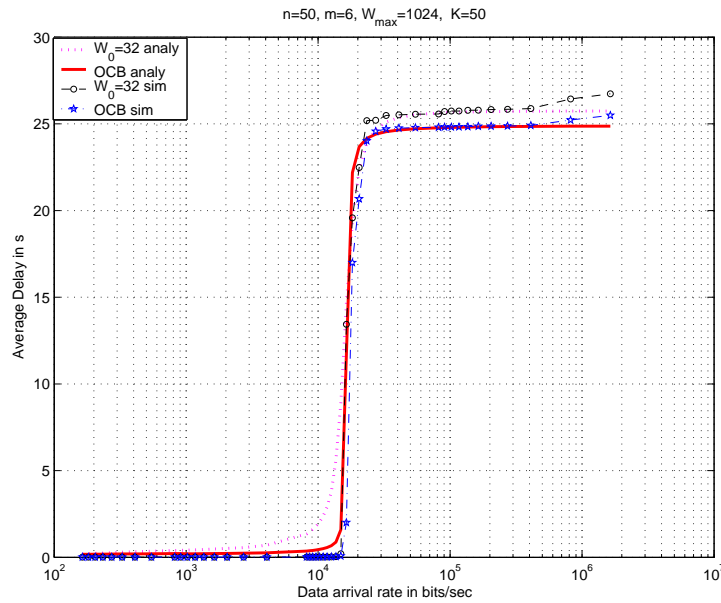


Figure 7.9: Délai du modèle theorique vs. simulation

2.2 Réseaux Multi-bonds

Les limitations physiques ou système des puissances d'émission produisent des situations où les noeuds ne partagent pas tous le même voisinage. Les protocoles CAC ont alors à résoudre en plus le problème du terminal caché qui détériore les performances de tout mécanisme basé sur l'écoute ou la réservation du canal.

2.2.1 IEEE803.11 DCF, Amélioration & Optimisation

Afin de résoudre le problème du terminal caché, le protocole IEEE 802.11 DCF a intégré un mécanisme secondaire d'accès qui effectue une réservation du canal dans les voisinages de l'émetteur et du récepteur. La réservation est obtenue par l'échange de deux messages de signalisation RTS et CTS qui bloquent l'accès au canal des terminaux qui les reçoivent. Cependant, il a été montré que RTS/CTS ne résout pas complètement le problème du noeud caché, et qu'il peut même atteindre des performances inférieures à celles du schéma d'accès basic de DCF dans certains réseaux multi-bonds [70]. Ceci

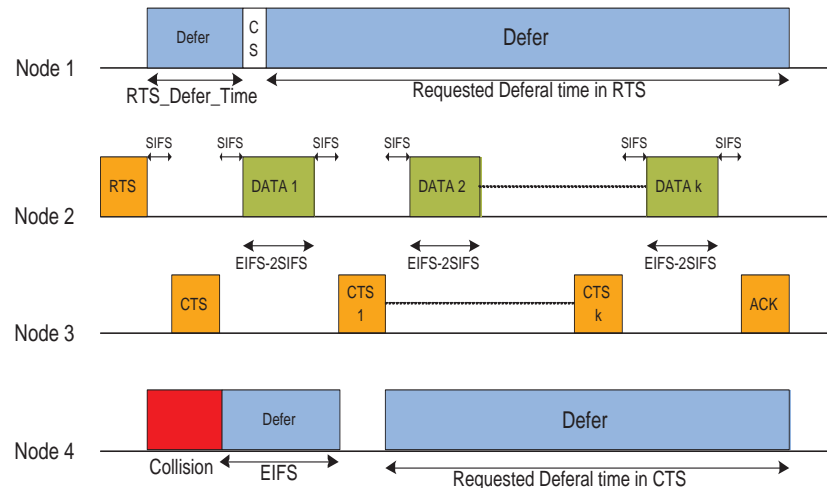


Figure 7.10: Illustration du mécanisme RTS/R-CTS

est dû au fait que le fonctionnement correcte de RTS/CTS nécessite que tous les nœuds du réseau aient accès aux messages de réservation. Cette contrainte est impossible à respecter dans les réseaux multi-bonds à cause du terminal masqué [69]. Beaucoup de travaux dans la littérature ont adressé ce problème et ont proposé des améliorations au mécanisme RTS/CTS [69, 71–73]. Dans le chapitre 4, nous présentons une modification du mécanisme de réservation RTS/CTS pour résoudre correctement le problème du terminal caché et celui du terminal masqué. Le nouveau mécanisme, baptisé RTS/R-CTS, est basé sur la répétition du message CTS et sur les contraintes temporelles de DCF afin de protéger la réception des paquets de données Fig. (7.10). Ensuite, nous analysons les performances du protocole résultant, et nous proposons un algorithme distribué basé sur la théorie des Approximations Stochastiques pour contrôler la longueur de la fenêtre de compétition afin de maximiser le débit en émission et en réception de chaque nœud. De cette manière, nous avons évité le comportement agressif des utilisateurs, et nous avons limité la dépendance de chaque nœud à l'information des autres utilisateurs.

2.2.2 ALOHA Multi-Canaux, Conception & Optimisation

Dans le chapitre 5, nous proposons un nouveau protocole ALOHA pour les réseaux ad hoc multi-canaux. Pour éviter le problème d'assignement de

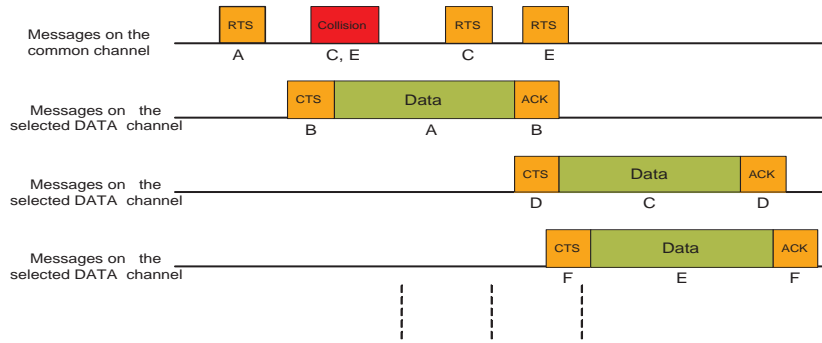


Figure 7.11: Exemple du fonctionnement du protocole ALOHA multi-canaux

canaux, un canal commun (cc) est consacré à la diffusion du message de signalisation initiale RTS, alors que les autres canaux (canaux de données) sont utilisés aléatoirement par tous les noeuds pour terminer la signalisation et éventuellement pour le transfert des paquets de données. Ceci simplifie le fonctionnement du protocole puisqu'aucune collaboration entre les noeuds n'est nécessaire pour réserver les canaux de données. Chaque noeud est équipé d'un émetteur récepteur semi-duplex simple, mais peut commuter sur tous les canaux. L'écoute du canal n'est pas utilisée, même sur les canaux de données. Sur le canal commun parce qu'elle est sans intérêt puisque le message RTS est de petite durée, et comme chaque noeud ne peut fonctionner que sur un canal à la fois, l'écoute des canaux de données peut prendre du temps de sorte que l'information rassemblée pendant la phase d'écoute devienne inexacte à la fin de l'opération d'écoute Fig. (7.11).

Les performances du protocole sont analysées pour un réseau multi-bonds de topologie symétrique et en saturation. On en dérive alors un schéma de retransmission optimal qui permet d'atteindre de très bonnes performances en terme de débit du réseau Fig. (7.12).

Nous nous intéressons ensuite à montrer l'existence d'un nombre optimal de canaux de données qui dépend non seulement de la taille du réseau n , mais aussi de la durée des paquets de données L . Fig. (7.13,7.14) pour des réseaux de taille 10 et 50, et différentes valeurs de L . En effet, d'un point de vue capacité du réseau, il a été montré dans [4] que le nombre optimal de canaux est égale à $\log n$ indépendamment de L .

L'analyse est alors prolongée pour considérer des conditions de trafic générales. Nous montrons encore qu'il est suffisant d'employer la fenêtre optimale de

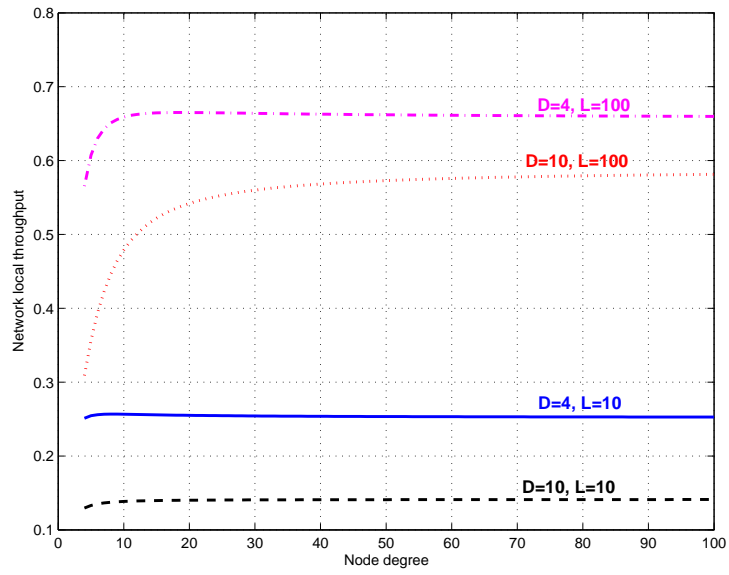
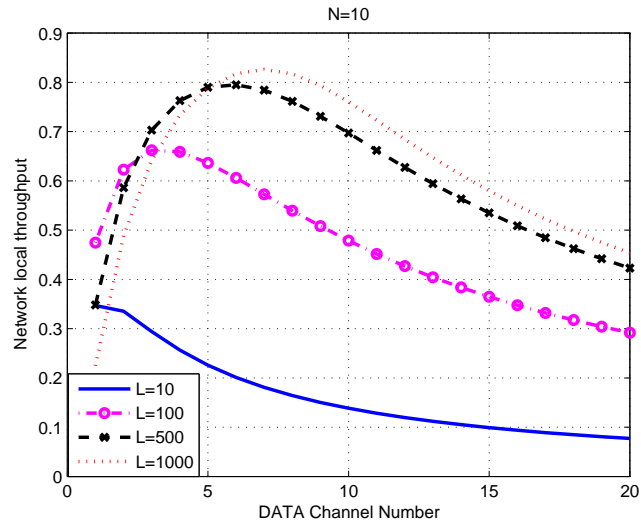


Figure 7.12: Débit du réseau

Figure 7.13: Network Throughput vs. Packet duration L for $N = 10$

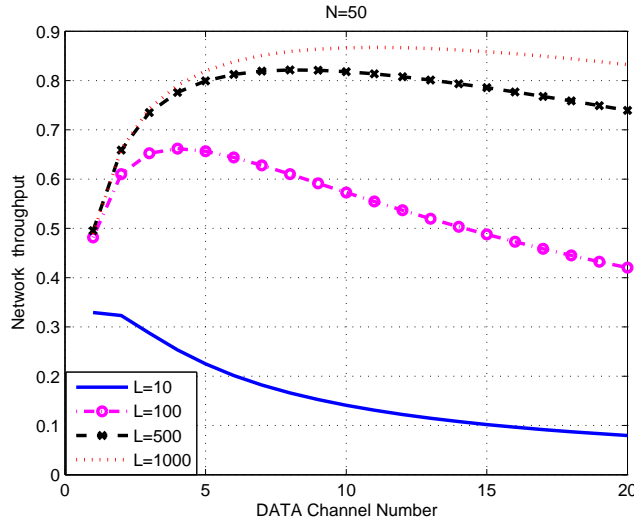


Figure 7.14: Network Throughput vs. Packet duration L for $N = 50$

saturation sous toutes les charges pour atteindre un débit quasi-optimal. Ce résultat est semblable à celui obtenu par DCF, mais ici sans utilisation de l'écoute du canal, Fig. (7.15).

2.3 Estimation du Temps d'Arrivée des Signaux UWB

Dans le chapitre 6 de la thèse, nous étudions les performances fondamentales de quelques estimateurs cohérent et non-cohérent du temps d'arrivée des signaux IR-UWB. Nous commençons par donner la bande minimale sur la variance de l'erreur de l'estimation. Puisque les signaux UWB possèdent une faible densité spectrale de puissance, il est plus approprié de caractériser la variance minimale d'erreur par la bande de Ziv-Zakai (IZZLB) [14] et non par la bande de Cramer-Rao [15, 16].

Nous appliquons alors la bande IZZLB pour dériver la limite inférieure sur la variance de l'erreur de l'estimation obtenue par un estimateur de maximum de vraisemblance (MV) ayant une connaissance parfaite des statistiques du deuxième ordre du signal reçu Fig. (7.16).

Nous nous intéressons ensuite à l'études des performances de certains estimateurs pratiques et sous-optimaux. Vue leurs sous-optimalité, il est

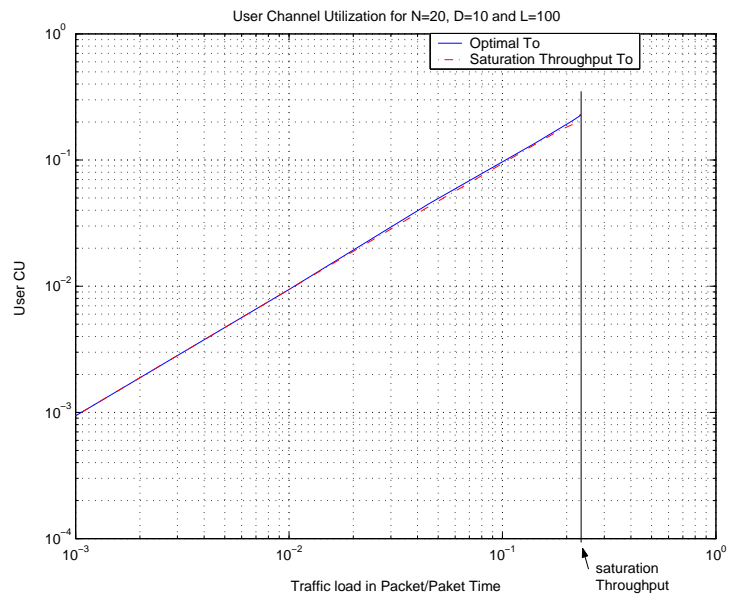


Figure 7.15: Débit utilisateur Vs. charge du trafic

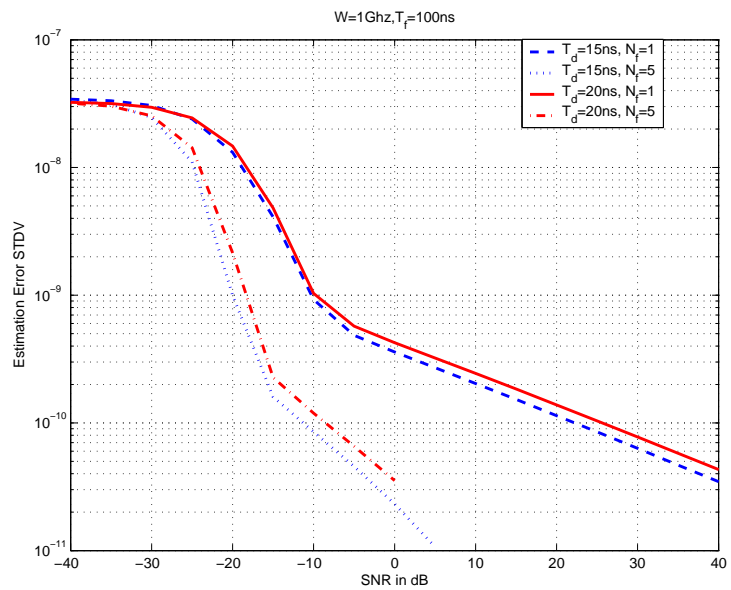


Figure 7.16: La bande IZZLB sur la variance de l'erreur d'estimation

nécessaire de caractériser leurs performances en terme de bandes supérieures sur la variance de leurs erreurs. Pour ceci, on donne d'abord une nouvelle bande supérieure sur les performances de n'importe quel estimateur. La nouvelle bande est simple à dériver et s'inspire de la bande de Ziv-Zakai. On applique ensuite cette bande pour un estimateur de vraisemblance ayant une connaissance bruitée des statistiques du signal reçu, et pour un estimateur aveugle qui effectue une combinaison, à niveau égale de puissance, du signal reçu. Enfin, on applique la bande pour un estimateur aveugle à temps discret qui effectue une collection de l'énergie du signal reçu. Ce dernier estimateur est facilement implementable dans un système pratique. On montre alors qu'il eut atteindre de très bonnes performance dans cas où le signal est répété suffisamment dans le temps et où la taille de la fenêtre de collection d'énergie est bien choisie Fig. (7.17).

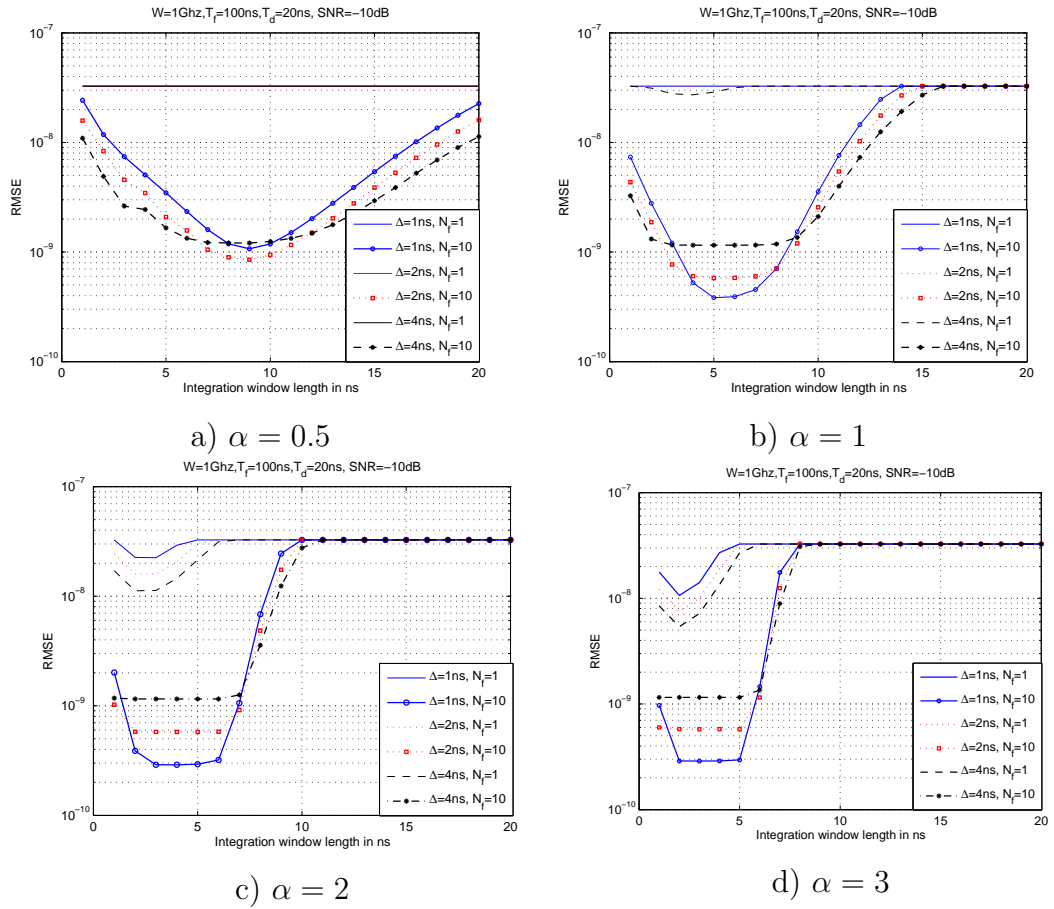


Figure 7.17: Bande supérieure sur la variance de l'erreur d'estimation de l'estimateur effectuant une collection d'énergie

Bibliography

- [1] P. Gupta and P. R. Kumar, “The capacity of wireless networks,” *IEEE transactions on Information theory*, vol. 46, pp. 388–404, 2000.
- [2] S. Toumpis and A. J. Goldsmith, “Capacity regions for wireless ad hoc networks,” *IEEE Transactions on Wireless Communications*, vol. 2, pp. 736–748, 2003.
- [3] M. Grossglauser and D. N. C. Tse, “Mobility increases the capacity of ad hoc wireless networks,” *IEEE/ACM Transactions on Networking*, vol. 10, pp. 477–486, 2002.
- [4] P. Kyasanur and N. H. Vaidya, “Capacity of multichannel wireless networks: Impact of number of channels and interfaces,” *Proceed. ACM MOBICIM*, 2005.
- [5] I. D. S. 802.11e, “Amendment: Medium access control (mac) enhancements for quality of service (qos), d2.0a,” 2001.
- [6] F. document 00-163, “Revision of part 15 commission rules et docket no. 98-153 regarding uwb transmission systems,” adopted 2-14-2002.
- [7] 802.15.3, “<http://www.ieee802.org/15/pub/tg3a.html>,”
- [8] I. D. 802.15.3, “Wireless medium access control (mac) and physical layer specifications for wireless personal area networks (wpan),” 2003.
- [9] 802.15.4, “<http://www.ieee802.org/15/pub/tg4a.html>,”
- [10] E. A. Homier and R. A. Scholtz, “Rapid acquisition of ultra-wideband signals in the dense multipath channel,” *Proceed. IEEE Conference on UWB Systems and Technologies*, pp. 245–250, 2002.

-
- [11] M. Z. Win and R. A. Scholtz, "On the energy capture of ultrawide bandwidth signals in sense multipath environments," *IEEE Communications Letters*, vol. 2, pp. 245–247, 1998.
 - [12] L. G. Roberts, "Aloha packet system with and without slots and capture," *Computer Communications Review*, vol. 5, pp. 28–42, 1975.
 - [13] IEEE, "Wireless lan medium access control (mac) and physical layer (phy) specifications," *IEEE 802.11 standards*, 1999.
 - [14] D. Chasan, M. Zakai, and J. Ziv, "Improved lower bounds on signal parameter estimation," *IEEE transactions on Information Theory*, vol. 21, pp. 90–93, 1975.
 - [15] H. Cramér, *Mathematical Methods of Statistics*. Princeton University Press, 1946.
 - [16] C. R. Rao, "Information and accuracy attainable in the estimation of statistical parameters," *Bull. of Calcutta Mathematical Society*, vol. 37, pp. 81–91, 1945.
 - [17] N. Abramson, "The aloha system-another alternative for computer communications," *Proceed. AFIPS*, pp. 695–702, 1970.
 - [18] A. B. Carleial and M. E. Hellman, "Bistable behavior of aloha-type systems," *IEEE transactions on Communications*, vol. 23, pp. 401–410, 1975.
 - [19] L. Kleinrock and S. S. Lam, "Packet switching in a multiaccess broadcast channel: performance evaluation," *IEEE transactions on Communications*, vol. 23, pp. 410–423, 1975.
 - [20] G. Fayolle, E. Gelembé, and J. labetoulle, "Stability and optimal control of the packet switching broadcast channel," *Journal of the Association of Computer Machines*, vol. 24, pp. 375–386, 1977.
 - [21] M. J. Fergusson, "On the control, stability, and waiting time in a slotted aloha random-access system," *IEEE transactions on Communications*, 1975.

-
- [22] S. S. Lam and L. Kleinrock, "Packet switching in a multiaccess broadcast channel: dynamic control procedures," *IEEE transactions on Communications*, vol. 23, pp. 891–904, 1975.
- [23] B. Hajek and T. V. Loon, "Decentralized dynamic control of a multi-access broadcast channel," *IEEE transactions on Automatic Control*, vol. 27, pp. 559–569, 1982.
- [24] J. I. Capetanakis, "The multiple access broadcast channel: protocol and capacity considerations," *IEEE transactions on Information Theory*, vol. 25, pp. 505–515, 1979.
- [25] B. S. Tsybakov and V. A. Mikhailov, "Random multiple access of packets: part and try algorithms," *Probl. Pered. Inform.*, vol. 16, pp. 65–79, 1980.
- [26] R. G. Gallager, "Conflict resolution in random access broadcast networks," *Proc. AFOSR Workshop Communication Theory and Applications*, pp. 74–76, 1978.
- [27] J. Mosely and P. A. Humblet, "A class of efficient contention resolution algorithms for multiple access channels," *IEEE transactions on Communications*, vol. 33, pp. 145–151, 1985.
- [28] M. Coupechoux, B. Baynat, C. Bonnet, and V. Kumar, "Croma an enhanced slotted mac protocol for manets," *Kluwer/ACM Mobile Networks and Applications*, vol. 10, pp. 183–197, 2005.
- [29] C. Zhu and M. Corson, "A five-phase reservation protocol (fprp) for mobile ad hoc networks," *Proceed IEEE INFOCOM*, 1998.
- [30] L. Kleinrock and F. A. Tobagi, "Packet switching in radio channels: Part I - carrier sense multiple-access modes and their throughput-delay characteristics," *IEEE transactions on Communications*, vol. 23, 1975.
- [31] G. Bianchi, "Performance analysis of the ieee 802.11 distributed coordination function," *IEEE Journal on Selected Area in Communications*, vol. 18, 2000.
- [32] E. Ziouva and T. Antonakopoulos, "Csma/ca performance under high traffic conditions: throughput and delay analysis," *Computer Communications*, vol. 25, pp. 313–321, 2002.

-
- [33] P. Chatzimisios, A. C. Boucouvalas, and V. Vistas, "Ieee 802.11 packet delay-a finite retry limit," *Proceed. IEEE GLOBECOM'03*, 2003.
- [34] M. M. Carvalho and J. Garcia-Luna-Aceves, "Delay analysis of ieee 802.11 in single-hop networks," *Proceed. IEEE ICNP'03*, 2003.
- [35] F. A. Shabdiz and S. Subramaniam, "A finite load analytical model for the ieee 802.11 distributed coordination function mac," *Proceed. WiOpt'03*, 2003.
- [36] C. B. G. R. cantieni, Q. Ni and T. Turletti, "Performance analysis under finite load and improvement for multirate 802.11," *Elsevier Computer Communications*, vol. 28, pp. 1095–1109, 2005.
- [37] D. Malone, K. Duffy, and D. J. Leith, "Modeling the 802.11 distributed coordination function with heterogenous finite load," *Proceed. Resource Allocation in Wireless Networks*, 2005.
- [38] C. E. Koksal, H. Kassab, and H. Balakrishnan, "An analysis of short-term fairness in wireless media access protocols," *Proceed. ACM Sigmetrics*, 2000.
- [39] O. G. G. Berger-sabbatel, A. Duda and F. Rousseau, "Fairness and its impact on delay in 802.11 networks," *Proceed. IEEE GLOBECOM'04*, 2004.
- [40] V. Barghavan, A. Demers, S. Shenker, and L. Zhang, "Macaw: A media access protocol for wireless lans," *Proceed. ACM SIGCOMM'94*, 1994.
- [41] Y. Kwon, Y. Fang, and H. Latchman, "A novel mac protocol with fast collision resolution for wireless lans," *Proceed. IEEE INFOCOM'03*, 2003.
- [42] N. O. Song, B. J. Kwak, and L. E. Miller, "Enhancement of ieee 802.11 distributed coordination function with exponential increase exponential decrease backoff algorithm," *Proceed. IEEE VTC Spring'03*, 2003.
- [43] D. Qiao and K. G. Shin, "Achieving efficient channel utilization and weighted fairness for data communications in ieee 802.11 wlan under the dcf," *Proceed. International Workshop on Quality of Service*, 2002.

-
- [44] L. Bononi, M. Conti, and E. Gregori, "Runtime optimization of ieee 802.11 wireless lans performance," *IEEE transactions on Parallel and Distributed Control*, vol. 15, 2004.
 - [45] R. G. M. Heusse, F. Rousseau and A. Duda, "Idle sens: An optimal access method for high throughput and fairness in rate diverse wireless lans," *Proceed. ACM SIGCOMM05*, 2005.
 - [46] Y. Chen, Q-A.Zeng, and D. P. Agrawal, "Analysis and enhancement of ieee 802.11 mac protocol," *Proceed. ICT'03*, 2003.
 - [47] G. B.-s. M. Heusse, F. Rousseau and A. Duda, "Performance anomaly of 802.11b," *Proceed. IEEE INFOCOM'03*, 2003.
 - [48] G. Tan and J. Guttag, "Time-based fairness improves performance in multi-rate wireless lans," *Proceed. USENIX'04*, 2004.
 - [49] D. Pong and T. Moors, "Fairness and capacity trade-off in ieee 802.11 wlans," *Proceed. IEEE ICLCN'04*, 2004.
 - [50] S. P. et al., "Delay improvement of ieee 802.11 distributed coordination function using size-based scheduling," *Proceed. IEEE ICC'05*, 2005.
 - [51] R. J. et al., "A quantitative measure of fairness and discrimination for ressource allocation of shared computer systems," *DEC technical report TR-301*, 1984.
 - [52] B.-J. Kwak, N.-O. Song, and L. E. Miller, "Performance analysis of exponential backoff," *IEEE transactions on Networking*, vol. 13, 2004.
 - [53] D. gross and C. Harris, *Fundamentals of queueing theory*. John Wiley & sons, 1998.
 - [54] L. Kleinrock and F. A. Tobagi, "Packet switching in radio channels: Partii - the hidden terminal problem in carrier sense multiple-access and the busy-tone solution," *IEEE transactions on Communications*, vol. 23, 1975.
 - [55] P. Karn, "Maca-a new channel access protocol for packet radio," *Proceed. ARRL/CRRL Amateur Radio Ninth computer Networking conference*, pp. 134-140, 1990.

- [56] Y. Zhou and S. M. Nettles, "Balancing the hidden and exposed node problems with power control in csma/ca-based wireless networks," *Proceed. IEEE Wireless Communications and Networking Conference*, pp. 683–688, 2005.
- [57] F. Ye, S. Yi, and B. Sikdar, "Improving spatial reuse of ieee 802.11 based ad hoc networks," *Proceed. IEEE GLOBECOM*, pp. 1013–1017, 2003.
- [58] X. Guo, S. Roy, and W. S. Conner, "Spatial reuse in wireless ad-hoc networks," *IEEE*, pp. 1437–1442, 2003.
- [59] J. Deng, B. Liang, and P. K. Varshney, "Tuning the carrier sensing range of ieee 802.11 mac," *Proceed. IEEE GLOBECOM*, pp. 2987–2991, 2004.
- [60] X. Yang and N. Vaidya, "On physical carrier sensing in wireless ad hoc networks," *Proceed. IEEE INFOCOM*, pp. 2525–2535, 2005.
- [61] J. Zhu, L. L. Yang, and W. S. Conner, "Leveraging spatial reuse in 802.11 mesh networks with enhanced carrier sensing," *Proceed. IEEE ICC*, 2004.
- [62] Z. Li, S. Nandi, and A. K. Gupta, "Improving mac performance in wireless ad hoc networks using enhanced carrier sensing (ecs)," *Proceed. Third IFIP Networking Conference*, 2004.
- [63] C. E. Shannon, "A mathematical theory of communication," *Bell System Technical Journal*, vol. 27, pp. 379–423, 1948.
- [64] J. Zander, "Distributed cochannel interference control in cellular radio systems," *IEEE transactions on vehicular Technology*, vol. 41, pp. 305–311, 1992.
- [65] G. Foschini and Z. Miljanic, "A simple distributed autonomous power control algorithm and its convergence," *IEEE transactions on vehicular Technology*, vol. 42, pp. 641–646, 1993.
- [66] R. Yates, "A framework for uplink power control in cellular radio systems," *IEEE Journal on selected Area in Communications*, vol. 13, pp. 1341–1348, 1995.

- [67] S. Ulukus and R. Yates, "Stochastic power control for cellular radio systems," *IEEE transactions on Communications*, vol. 46, pp. 784–798, 1998.
- [68] R. Knopp and P. A. Humblet, "Information capacity and power control in single-cell multiuser communications," *Proceed. IEEE ICC*, pp. 18–22, 1995.
- [69] J. L. Sobrinho, R. D. Haan, and J. M. Brazio, "Why rts-cts is not your ideal wireless lan multiple access protocol," *IEEE*, pp. 1516–1521, 2003.
- [70] S. ray nd J. B. Carruthers and D. Starobinski, "Evaluation of the masked node problem in ad hoc wireless lans," *IEEE Transactions on Mobile computing*, vol. 4, pp. 430–442, 2005.
- [71] S. Xu and T. Saadawi, "Does the ieee 802.11 mac protocol work well in multihop networks?," *IEEE Communications Magazine*, vol. 39, pp. 130–137, 2001.
- [72] S. Ray, J. B. Carruthers, and D. Starobinski, "Rts/cts-induced congestion in ad hoc wireless lans," *IEEE*, pp. 1516–1521, 2003.
- [73] K. Xu, M. Gerla, and S. Bae, "How effective is the ieee 802.11 rts/cts handshake in ad hoc networks," *Proceed. IEEE GOLBECOM*, pp. 72–76, 2002.
- [74] H. J. Kushner and J. Yin, *Stochastic Approximation Algorithms and Applications*. Springer-Verlag, 1997.
- [75] H. Robins and S. Monroe, "A stochastic approximation method," *Ann. Math. Statist.*, vol. 22, pp. 400–407, 1951.
- [76] J. Kiefer and J. Wolfowitz, "Stocahstic etimation of the maximum of a regression function," *Ann. Math. Statist.*, vol. 23, pp. 462–466, 1952.
- [77] P. W. Glynn, "Likelihood ratio gradient estimation for stochastic systems," *communications of the ACM*, vol. 33, pp. 75–84, 1990.
- [78] P. Glasserman and P. W. Glynn, "Gradient estimation for regenerative processes," *Proceed. Winter Simulation Conf.*, pp. 280–288, 1992.

- [79] X. R. Cao and Y.-W. Wan, "Algorithms for sensitivity analysis of markov systems through potentials and perturbation realization," *IEEE transactions on Control System Techniques*, vol. 6, pp. 482–494, 1998.
- [80] E. K. P. Chong and P. J. Ramadage, "Stochastic optimization of regenerative systems using infinitesimal perturbation analysis," *IEEE transactions on automatic Control*, vol. 39, pp. 1400–1410, 1994.
- [81] J. C. Spall, "adaptive stochastic approximation by the simultaneous perturbation method," *IEEE transactions on automatic Control*, vol. 45, pp. 1839–1853, 2000.
- [82] E. altman, R. El-Azouzi, and T. Jiménez, "Slotted aloha as a game with partial information," *Elsevier Computer Networks*, vol. 45, pp. 701–713, 2004.
- [83] F. J. Vazquez-Abad, G. C. Cassandras, and V. Julka, "Centralized and decentralized asynchronous optimization of stochastic discrete-event systems," *IEEE Transactions on automatic Control*, vol. 45, pp. 631–655, 1998.
- [84] E. S. Sousa and J. A. Silvester, "Spreading code protocols for distributed spread-spectrum packet radio networks," *IEEE transactions on Communications*, vol. 36, pp. 272–281, 1988.
- [85] Y.-C. T. S.-L. Wu, C.-Y. Lin and J.-P. Sheu, "A new multi-channel mac protocol with on-demand channel assignment for multi-hop mobile ad hoc networks," *Proceed. Intl Symposium on Parallel Architectures, Algorithms and Networks (I-SPAN)*, 2000.
- [86] J. So and N. H. Vaidya, "Multi-channel mac for ad hoc networks: Handling multi-channel hidden terminals using a single transceiver," *Proceed. 5th ACM MOBIHOC*, 2004.
- [87] A. Nasipuri and S. R. Das, "A multichannel csma mac protocol for mobile multihop networks," *Proceed. IEEE Wireless Communications and Networking Conference (WCNC)*, 1999.

-
- [88] A. Nasipuri and S. R. Das, "Multichannel csma with signal power-based channel selection for multihop wireless networks," *Proceed. IEEE Vehicular Technology Conference (VTC)*, 2001.
- [89] N. Jain and S. R. Das, "A multichannel csma mac protocol with receiver-based channel selection for multihop wireless networks," *Proceed. of the 9th Int. Conf. On Computer Communications and Networks (IC3N)*, 2001.
- [90] Z. Tang and J. J. Garcia-Luna-Aceves, "Hop-reservation multiple access (hrma) for ad-hoc networks," *Proceed. IEEE INFOCOM*, 1999.
- [91] A. Tzamaloukas and J. Garcia-Luna-Aceves, "Receiver-initiated collision-avoidance protocol for multi-channel networks," *Proceed. IEEE INFOCOM*, 2002.
- [92] L. Kleinrock and J. Silvester, "Optimum transmission radii for packet radio network or why six is a magic number," *Procd. IEEE National elecommunications Conference*, pp. 431–435, 1987.
- [93] H. takagi and L. kleinrock, "Optimal transmission ranges for randomly distributed paket radio terminals," *IEEE transactions on Communications*, vol. 32, 1984.
- [94] F. P. Kelly, *Reversibility and stochastic networks*. Wiley, 1979.
- [95] R. F. Serfozo, *Introduction to stochastic networks*. Springer Verlag, 1999.
- [96] R. J. Cramer, R. A. Scholtz, and M. Z. Win, "Evaluation of an ultra-wide-band propagation channel," *IEEE Transactions on Antennas Propagation*, vol. 50, pp. 561–570, 2002.
- [97] J. Zhang, R. A. Kennedy, and T. D. Abhayapala, "Cramer-rao lower bound for the time delay estimation of uwb signals," *Proceed. IEEE 5th Workshop on Signal Processing Advances in Wireless Communications*.
- [98] A. L. Deleuze, C. L. Martret, P. Ciblat, and E. Serpedin, "Cramer-rao bound for channel parameters in ultra-wide band based system," *Proceed. IEEE 5th Workshop on Signal Processing Advances in Wireless Communications*.

- [99] G. Tian and G. B. Giannakis, "A glrt approach to data-aided timing acquisition in uwb radios part i: Algorithms," *IEEE transactions on Wireless Communications*.
- [100] G. Tian and G. B. Giannakis, "A glrt approach to data-aided timing acquisition in uwb radios . part ii: Training sequence design," *IEEE transactions on Wireless Communications*.
- [101] L. P. Seidman, "Performance limitations and error for parameter estimation," *IEEE transactions on Information Theory*, vol. 58, pp. 644–652, 1970.
- [102] E. Weinstein and A. J. Weiss, "Fundamental limitations in passive time-delay estimation-part i: Narrow-band systems," *IEEE transactions on Acoustic, Speech, and Signal Processing*, vol. 31, pp. 472–486, 1983.
- [103] E. Weinstein and A. J. Weiss, "Fundamental limitations in passive time-delay estimation-part ii: Wide-band systems," *IEEE transactions on Acoustic, Speech, and Signal Processing*, vol. 32, pp. 1064–1078, 1984.
- [104] K. Bell, Y. Ephraim, and H. V. Trees, "Explicit ziv-zakai lower bound for bearing estimation," *IEEE Transactions on Signal Processing*, vol. 44, pp. 2810–2824, 1996.
- [105] P. Ciblat and M. Ghogho, "Ziv-zakai bound for harmonic retrieval in multiplicative and additive gaussian noise," *Proceed. IEEE Workshop on Statistical Signal Processing*.
- [106] D. Cassioli, M. Win, F. Valataro, and A. F. Molisch, "Performance of low-complexity rake reception in a realistic uwb channel," *Proceed. IEEE ICC*, vol. 2, pp. 763–767, 2002.
- [107] J. Foerster, "Channel modeling sub-committee report final," *IEEE P802.15 02/490r1 SG3a*, 2003.
- [108] A. Menouni-Hayar, R. Knopp, and R. Saadane, "Subspace analysis of indoor uwb channels," *EURASIP Journal on applied signal processing*, vol. 3, pp. 287–295, 2005.

-
- [109] B. Mielczarek, M. Wessman, and A. Svensson, "Performance of coherent uwb rake receivers using different channel estimators," *Proceed. International Workshop on Ultra Wideband Systems (IWUWBS)*, 2003.
- [110] J. D. Choi and W. E. Stark, "Performance of ultra-wideband communications with suboptimal receivers in multipath channels," *IEEE Journal on Selected Areas in Communications*, vol. 20, pp. 1754–1766, 2002.
- [111] R. Saadane and D. A. and A. Menouni-Hayar, "A statistical uwb channel model based on physical analysis," *Advanced International Conference on Telecommunications*, 2006.
- [112] V. Lottici, A. DAndrea, and U. Mengali, "Channel estimation for ultra-wideband communications," *IEEE Journal on Selected Areas in Communications*, vol. 20, pp. 1638–1644, 2002.
- [113] Y. Souilmi and R. Knopp, "On the achievable rates of ultra-wideband ppm with non-coherent detection in multipath environments," *IEEE ICC*, vol. 5, pp. 3530–3534, 2003.
- [114] M. Zakai and J. Ziv, "Some lower bounds on signal parameter estimation," *IEEE transactions on Information Theory*, vol. 15, pp. 386–391, 1969.
- [115] L. P. Seidman, "An upper bound on average estimation error in nonlinear systems," *IEEE Transactions on Information Theory*, vol. 14, pp. 243–250, 1968.
- [116] R. M. Hawkes and J. B. Moore, "An upper bound on the mean-square error for bayesian parameter estimators," *IEEE Transactions on Information Theory*, vol. 22, pp. 610–615, 1976.
- [117] D. Mary and D. Slock, "Comparison between unitary and causal approaches to backward adaptive transform coding of vectorial signals," *IEEE Conference on Acoustics, Speech, and Signal Processing*, vol. 3, pp. 2533–2536, 2002.
- [118] H. Urkowitz, "Energy detection of unknown deterministic signals," *Proceed. IEEE*, vol. 55, pp. 523–531, 1967.

-
- [119] F. F. Digham, M.-S. Alouini, and M. K. Simon, "Energy detection of unknown deterministic signals," *Proceed. IEEE*, vol. 55, pp. 523–531, 1967.
 - [120] C. W. Helstrom, *Elements of Signal detection & estimation*. Prentice Hall, 1995.
 - [121] H. L. V. Trees, *Detection, Esimation, and Modulation Theory, Part I*. John Wiley & sons, 2001.
 - [122] Q. Zhang and D. liu, "A simple capacity formula for correlated diversity rician fading channels," *IEEE Communications letters*, vol. 6, pp. 481–483, 2002.
 - [123] M. Simon and M.-S. Alouini, "On the difference of two chi-square variates with application to outage probability computation," *IEEE transactions on Communications*, vol. 49, pp. 1946–1954, 2001.

List of Publications

Conferences

- H. Anouar, Y. Souilmi, C. Bonnet, '*A Self-Balanced Receiver-Oriented MAC Protocol for Ultra-Wideband Ad Hoc Networks*', IWUWBS'2003 International Workshop on Ultra Wideband Systems, June 2-5, 2003-Oulu, Finland.
- H. Anouar, C. Bonnet, '*A Self-Balanced Receiver-Oriented MAC Protocol for Multiple channels Multihop Ad-Hoc Networks*', VTC' Spring 2005, 61st Semiannual IEEE Vehicular Technology Conference, 30th May - 1st June, 2005, Stockholm, Sweden. H. Anouar, A. Menouni Hayar, R. Knopp, C. Bonnet,
- '*Ziv-Zakai Lower Bound on The Time Delay Estimation of UWB Signals*', ISCCSP 2006, 2nd IEEE-EURASIP International Symposium on Control, Communications, and Signal Processing 13-15 March 2006, Marrakech, Morocco.
- H. Anouar, C. Bonnet, '*Optimal Constant-Window Backoff Scheme for IEEE 802.11 DCF in General Load Single-Hop Wireless Networks*', 9th ACM/IEEE International Symposium on Modeling, Analysis and Simulation of Wireless and Mobile Systems MSWIM 2006.

Reports

- H. Anouar, C. Bonnet, '*Optimal Constant-Window Backoff Scheme to Increase Throughput and Fairness of IEEE 802.11 DCF in Single-Hop Networks*', Research Report RR-05-153.
- H. Anouar, C. Bonnet, '*Design, Design, Analysis, and Optimization of Aloha-Like Protocol for Multichannel Multihop Ad Hoc Networks*', Research Report RR-05-154.
- H. Anouar, A. Menouni Hayar, R. Knopp, C. Bonnet, '*Fundamental Limitations in Time-Delay Estimation of IR-UWB Signals*', Research Report RR-06-167.

Journals

- H. Anouar, C. Bonnet, '*Optimal Constant-Window Backoff Scheme for IEEE 802.11 DCF in General Load Single-Hop Wireless Networks*', Submitted to Springer Wireless Networks Journal.
- H. Anouar, C. Bonnet, '*Design, Analysis and Optimization of Aloha-Like Protocol for Multichannel Multihop Ad Hoc Networks*', To be submitted.